THE BIOLOGICAL CHARACTERISATION OF TRIPLE NEGATIVE BREAST CANCER IN CYCLIC HYPOXIA

Charlotte Simpson
MSc by Research Thesis
St Catherine's College

Supervised by
Ester Hammond
and
Kristoffer Petersson

Department of Oncology
University of Oxford
Trinity Term, 2021

DECLARATION

This thesis is submitted for the degree of Master by Research in Oncology. I hereby declare that the results presented in this thesis are my own and that this dissertation does not exceed the word limit.

ACKNOWLEDGEMENTS

I would first like to thank my supervisor, Ester Hammond, for giving me the opportunity to be a student in her lab this year. Ester has provided me with invaluable support, feedback and guidance as well as incredible opportunities to learn as many techniques as possible and help with paper revisions. I have loved every moment in the lab, and the enthusiasm for research Ester brings to the lab is inspiring and something I will carry on with me.

I would like to thank my secondary supervisor Kristoffer Petersson for giving me the opportunity to do FLASH, as well as providing helpful and constructive feedback.

I would also like to thank all the members of the Hammond lab, past and present, for their support during this MSc(Res). Specifically I would like to thank Hannah Bolland, Tiffany Ma, Hala Estephan and Çağla Tosun, as well as, Susan Kilgas from the Ramadan Lab for their friendship, guidance, enthusiasm and laughs in and outside of lab. To Hannah, Tiff and Hala, thank you for taking time to teach me so many different techniques and provide constructive feedback on my work. I will miss working with you all.

Finally, I would like to thank my family and friends for their support and encouragement throughout this year, to Walter, Juliette, Cliodhna, Izzy and Liv, thank you!

ABSTRACT

Regions of insufficient oxygen, hypoxia, occur in most solid tumours, including breast cancer. Hypoxia occurs due to malformed tumour vasculature and uncontrolled cell proliferation and is associated with therapy resistance and an overall poor patient prognosis. Of all the breast cancer subtypes, hypoxia is particularly evident in triple negative breast cancer (TNBC). A wealth of evidence suggests that cyclic hypoxia is commonplace in solid tumours and is associated with the most aggressive disease including increased metastasis. Our laboratory has recently developed a physiologically relevant cyclic protocol that fluctuates between <0.1% O_2 and 2% O_2. The aim of this project was to characterise the biological response of TNBC to cyclic hypoxia compared to static <0.1% O_2 and static 2% O_2. We found that cyclic hypoxia induces a differential gene expression profile compared to static <0.1% O_2 and static 2% O_2, in which there are 87 uniquely expressed genes in cyclic hypoxia. The cell cycle dynamics between the three hypoxic conditions were distinct, with cyclic hypoxia inducing an S-phase accumulation. Cyclic hypoxia exposed TNBC showed decreased radiosensitivity comparative to 2% O_2, which we attribute to the S-phase accumulation. Despite a decrease in radiosensitivity of TNBC exposed to cyclic hypoxia, cyclic hypoxia appears a challenging environment for TNBC cell lines and results in decreased cell viability compared to <0.1% O_2 and 2% O_2. Together, our data shows that the biological response to hypoxia is dependent on the exact nature of the hypoxic conditions to which the cells are exposed, and that cyclic hypoxia can increase therapy resistance.

Table of Contents

DECLARATION 1

ACKNOWLEDGEMENTS 2

ABBREVIATIONS 9

CHAPTER 1: INTRODUCTION 12

1.1. Cancer: origin to today 12

1.2. The hallmarks of cancer 12

1.3. Hypoxia and cancer 18

1.4. Mild hypoxia 23

1.5. Severe hypoxia 24

1.6. Cyclic hypoxia 29

1.7. Breast cancer 31

1.8. Aims of this project 34

CHAPTER 2: MATERIALS AND METHODS 36

2.1. Solutions and Reagents 36

2.1.1 Primary Antibodies 36

2.1.2 Secondary antibodies 36

2.1.3 Buffers 37

2.2. Cell lines and cell culture 38

2.2.1 Cell lines and specifications 38

2.2.2 Culture Conditions 38

2.2.3 Mycoplasma testing 38

2.2.4 Cryopreservation 39

2.2.5 Thawing 39

2.3. Hypoxia treatment 39

2.4. Irradiation 40

2.5. Laboratory techniques 41
2.5.1 Colony Survival Assay 41
2.5.2 Cell Lysis 42
2.5.3 Western Blotting 42
2.5.4 3-(4,5-dimethylthiazol-2-yl)-2,5-diphenyl-2H-tetrazolium bromide (MTT) assay 43
2.5.5 RNA extraction and purification 43
2.5.6 cDNA library creation 44
2.5.7 qPCR 45
2.5.8 Fluorescence activated cell sorting (FACS) 46
2.5.9 Small interfering RNA gene knockdown (siRNA) transfection 47
2.6. Statistical analysis 48
CHAPTER 3: The biological response to cyclic hypoxia 49
Introduction 49
3.1. Cyclic hypoxia appears to induce the UPR but not the DDR 50
3.2. Cell cycle dynamics vary between different oxygen conditions 51
3.3. Cyclic hypoxia reduces cell viability in four TNBC cell lines 54
3.4. The oxygen conditions tested induce differential gene expressions 57
3.5. Expression analysis of genes in the Buffa hypoxia signature indicates the signature cannot distinguish between the different oxygen conditions 64
3.6. The differing oxygen conditions lead to distinct upregulation in gene ontologies 66
3.7. Cyclic hypoxia is most relevant to breast cancer 71
Discussion 74
CHAPTER 4: The therapeutic response to cyclic hypoxia 77
Introduction 77
4.1 The role of EphA3 in cyclic hypoxia 79
4.2. Cyclic hypoxia leads to increased radioresistance compared to 2% O_2 but increased radiosensitivity compared to <0.1% O_2 80

4.3. FLASH 84

Discussion 88

CHAPTER 5: Discussion **91**

Therapeutic potential for cyclic hypoxia 96

Future Directions 97

REFERENCES **99**

APPENDIX: Published papers from this MSc by Research **114**

List of Figures

Figure 1.2.1: The six hallmarks of cancer 13

Figure 1.2.2: The enabling characteristics and emerging hallmarks of cancer 16

Figure 1.3.1: The regulation of HIF-1α in normoxia compared to hypoxia 20

Figure 1.3.2: Chronic versus acute hypoxia. 23

Figure 1.5: The oxygen depletion hypothesis for FLASH radiotherapy 28

Figure 1.8: Cyclic hypoxia protocol 35

Figure 2.3: Cyclic hypoxia oxygen readout 40

Figure 2.4: Radiation box 41

Figure 3.1: Static and cyclic hypoxia elicit different biological responses. 51

Figure 3.2.1: MDA-MB-231 cell cycle shows distinct profiles in cell proliferation and cycle stage depending on O_2 condition 52

Figure 3.2.2: CAL51 cell cycle shows distinct profiles in cell proliferation and cycle stage depending on O_2 condition 53

Figure 3.3.1: Cyclic hypoxia leads to decreased cell viability in four TNBC cell lines 55

Figure 3.3.2: Colony survival in CAL51 supports the cell viability results determined by MTT assay. 56

Figure 3.3.3: MDA-MB-231 appear to decrease in cell viability in 2% O_2 56

Figure 3.4.1: Gene expression of CAIX and GLUT-1 confirm different hypoxic conditions..... 57

Figure 3.4.2: Pearson correlation coefficient of gene expression levels between samples supports repeat validity..... 58

Figure 3.4.3: Differential gene expression profiles occur in response to the varied hypoxic conditions 60

Figure 3.4.4: The distribution of differentially expressed genes in 2% O_2, <0.1% O_2 and cyclic hypoxia comparative to 21% O_2. 62

Figure 3.4.5: Differential gene expression of four HIF-1α mediated genes in our different hypoxic conditions. 63

Figure 3.5.1: Differential expression of the 15 top-ranked genes from the Buffa hypoxia signature in our range of hypoxia conditions. 65

Figure 3.5.2: The expression of the Buffa hypoxia gene signature in MDA-MB-231 cells exposed to 16 h of 21% O_2, 2% O_2, <0.1% O_2 and cyclic hypoxia 66

Figure 3.6.1: Distinct gene ontologies are enriched dependent on the hypoxic conditions, with cyclic hypoxia and 2% O_2 enriching metabolic reprogramming and <0.1% O_2 enriching the UPR. 68

Figure 3.6.2: The cellular component of the GO highlights the induction of UPR in cyclic hypoxia. 70

Figure 3.7: Cyclic hypoxia is the only condition in which, comparative to 21% O_2, cancer-related gene enrichment is significant in breast cancer 72

Figure 4.1.1: Cyclic-specific induction of *EPHA3* in the RNA-seq was validated with qPCR. .. 79

Figure 4.1.2: No significant reduction on *EPHA3* mRNA is observed 80

Figure 4.2.1: An OER of 2.05 between 21% O_2 and <0.1% O_2 provides confidence in our radiation boxes being airtight. 82

Figure 4.2.2: Cyclic hypoxia induces a distinct radioresistance response to 2% O_2 and <0.1% O_2. 83

Figure 4.3.1: Preliminary experiment to determine if T12.5s can maintain hypoxia during irradiation. 85

Figure 4.3.2: FLASH versus Conv radioresistance across 21% O_2, 2% O_2 and <0.1% O_2..... 86

Figure 4.3.3. Cyclic hypoxia may induce differing radiosensitivity responses to FLASH compared to Conv 87

List of Tables

Table 1.7: Breast cancer classification based on ER, PR and HER2 status with Ki67 as an additional determinant for Luminal A and Luminal B.. 32

Table 2.1.1 Primary Antibodies 36

Table 2.1.2 Secondary antibodies 36

Table 2.2.1: Cell lines and specifications 38

Table 2.5.1: The seeding densities and plating efficiencies of the human carcinoma cell lines used for clonogenic assays 42

Table 2.5.7: qPCR primers 46

ABBREVIATIONS

APOBEC	Alipoprotien B mRNA editing enzyme, catalytic polypeptide like
APOBEC3B	Apolipoprotein B mRNA-editing enzyme, catalytic polypeptide-like 3B
ATM	Ataxia telangiectasia mutated
ATR	ATM-related and RAD3-related
BET	Bromodomain and extra-terminal
BrdU	Bromodeoxyuridine
CAFs	Cancer-associated fibroblasts
CBP	CREB-binding protein
CDK	Cyclic dependent kinase
Chk1	Checkpoint kinase
Conv	Conventional radiotherapy
Cs	Caesium
DDR	DNA damage response
DEPC	Diethylpyrocarbonate
DMEM	Dulbecco's modified Eagle's medium
DMSO	Dimethylsulphoxide
DNA	Deoxyribonucleic acid
DNA-PKcs	DNA-phosphokinases
dNTP	Deoxynucleotide
DO	Disease ontology
DSB	Double stranded break
DSBs	Double stranded breaks
ECM	Extracellular matrix
EMT	Epithelial mesenchymal transition
ER	Oestrogen receptor
FACS	Fluorescent activated cell sorting
FBS	Fetal bovine serum
FIH	Factor inhibiting HIF-1
GO	Gene ontology

HCl	Hydrochloric acid
HIF	Hypoxia inducible factor
HRE	Hypoxia response element
LDHA	Lactate Dehydrogenase A
LOX	Lysyl oxidase
LSD1	Lysine-specific demethylase 1
mRNA	Messenger RNA
MTT	3-(4,5-dimethylthiazol-2-yl)-2,5-diphenyl-2H-tetrazolium bromide
NAC	N'acetylcysteine
OER	Oxygen enhancement ratio
PBS	Phosphate buffered saline
PCR	Polymerase chain reaction
PDI	Protein disulphide isomerase
PHD	Prolyl hydroxylase domain proteins
PI	Propidium iodide
PR	Progesterone receptor
PTM	Post translational modification
qPCR	Quantitative polymerase chain reaction
RB	Retinoblastoma-associated
RNA	Ribonucleic acid
RNR	Ribonucleotide reductase
ROS	Reactive oxygen species
RPA	Replication protein A
RRM1	Ribonucleotide reductase regulatory subunit M1
RRM2	Ribonucleotide reductase regulatory subunit M2
RRM2B	Ribonucleotide reductase regulatory subunit M2B
SDS	Sodium dodecyl sulphate
SETX	Senataxin
ssDNA	Single stranded DNA
siRNA	Small interfering RNA
SSB	Single stranded break
ssDNA	Single stranded DNA

STAT3	Signal transducer and activator of transcription 3
TME	Tumour microenvironment
TNBC	Triple negative breast cancer
UPR	Unfolded protein response
VEGF-A	Vascular endothelial growth factor A
VHL	Von Hippel-Lindau

CHAPTER 1: INTRODUCTION

1.1. Cancer: origin to today

Cancer was first described in the Hippocratus Corpus (*c*. 410 – 360 BCE) by the Greek physician Hippocrates. Hippocrates used the words carcinos, meaning crab, and carcinoma to describe a range of tumours and refer to the crab-like projections spreading from tumour masses (David and Zimmerman, 2010). Today, cancer is a leading cause of death, and specifically premature death, worldwide. The year 2020 saw 19.3 million new cancer cases and close to 10 million cancer deaths (Bray et al., 2021, Sung et al., 2021). Female breast cancer is the most commonly diagnosed cancer with around 2.3 million diagnoses per year (11.7% of all new cancer diagnoses), followed by lung, colorectal, prostate, and stomach cancers. Lung cancer is the leading cause of cancer death, resulting in an estimated 1.8 million deaths per year, followed by colorectal, liver, stomach, and female breast cancers. It has been projected that in 2040, the global cancer burden will increase to 28.4 million cases (Sung et al., 2021).

1.2. The hallmarks of cancer

Cancer is characterised by neoplasia, the uncontrolled proliferation of cells, and the invasion of these malignant cells to surrounding tissue and distant organs. The origin of cancer is complex and involves the accumulation of genomic mutations, specifically aberrations that result in gain of function oncogenes and loss of function tumour suppressor genes (Lee and Muller, 2010). As normal cells transform into this neoplastic, malignant state they undergo a

series of changes that enable tumour growth and metastatic dissemination. Described first by Hanahan and Weinberg, these complex changes can be organised into six broad categories that provide the foundation of cancer biology, known as the hallmarks of cancer. The hallmarks are as follows: sustaining proliferative signalling, evading growth suppressors, activating invasion and metastasis, enabling replicative immortality, inducing angiogenesis and finally, resisting cell death (Figure 1.2.1) (Hanahan and Weinberg, 2000).

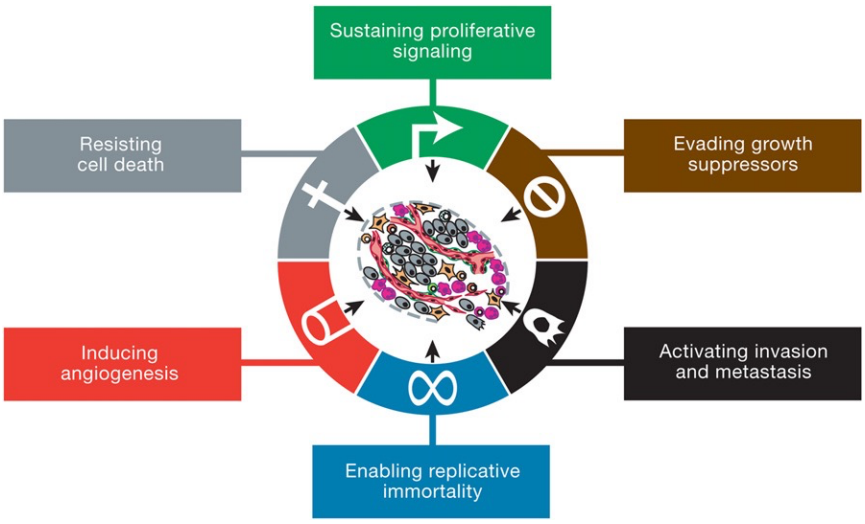


Figure 1.2.1: The six hallmarks of cancer. This figure was reproduced from (Hanahan and Weinberg, 2011). Permission date: 02 August 2021

In normal tissues, the production and release of growth promoting signals that control entry and progression through the cell cycle are carefully controlled. Cancer cells deregulate these signals. High throughput DNA sequencing of cancer cell genomes shows that specific somatic mutations predict for constitutive activation of signalling circuits usually triggered by the activation of growth factor receptors that regulate progression through the cell cycle as well as cell growth. Therefore, this autocrine signalling network leads to sustained proliferative cell growth (Davies and Samuels, 2010). Tumour suppressors act to constrain cell proliferation

and growth. Retinoblastoma-associated (RB) and p53 proteins are encoded by the two prototypical tumour suppressors. These proteins operate within cellular regulatory networks to govern proliferation, senescence and apoptosis. With mutation of these tumour suppressor genes comes the ability to evade growth suppressor signals and sustain proliferation while also avoiding cell death (Amin et al., 2015, Hickman et al., 2002). In addition to mutation in *TP53* and *RB*, malignant cells may achieve similar evasion of apoptosis through increasing the expression of antiapoptotic regulators, such as members of the Bcl-2 family, or of survival signals, such as IGF1/2, through the downregulation of proapoptotic factors such as Bim, Bax or Puma (O'Connor et al., 1998, Oltvai et al., 1993, Yin et al., 1997, Yu et al., 2003). In normal, healthy cells the DNA polymerase that adds telomere repeat segments to the 3' end of telomeres, telomerase, is expressed at negligible levels. Strikingly, in cancer cells this protein is expressed at high levels. This ability to extend telomeric DNA counteracts the otherwise present progressive telomeric erosion. Cells will therefore not reach the Hayflick limit, rendering them resistant to senescence as well as apoptosis and hence, replicative immortality is enabled (Jafri et al., 2016). Some oncogenes, such as *Myc* and *Ras*, upregulate the expression of angiogenic factors, such as vascular endothelial growth factor-A (VEGF-A), leading to a tumour-associated neovasculature (Rak et al., 1995, Shchors et al., 2006). This neovasculature is characterised by excessive vessel branching, inconsistent blood flow and leakiness which ultimately help sustain the developing neoplastic growth (Nagy et al., 2010). Finally, the hallmark responsible for the poorest patient prognosis is metastasis. This is the spread of cancer cells from the primary tumour to surrounding tissue and distant organs. Metastasis consists of two main steps: dissemination of primary tumour cells to distant tissues/organs, and the adaption of these primary cancer cells to the new tissue microenvironments resulting in successful colonisation (Polyak and Weinberg, 2009,

Thiery et al., 2009). Epithelial mesenchymal transition (EMT) broadly regulates invasion and metastasis, but crosstalk between cancer cells and their microenvironment is also vital (Egeblad et al., 2010, Joyce and Pollard, 2009, Karnoub et al., 2007, Wyckoff et al., 2007)

Since the hallmarks were established in 2000, further cancer cell adaptations have been acknowledged. The ability of cancer cells to reprogramme their cellular metabolism to support neoplasia, as well as the ability of cancer cells to evade immune attack are now recognised as emerging cancer hallmarks (Figure 1.2.2) (Hanahan and Weinberg, 2011). Due to the uncontrolled proliferation of neoplasia, adjustments to cancer metabolism are required to fuel this growth. Cancer cells therefore see a shift from mitochondrial oxidative phosphorylation to glycolysis. This was first observed by Warburg, and hence is coined the Warburg effect (Warburg, 1956). Even in the presence of oxygen cancer cells undergo this metabolic shift. This leads to a state that has been termed aerobic glycolysis. However, the reliance on glycolysis is further accentuated under hypoxic conditions, where oxygen availability is diminished. Here the shift from oxidative to glycolytic metabolism that occurs in periods of prolonged hypoxia allows the maintenance of redox homeostasis and cell survival (Semenza, 2010b, Kim et al., 2006, Papandreou et al., 2006)

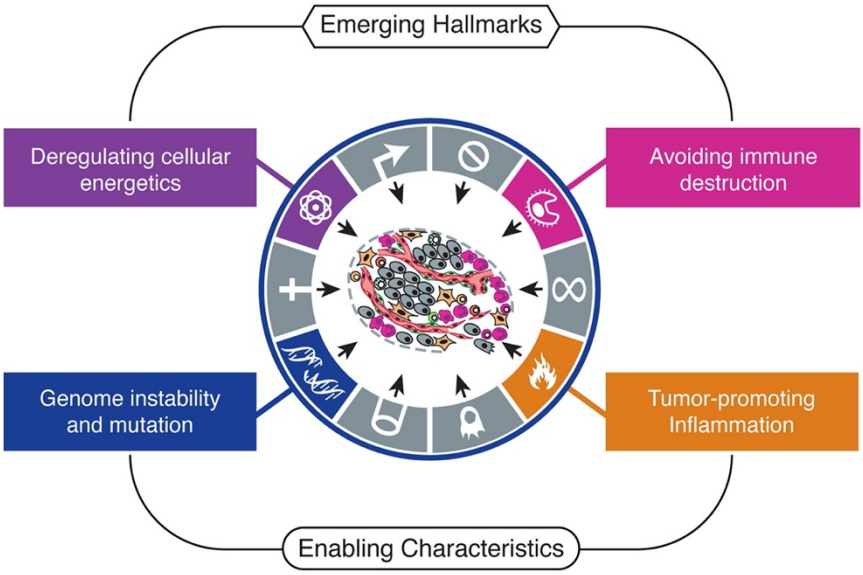


Figure 1.2.2: The enabling characteristics and emerging hallmarks of cancer. This figure was reproduced from (Hanahan and Weinberg, 2011). Permission date: 02 August 2021

Despite the universal cancer hallmarks, intertumoural and intratumoural heterogeneity also exists. It is important to understand tumour heterogeneity as it impacts tumour evolution, metastasis, immune response and drug resistance (Caswell and Swanton, 2017). The advent of sequencing technology has allowed the investigation into genetic heterogeneity, which is driven by somatic mutations and epigenetic modifications. These mutations build upon the pre-existing cancer genetic landscape and Darwinian evolution allows malignant sub-clones to develop in the mutating tumour (Caswell and Swanton, 2017, Keats et al., 2012, Shah et al., 2009, Varley et al., 2009). One such example of an endogenous driver of genetic heterogeneity are the apolipoprotein B mRNA editing enzyme catalytic polypeptide (APOBEC) family. APOBECs are cytidine deaminases. Cytosine deamination to uracil primarily occurs in regions of ssDNA. An ABOBEC mutational signature has been characterised in response to APOBEC-induced C to T and C to G mutations seen within the APOBEC consensus deamination sequence of patients (Alexandrov et al., 2013, Roberts et al., 2013).

Beyond genetic mutations, heterogeneity is also driven by non-genetic factors, resulting in highly dynamic and complex tumour cell populations. Tumours not only consist of cancer cells but also an array of extracellular matrix (ECM) proteins, resident and infiltrating cells, such as immune cells and fibroblasts, as well as secreted factors. These components are collectively known as the tumour microenvironment (TME) (Petitprez et al., 2018). TME cues are a source of non-genetic tumour heterogeneity. Therefore, local variations of the TME results in functional variability of genetically identical cells in the same tumour (Baghban et al., 2020, Caiado et al., 2016). TME variability depends on many factors, such as immune infiltrate, cancer-associated fibroblasts (CAFs), acidosis and hypoxia.

Immune infiltration by cytotoxic T cells and T helper cells prevents tumour growth through attacking antigenic cancer cells, whereas tumour-associated neutrophils, macrophages and mast cells act in a tumour promoting capacity (Fridman et al., 2012, Vesely et al., 2011, Wang et al., 2020). CAFs secrete an array of factors that promote tumour progression, such as development and metastasis (Ping et al., 2021). Acidosis results from poor tumour vasculature and increased carbon flux as a result of glycolysis. An acidic microenvironment promotes tumour progression through stimulating angiogenesis and metastasis, as well as ECM remodelling and suppresses T cell activity (Estrella et al., 2013, Lardner, 2001, Moellering et al., 2008, Xu et al., 2002). Hypoxia is defined as a lack of sufficient oxygen. Hypoxia is present in the majority of solid tumours and occurs from an imbalance between increased oxygen demands of the neoplastic cells as well as impaired oxygen supply (Jing et al., 2019). Hypoxia will now be explored further in the following sections of this introduction.

1.3. Hypoxia and cancer

Oxygen is vital, it is required for cell survival and tissue homeostasis as well as development processes. In the tumour microenvironment, oxygen delivery to cells is impaired due to aberrations in the tumour vasculature, characterised by distended, leaky capillaries. A combination of this with the increased oxygen demand for the highly proliferative neoplastic cells leads to regions of insufficient oxygen in most solid tumours. This is called tumour hypoxia and is associated with metastatic potential, therapy resistance and overall poor patient prognosis. Hypoxia is associated with the stabilisation of hypoxia inducible factor-1 (HIF-1). This stabilisation occurs in a wide range of oxygen concentrations ranging from 3% O_2 to <0.1% O_2 (Rankin and Giaccia, 2016).

HIF-1 is a heterodimeric protein comprised of an oxygen-regulated subunit, HIF-1α, and a constitutively expressed HIF-1β subunit (Wang et al., 1995). HIF-1α undergoes oxygen-dependent hydroxylation on the proline residues 402 and 546, either alone or in tandem, by prolyl hydroxylase domain proteins (PHDs) (Snell et al., 2014). The von Hippel-Lindau protein (VHL) interacts with the hydroxylated prolines and subsequently recruits an E3 ubiquitin ligase. The E3 ubiquitin ligase catalyses ubiquitination of HIF-1α, and consequently targets it for proteasomal degradation. The PHDs are part of the Fe(II) and 2-oxoglutarate dependent oxygenase superfamily, therefore they are oxygen dependent (Kaelin and Ratcliffe, 2008). Consequently, in hypoxia, HIF-1α hydroxylation is suppressed and the subunit accumulates, translocates to the nucleus and dimerises with the HIF-1β subunit (Wang et al., 1995). In the nucleus the HIF-1 complex transcriptionally activates target genes to control the adaptive cellular response to the low oxygen levels, such as cell proliferation, differentiation,

apoptosis, angiogenesis and erythropoiesis (Semenza, 2010a). Some of the most characterised hypoxia-induced genes include carbonic anhydrase IX (*CAIX*), glucose transporter (*GLUT-1*), erythropoietin (*EPO*) and vascular endothelial growth factor A (*VEGF-A*) (Hammond et al., 2014). Transcription occurs through binding of HIF-1 to a hypoxia response element (HRE) containing the consensus DNA binding sequence 5'-RCGTG-3'. Following binding, co-activators p300 and CREB-binding protein (CBP) are recruited, and transcription is activated (Figure 1.3.1) (Mole et al., 2009, Semenza, 2010a). Another mechanism to suppress HIF-1 activity in normoxia is the factor inhibiting HIF-1 (FIH-1) oxygen-dependent hydroxylation of asparagine-803. Under normoxic conditions, FIH-1 inhibits the interaction of HIF-1α with the co-activators p300/CBP (Lando et al., 2002). HIF-2α has extensive sequence similarity to HIF-1α and is regulated in the same manner by proline and asparagine hydroxylation. HIF-2α dimerises with HIF-1β and mediates transcription of target genes. HIF-2α target genes may overlap or be distinct from HIF-1α target genes (Lau et al., 2007). The binding of HIF-1 to hypoxia-induced target genes has been shown by chromatin-immunoprecipitation assays. Genome-wide studies of HIF DNA binding have defined more than 600 sites in which HIF-1α, HIF-2α or both proteins bind (Mole et al., 2009, Schödel et al., 2011).

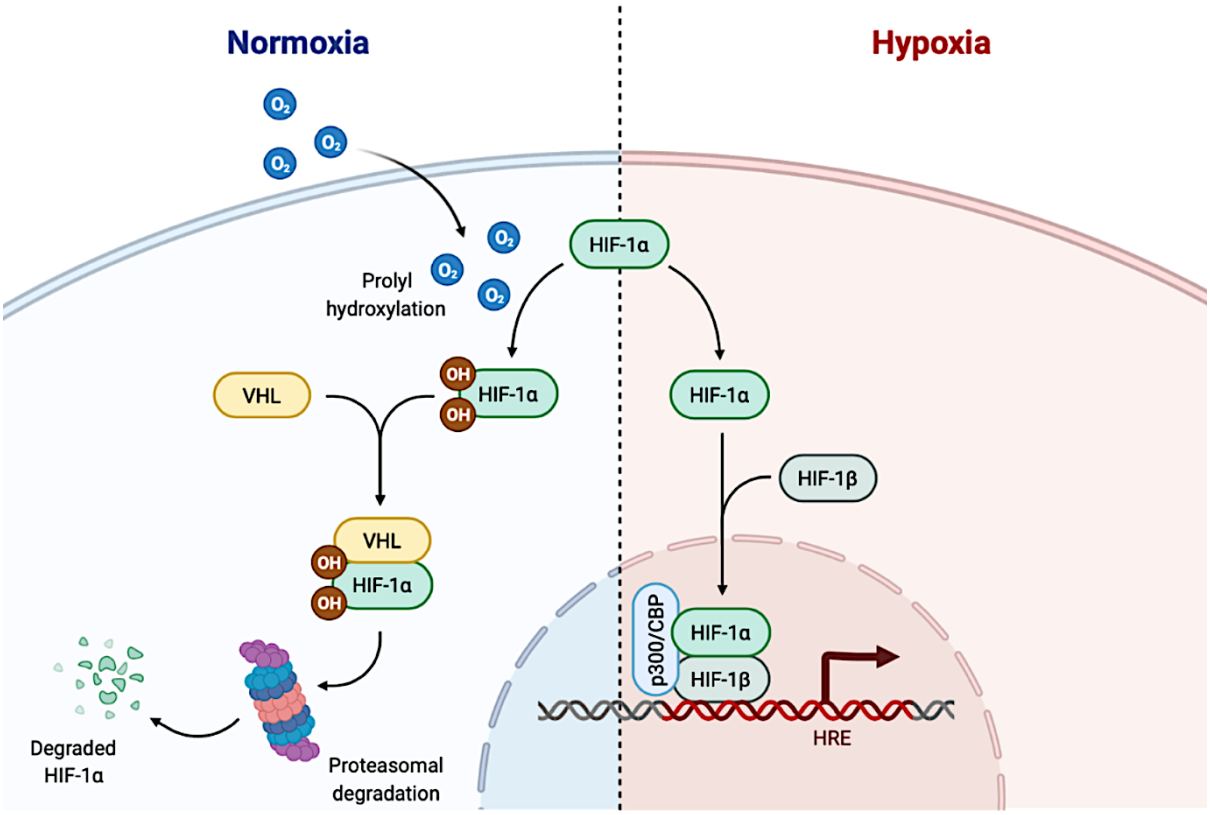


Figure 1.3.1: The regulation of HIF-1α in normoxia compared to hypoxia. Under normoxia HIF-1α is hydroxylated by PHDs, ubiquitinated by VHL and targeted for degradation by the proteasome. In hypoxia, the oxygen-dependent prolyl hydroxylases cannot hydroxylate HIF-1α, and therefore HIF-1α enters the nucleus and binds to HIF-1β. HIF-1 binds to co-activators p300/CBP and transcribes HIF-1 target genes through binding to HRE sequences. Figure made on BioRender.

In addition to HIF-1α and HIF-2α, HIF-3α is a third transcriptional regulator that also binds to HIF-1β in the hypoxic response. HIF-3α binds to HIF-1β and forms a non-functional transcription factor that can act as a means of negatively regulating HIF-1α and HIF-2α signalling, however, the eight HIF-3α variants need to be better characterised for increased understanding of this role (Duan, 2016, Makino et al., 2007).

Cancer hallmark associated HIF target genes promote angiogenesis, altered bioenergetics and metastasis. HIF acts to induce the expression of a large number of pro-angiogenic factors, including VEGF; the VEGF receptors FLK-1 and FLT-1; matrix metalloproteinases MMP-2 and MMP-9; angiopoietins; and, platelet-derived growth factor B. Of these factors VEGF-A is the most widely upregulated, as reported in many human tumours (Hickey and Simon, 2006, Lv et al., 2017). HIF, specifically HIF-1α, plays a key role in the switch from oxidative phosphorylation to anaerobic glycolysis in tumours. This is achieved through increasing the expression of glucose transporters Glut1 and Glut3, as well as glycolytic enzymes such as lactate dehydrogenase A (LDHA), hexokinases (HK1 and HK2) and phosphoglycerate kinase 1 (Haider et al., 2016).

HIF can directly influence multiple steps within the metastatic cascade, from migration to extravasation as well as establishing the premetastatic niche and promoting cell survival and growth at the secondary site. In the early stages of metastasis, HIF directly activates key EMT genes such as *SNAI1*, *ZEB1* and *TWIST1* (Luo et al., 2011, Yang et al., 2008). Additionally, HIF indirectly promotes EMT through several cell signalling pathways, including TGF-β, Wnt, Notch, and Hedgehog (Rankin et al., 2014, Copple, 2010, Sahlgren et al., 2008, Spivak-Kroizman et al., 2013, Zhang et al., 2015). In the late stages of metastasis, disseminated tumour cells colonise distant tissues/organs. *In vivo* murine experiments have shown that a tumour-promoting pre-metastatic niche in these secondary sites is required for the extravasation and colonisation of metastatic tumour cells (Kaplan et al., 2005). HIF signalling in primary tumour cells promotes the production of secreted factors that aid in the formation of the premetastatic niche (Rankin and Giaccia, 2016). For example, HIF induces an increased expression and consequent secretion of lysyl oxidase (LOX) in breast cancer cells. The collagen

matrix of the lung is modified by LOX and consequent recruitment of bone marrow derived cells occurs that prepare the lung for breast metastatic colonisation (Wong et al., 2011).

Hypoxia within the tumour microenvironment is highly heterogenous and the percentage of oxygen associated with tumour hypoxia is within the range of 0% O_2 to 6% O_2 (Bader et al., 2020, Vaupel et al., 1989, Vaupel et al., 2002). Hypoxia occurs in two different states: chronic or acute (Figure 1.3.2). Chronic hypoxia is diffusion limited. This leads to a gradient in oxygen tension within a tumour as the distance from blood vessels increase. Mild hypoxia (between 3% O_2 and <0.5% O_2) and severe hypoxia (<0.1% O_2) are used to define differing degrees of chronic hypoxia (Hompland et al., 2021). Acute hypoxia is perfusion limited. It occurs when the malformed vasculature of the tumour microenvironment results in temporary closing and opening of blood vessels. Therefore, temporal pO_2 fluctuations around 1.3% O_2 occur (Dewhirst, 2009). Acute hypoxia is transient and dynamic; it is also termed cyclic hypoxia (Bader et al., 2020). These varying definitions and distinctions within tumour hypoxia are required as cancer cells are impacted in a profoundly different manner at different oxygen concentrations. Generally, 200 μm is the furthest distance from the vasculature where cells are able to survive before becoming necrotic (Wijffels et al., 2000). Mild, severe and cyclic hypoxia shall now be discussed in greater detail.

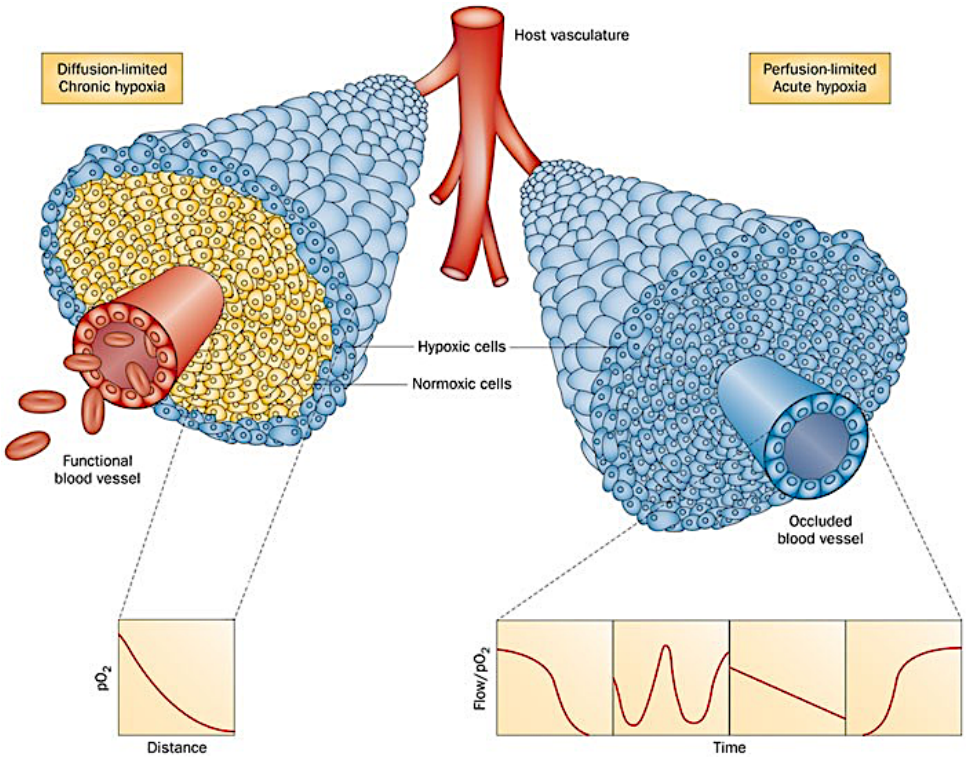


Figure 1.3.2: Chronic versus acute hypoxia. Chronic hypoxia (left) is diffusion limited, cells further away from the blood vessel experience a decrease in pO_2. Acute hypoxia (right) is perfusion limited. Tumours have malformed vasculature in which vessels can undergo transient occlusion. Consequent changes in pO_2 depend on the occlusion, but overall may consist of rapid decreases, recovery and fluctuations in pO_2. This figure was reproduced from (Horsman et al., 2012). Permission date: 02 August 2021

1.4. Mild hypoxia

Mild hypoxia refers to regions within the tumour that experience a state of chronic hypoxia at an oxygen concentration between 3% O_2 and <0.5% O_2 (Hompland et al., 2021). As expected, in mild hypoxia HIF-induced transcription of genes due to HIF-α subunit stabilisation is seen. Mild hypoxia also acts to induce changes in chromatin conformation to affect transcriptional activity. For example, the expression of histone lysine demethylates are

increased by HIF-1α. Some of these demethylases act to augment gene transcription through demethylation of H3K27 or H3K9, whereas other demethylases repress transcription through the demethylation of activating marks H3K4me2 and H3K4me3 sites (Salminen et al., 2016). Aside from transcriptional changes, cells experiencing mild hypoxia slow down protein synthesis. This is hypothesised to be as a means to conserve energy before oxygen is metabolically limiting (Hompland et al., 2021). For example, cap-dependent mRNA translation is supressed through the inhibition of eEF2 and mTOR signalling at 1.5% O_2 (Liu et al., 2006). The means by which cells alternatively synthesise proteins for the newly transcribed hypoxia responsive genes is still under investigation (Chee et al., 2019). In addition to slowing down protein synthesis, a metabolic shift from oxidative phosphorylation to anaerobic glycolysis is favoured in mildly hypoxic cells. Nonetheless, oxygen is not a limiting factor of oxidative phosphorylation until severe hypoxia (Wilson et al., 1988). The increase in glycolytic activity seen in mild hypoxia also acts to inadvertently promote cell proliferation through playing a role in apoptosis resistance, converse to severe hypoxia whereby growth arrest is induced (Gwak et al., 2005).

1.5. Severe hypoxia

We define severe hypoxia as <0.1% O_2. As seen in mild hypoxia, severe hypoxia has HIF-induced transcription of genes and a shift in metabolism to anaerobic glycolysis. In contrast to mild hypoxia, there are distinct differences in the biological response of cancer cells to <0.1% O_2.

The DNA damage response (DDR) is induced at <0.1% O_2. The DDR is a signalling pathway, which is initiated by sensors of DNA damage followed by a cellular signalling cascade to promote repair, cell cycle arrest or in extreme cases, cell death. The DDR is controlled by three apical kinases: DNA-phosphokinases (DNA-PKcs), ataxia telangiectasia mutated (ATM) and ataxia telangiectasia and Rad3 related (ATR) (Blackford and Jackson, 2017). These DDR kinases have numerous targets, many of which are overlapping, including p53. Severe hypoxia results in a p53 accumulation that can result in p53-mediated apoptosis (Hammond et al., 2002, Leszczynska et al., 2015). As a result of this p53-induced apoptosis in severe hypoxia, a selection pressure occurs in which subpopulations arise from cells with a diminished potential to undergo apoptosis (Graeber et al., 1996).

In severe hypoxia, stalled replication forks and consequent replication stress is observed, which can be attributed to decreased nucleotide availability (Pires et al., 2010b). Regions of replication protein A (RPA) coated single stranded DNA (ssDNA) accumulate when DNA replication forks stall. Notably, DNA damage has not been observed in severe hypoxia, highlighted by a lack of detectable double stranded breaks (DSBs) and single stranded breaks (SSBs) (Olcina et al., 2013). ATR mediated signalling is induced in severe hypoxia, including the phosphorylation of p53 (S15), CHK1 (S345), H2AX (S139) and RPA (the phosphorylation of which occurs at multiple sites) (Hammond et al., 2014, Pires et al., 2012, Pires et al., 2010a). ATM is also activated in hypoxia, despite the lack of DSBs, and is dependent on a heterochromatin-like context including increased levels of H3K9me3 and replication stress (Bencokova et al., 2009, Olcina et al., 2013, Olcina et al., 2016). The ability of hypoxic cells to experience replication stress but not accumulate DNA damage suggests a level of sustained DNA replication. Deoxyribonucleotide triphosphate (dNTP) *de novo* synthesis is carried out by

the ribonucleotide reductase (RNR) enzyme. In normoxic conditions, RNR is composed of homodimeric subunits RRM1/RRM2. However, in severe hypoxia the activity of this enzyme is lost due to the oxygen-dependency of RRM2. Consequently, hypoxic cells compensate for this through favouring the alternative subunit, RRM2B and forming the RRM1/RRM2B conformation of RNR. In severe hypoxia, the RRM1/RRM2B conformation remains catalytically active for longer. Sufficient dNTP pools can therefore be maintained in severe hypoxia due to this RNR conformational switch and hence, DNA damage can be prevented (Foskolou et al., 2017). In addition to replication stress, global repression of RNA synthesis, termed transcriptional stress, has also been identified to promote the DDR in severe hypoxia (Johnson et al., 2008). Alongside this DDR in the apparent absence of detectable DNA damage, DNA repair proteins are suppressed. For example, the inhibition of MLH1, MSH2 and MSH6 occurs and this leads to mismatch repair deficiency (Koshiji et al., 2005, Mihaylova et al., 2003, Bindra and Glazer, 2007). Additionally, the RNA expression of HR-related genes such as *RAD51*, *BRCA1* and *BRCA2* and the genes encoding other NHEJ related proteins such as Ku70, XRCC4 and DNA-PKCs are decreased (Kumareswaran et al., 2012).

In addition to induction of the DDR, the unfolded protein response (UPR) is also induced in severe hypoxia. The UPR is an endoplasmic reticulum stress response pathway that is activated by the detection of misfolded proteins and subsequently acts to maintain protein homeostasis. Disulphide bonds are present in many secreted proteins and membrane proteins. The formation of disulphide bonds is oxygen-dependent, and requires protein disulfide isomerase (PDI), which is a soluble thiol-disulfide oxireductase as well as the endoplasmic reticulum oxidoreductin, Ero1 (Bartoszewska and Collawn, 2020, Bolland et al., 2021). Due to the lack of oxygen in severe hypoxia, and hence the inability to form disulphide

bonds, there is an accumulation of misfolded proteins in the lumen of the endoplasmic reticulum causing the induction of the UPR (Koritzinsky et al., 2013). Once activated, the UPR inhibits protein synthesis, increases the protein folding capacity and upregulates UPR genes involved in redox homeostasis, protein folding and protein degradation (Bartoszewska and Collawn, 2020). Interestingly, the UPR and DDR are active in response to the same levels of hypoxia, prompting the question are these two responses linked? Despite few discovered links, one reported link is senataxin (SETX). SETX is an DNA/RNA helicase that is induced by the UPR. SETX has been shown to play a role in protecting cells from DNA damage that is induced during transcription, likely through its role in R-loop resolution (Ramachandran et al., 2021).

Severe hypoxia has also been defined as radiobiological hypoxia. Radiotherapy kills cells by inducing DNA damage, including DNA DSBs. In the presence of oxygen, radiation creates free radicals that are oxidised to form peroxyl radicals that cause fixed DNA damage. Consequently, a lack of oxygen decreases the damage induced in irradiated cells, promoting their survival (Brown and Wilson, 2004, Hammond et al., 2014). Despite being controversial (Ewing, 1998), this is coined the oxygen fixation hypothesis and well-oxygenated cells respond to therapy three times better than severe hypoxic cells (Gray et al., 1953). The oxygen fixation hypothesis is not unique to conventional radiotherapy, it also occurs in ultra-high dose radiotherapy, FLASH (Adrian et al., 2020). In FLASH, greater than 40 Gy/s are delivered compared to around 0.03 Gy/s in conventional (Conv) radiotherapy (Cao et al., 2021). FLASH is a highly promising clinical therapy due to its ability to ‘spare’ normal, healthy cells from the radiotherapy effect, while killing the cancer cells to the same extent as conventional radiotherapy. One explanation that has been proposed for this sparing effect is the oxygen

depletion hypothesis in which high doses of FLASH deplete oxygen within the cell during the ultra-short time of dose administration by inducing radical interaction. The irradiation time is too short for diffusion and reoxygenation of oxygen back into the cells, therefore, a radioresistant hypoxic phenotype is induced in normal cells (Figure 1.5) (Cao et al., 2021, Han et al., 2021, Adrian et al., 2020)

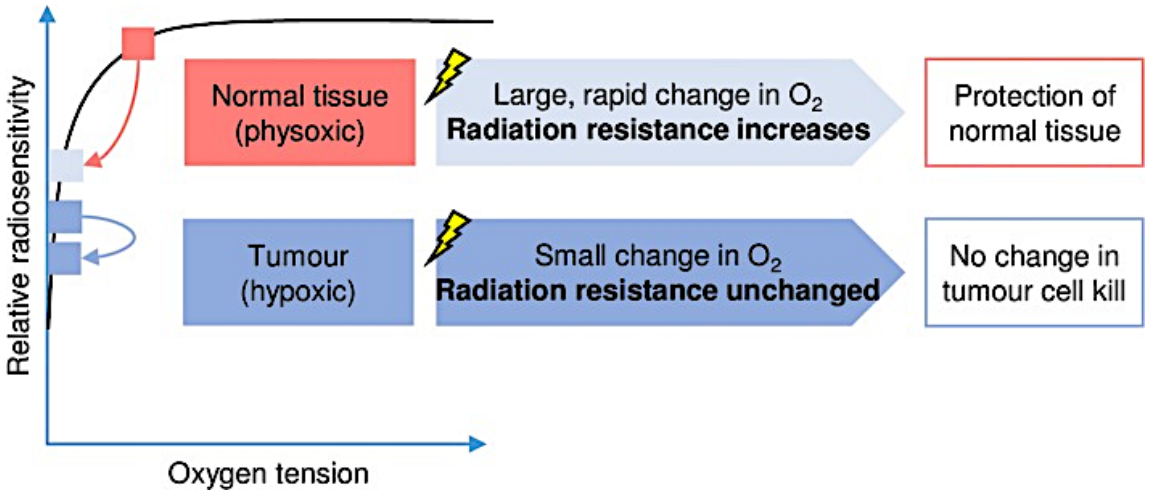


Figure 1.5: The oxygen depletion hypothesis for FLASH radiotherapy. The relationship between relative radiosensitivity and oxygen tension in normal tissue compared to tumour tissue subjected to FLASH radiotherapy. Normal cells are protected as a result of the oxygen depletion hypothesis. Reproduced from (Wilson et al., 2019), University of Oxford.

Severe hypoxia also leads to chemotherapy and immunotherapy resistance. Chemoresistance occurs in severely hypoxic tumours largely as a result of the perfusion and diffusion limitations of anti-cancer drugs in reaching the hypoxic tumour cells due to distance from the blood vessels (Mistry et al., 2017, Tannock et al., 2002). Additionally, cells can undergo hypoxia-induced reversible quiescence, therefore antiproliferative chemotherapeutic agents are unable to target these cancer cells effectively (Leontieva et al., 2012, Mistry et al., 2017). Finally, immunotherapy is also less effective in hypoxia. The shift of hypoxic tumour cell

metabolism to anaerobic glycolysis results in the overproduction of adenosine which is released into the extracellular matrix of the tumour microenvironment. A combination of this extracellular adenosine, which acts to suppress T cells, as well as the inhibitory effect of HIF-1α on the adaptive immune system dampen the immunotherapeutic response (Graham and Unger, 2018, Panther et al., 2003).

1.6. Cyclic hypoxia

As already described, the mild and severe hypoxic conditions are both chronic hypoxia. Cyclic hypoxia refers to a transient, fluctuating pO_2 environment. The dynamics of cyclic hypoxia are akin to tides and waves (Bader et al., 2020). Slow fluctuations, the tides, occur over a period of hours to days whereas the quicker fluctuations, the waves, occur between two to five times an hour (Braun et al., 1999, Ellingsen et al., 2012). Cyclic hypoxia was first described in 1979 (Yamaura and Matsuzawa, 1979). Yamaura and Matsuzawa saw transient vascular stasis on the periphery of a window chamber tumour that resulted in temporary radioresistance. It was concluded that variations in red blood cell flux and haemoglobin saturation are key factors that are responsible for the transience of cyclic hypoxia. Previous studies also support a role for thermoregulation in the short fluctuations seen in cyclic hypoxia (Dewhirst et al., 1996, Dewhirst et al., 1999, Gonçalves et al., 2015).

A wealth of murine *in vivo* imaging shows that in solid tumours cyclic hypoxia is commonplace (Matsumoto et al., 2010, O'Connor et al., 2019, Ron et al., 2019, Yasui et al., 2010). However, due to *in vitro* limitations, the majority of hypoxic studies have focused upon static conditions and those which are cyclic studies use ambient oxygen levels (21% O_2) as the oxygenation

portion of the cycling hypoxia schedule. Very few studies have fluctuated between physiologically relevant oxygen concentrations (Bader et al., 2020). Despite cyclic hypoxia being less well characterised than severe and mild hypoxia, *in vivo* studies suggest it results in a more aggressive form of disease. For example, cyclic hypoxia has been characterised to cause more aggressive metastases. Through the use of regulated gas supplies, *in vivo* mice studies have shown that subjects exposed to cyclic oxygen develop more metastases than those mice subjected to ambient oxygen (Chen et al., 2018, Daneau et al., 2010, Li et al., 2018, Rofstad et al., 2010). Cyclic hypoxia exposed cells have also shown an increased ability to efflux Rh123, a chemotherapeutic agent, compared to chronic hypoxic cells in an ABCB1-depedent manner (Hsieh et al., 2011). In addition to chemotherapy resistance, enhanced radioresistance has been seen in cells subjected to cyclic hypoxia comparative to chronic hypoxia (Hsieh et al., 2010, Martinive et al., 2006, Liu et al., 2010, Hlouschek et al., 2018b, Hlouschek et al., 2018a).

There are several other biological characterisations of cyclic hypoxia. For example, a recent study from our laboratory found that cyclic hypoxia was required to induce APOBEC3B expression and activity (Bader et al., 2021). Specifically, our laboratory found that sustained DNA replication under cyclic hypoxia led to a phenomenon termed replication catastrophe. Replication catastrophe is characterised by the presence of replication stress (stalled DNA replication forks) and an accumulation S-phase specific DNA damage (Toledo et al., 2013). Replication catastrophe leads to the induction of APOBEC3B expression and activity. Replication catastrophe and APBOBEC3B induction were not seen in chronic hypoxia (Bader et al., 2021). Similar to severe hypoxia, p53 induction is seen in cyclic hypoxia. In contrast to severe hypoxia in which a G1 accumulation is seen, cyclic hypoxia was shown to lead to an S-

phase accumulation (Bader et al., 2021). Additionally, the induction of reactive oxygen species (ROS) is reported to be greater in cyclic hypoxia compared to chronic hypoxia (Chen et al., 2015). This is supported by an increase in the mRNA and protein levels of NADPH oxidase 4, a major source of oxidative stress, in cyclic comparative to chronic hypoxia (Hsieh et al., 2011, Hsieh et al., 2012).

1.7. Breast cancer

Breast cancer is the leading cancer type that affects women, and although rare, also men. Breast cancer is a disease of the mammary epithelial cells, which acquire the ability to grow atypically while confined to the mammary ducts or lobules (non-invasive breast cancer). The confinement of these malignant cells to the breast ducts or lobules is an important factor to limit breast cancer progression, and if the cancer is found localised there is a 98% chance of no recurrence within 5 years (Howlader et al., 2011). Conversely, breast cancer prognosis significantly decreases in the event of invasive breast cancer, whereby cells metastasise beyond the ducto-lobular mesh into the surrounding stroma and/or beyond, through the blood and lymphatic systems to distant tissues/organs (Winters et al., 2017). A breast cancer diagnosis with already present metastasis results in a prognosis of 23% patient survival beyond 5 years following diagnosis (Howlader et al., 2011).

There are many risk factors for breast cancer; these vary from reproduction, hormonal intake and obesity to genetic mutations. Mutations of the genes *BRCA1* or *BRCA2*, which are located on chromosome 17q and chromosome 13q respectively, are causes of predisposition to breast, pancreatic, ovarian, as well as other cancers. BRCA1 and BRCA2 proteins play a key

role in the repair of DSBs (Moynahan et al., 2001). Most of the mutations in the *BRCA1* and *BRCA2* genes are insertions or deletions that lead to the translation of a truncated protein (Mavaddat et al., 2010, Winters et al., 2017). These mutations account for 20% of familial breast cancer cases (Turnbull and Rahman, 2008). Other relevant genetic mutations include single nucleotide polymorphisms of the genes *XRCC2* and *XRCC3*, which encode proteins involved in homologous recombination (Silva et al., 2010, Zhang et al., 2011). The risk of breast cancer can be increased by other high-penetrance mutations including *TP53* mutations, *PTEN* mutations, and *STK1* mutations (Mavaddat et al., 2010)

Breast cancer is highly heterogenous. It is clinically divided into three main subtypes by HER2 status and hormone receptor (oestrogen receptor (ER) and progesterone receptor (PR)). In addition, the nuclear antigen Ki67 is associated with cell proliferation and is a molecular marker of the breast cancer cell proliferation index. Ki67 expression is used in the classification determination between the Luminal A and Luminal B breast cancer subtypes (Gnant et al., 2015). The classifications are as follows (Table 1.7):

Table 1.7: Breast cancer classification based on ER, PR and HER2 status with Ki67 as an additional determinant for Luminal A and Luminal B.

	Luminal		**HER2 Positive**	**TNBC**
	Luminal A*	**Luminal B**		
ER	+/-	+/-	-	-
PR	+/-	+/-	-	-
HER2	-	+	+	-
Ki67	<14%	≥ 14%		

* Luminal A must have either ER + or PR + both cannot be negative

Most patients, irrelevant of breast cancer classification, begin their treatment course with locoregional therapy. This consists of either breast conserving therapy (removal of the tumour alone) or mastectomy (Loibl et al., 2021, Moo et al., 2018). Following tumour resection, postoperative adjuvant radiotherapy to eliminate the remaining tumour deposits occurs and is associated with a significant decrease in locoregional recurrence risk (O'Rorke et al., 2016, Bhoo-Pathy et al., 2015). Patients may also receive targeted therapies and/or chemotherapy specific to their classification of breast cancer. Endocrine therapy alongside a chemotherapeutic adjuvant is recommended for most patients with hormone receptor positive disease. Examples of endocrine therapy drugs include tamoxifen, which is most commonly used for premenopausal women, and aromatase inhibitors, most commonly used for postmenopausal woman (Kharb et al., 2020, Moo et al., 2018). HER2 positive breast cancers can be treated with HER2 targeted therapies and a chemotherapeutic adjuvant. An example of a HER2 targeted therapy is the monoclonal antibody trastuzumab, which is targeted against the HER2 receptor (Slamon et al., 2001, Loibl and Gianni, 2017). TNBC constitute 15% of overall breast cancer cases. Due to their negative ER, PR and HER2 status they do not benefit from endocrine or HER2 targeted therapies, hence the important role of adjuvant radiotherapy in TNBC patients (Bhoo-Pathy et al., 2015, He et al., 2018, O'Rorke et al., 2016). Novel therapies for TNBC have been proposed. For example, bromodomain and extra-terminal (BET) proteins are epigenetic readers that recognise and bind to acetylated lysine residues on chromatin and recruit transcription factors and epigenetic regulators. A BET inhibitor, JQ1, has been identified to impair the TNBC hypoxia mediated response driving tumour aggression (da Motta et al., 2017).

Hypoxia is associated with poor treatment response and aggressive disease in breast cancer patients. This association is particularly evident in the breast cancers which are triple negative. Of all the breast cancer subtypes, TNBC results in the worst patient prognosis, with patients often succumbing to brain, bone or lung metastases (Chen et al., 2014, Schwab et al., 2012, Bernardi and Gianni, 2014, Tan et al., 2009). As already mentioned, cyclic hypoxia is associated with a more aggressive cancer phenotype (Daneau et al., 2010, Li et al., 2018, Matsumoto et al., 2010, O'Connor et al., 2019, Rofstad et al., 2007, Ron et al., 2019, Yasui et al., 2010). Therefore, it is important to better understand and characterise the response of breast cancer, specifically TNBC, to cyclic hypoxia.

1.8. Aims of this project

As already discussed, hypoxia is associated with poor treatment response and aggressive disease in people with breast cancer, specifically TNBC (Chen et al., 2014). As cyclic hypoxia has been linked with the most aggressive forms of disease and metastasis there is a need to characterise the response of TNBC to cyclic hypoxia. The Hammond laboratory has recently developed a physiologically relevant *in vitro* cyclic hypoxia protocol using a variable atmosphere workstation in which the oxygen concentration fluctuates between <0.1% O_2 and 2% O_2 every two hours, as recently published in Bader et al. (2021) (Figure 1.8). The choice of the cyclic parameters is supported by the magnitude and periodicity of oxygen fluctuations in mouse xenograft tumours (Matsumoto et al., 2010). Using this cyclic hypoxia workstation, the two main aims of my project are as follows:

- To investigate differences in the biological response to cyclic hypoxia versus chronic hypoxia at both static 2% O_2 and <0.1% O_2. This will include an RNA-sequencing analysis.
- Determine the response of cyclic hypoxia exposed TNBC cells to DNA-damaging therapies, utilising radiotherapy

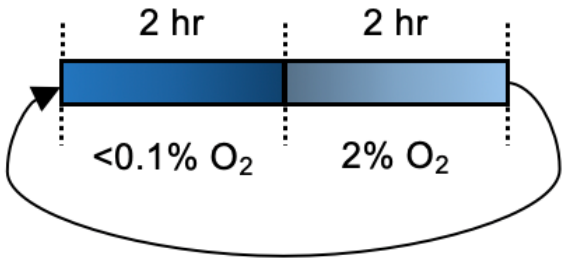


Figure 1.8: Cyclic hypoxia protocol Reproduced from (Bader et al., 2021), University of Oxford.

Overall, we hypothesised that the TNBC cells will respond differently to cyclic compared both static 2% O_2 and <0.1% O_2 and consequently will lead to different therapy responses.

CHAPTER 2: MATERIALS AND METHODS

2.1. Solutions and Reagents

2.1.1 Primary Antibodies

Name	Species	Dilution	Company	Catalogue Number	Application
β-Actin	mouse	1:10000	Santa Cruz	sc-69879	WB
HIF-1α	mouse	1:500	BD Biosciences	610958	WB
KAP1	rabbit	1:1000	Bethyl	A300-274A	WB
KAP1-S824	rabbit	1:2000	Bethyl	A300-767A	WB
RPA32	rat	1:2000	Cell Signaling	2208	WB
GRP78	mouse	1:1000	BD Biosciences	610978	WB
BrdU	mouse	1:50	BD Biosciences	347580	FACS

2.1.2 Secondary antibodies

Name	Species	Dilution	Company	Catalogue Number	Application
IRDye 800CW donkey anti-mouse IgG	mouse	1:10000	LI-COR	926-32212	WB
IRDye 680RD donkey anti-mouse IgG	mouse	1:10000	LI-COR	926-68072	WB
IRDye 800CW donkey anti-rabbit IgG	rabbit	1:10000	LI-COR	926-32213	WB
IRDye 680RD donkey anti-rabbit IgG	rabbit	1:10000	LI-COR	926-68073	WB
IRDye 800CW goat anti-rat IgG	rat	1:10000	LI-COR	926-32219	WB
Alexa Fluor 488-conjugated goat anti-mouse IgG	mouse	1:200	Invitrogen	A-11001	FACS

2.1.3 Buffers

Running buffer (10X): 25 mM Tris base, 192 mM glycine and 0.1% sodium dodecyl sulphate (SDS). Buffer is diluted to 1X with dH_2O for use.

Transfer buffer (10X): 25 mM Tris base, 192 mM glycine and 20% methanol. Buffer is diluted to 1X with dH_2O for use.

2X Laemmli buffer: 120 mM Tris-HCl pH 6.8, 20% glycerol, 10% SDS, 10% β-mercaptoethanol, and 0.01% Bromophenol blue.

UTB lysis buffer: 9 M Urea and 75 mM Tris-HCl pH 7.5. Supplemented with 0.15 M β-mercaptoethanol prior to use.

Tris buffered saline with Tween-20 (TBS-T) buffer (10X): 500 mM Tris base and 1.5 M NaCl. Make up solution to pH 7.6 and autoclave. Buffer is diluted to 1X with dH_2O for use and supplemented with 0.1% Tween-20.

Phosphate buffered saline (PBS) buffer: 1X of PBS was prepared through dissolving a singular PBS tablet (Oxoid) in 100 mL of dH_2O.

2.2. Cell lines and cell culture

2.2.1 Cell lines and specifications

Breast Cancer Cell Line	Tissue	ER status	PR status	HER2 status	Origin	Culture
MDA-MB-231	Breast	-	-	-	Prof. Humphrey, University of Oxford	DMEM
MCF-7	Breast	+	+	-	Prof. Humphrey, University of Oxford	DMEM
CAL51	Breast	-	-	-	Dr Parkes, University of Oxford	DMEM
MDA-MB-468	Breast	-	-	-	ATCC	DMEM
MDA-MB-436	Breast	-	-	-	Prof. Tarsounas, University of Oxford	RPMI
Other cell lines	**Tissue**				**Origin**	**Culture**
PSN1	Pancreatic adenocarcinoma				ATCC	DMEM

2.2.2 Culture Conditions

All cell lines were maintained in a 5% CO_2 humidified incubator at 37°C. Cells were passaged at 80% confluency. They were washed with 1x PBS and were then trypsinised with Trypsin-EDTA (Sigma-Aldrich). Trypsinised cells were then resuspended in Dulbecco's Modified Eagle's Medium (DMEM; Sigma-Aldrich) supplemented with 10% Foetal Bovine serum (FBS; Sigma-Aldrich) and split into a new culture flask (Corning) at the required flask size and cell density.

2.2.3 Mycoplasma testing

Cells were grown in media without antibiotics and harvested when 90% confluent. Cells were harvested and heated for 15 minutes at 100°C before resuspending 50 μL of the cell suspension in 200 μL of HEK Blue cell in HEK Blue detection medium (Invivogen). The resuspended cells were placed back in the incubator under normal tissue culture conditions

and observed over 24 h for a colour change. The colour blue indicated the presence of mycoplasma, the pink media colour was a negative result.

2.2.4 Cryopreservation

Confluent cells were trypsinised and centrifuged at 300 g for 5 min in complete media. The obtained pellet was then resuspended in a freezing mixture composed of 90% FBS and 10% dimethyl sulfoxide (DMSO) and aliquoted into cryovials (Thermo Fisher Scientific) at a concentration of ~2 x 10^6 cells/mL. The cryovials were stored at -80°C in Mr. Frosty (Nalgene), which contained 2-propanol, before later being transferred to liquid nitrogen.

2.2.5 Thawing

Cryovials of frozen cells were thawed quickly in a 37°C water bath. Cells were then resuspended in 5 mL of complete media and centrifuged for 5 min at 300 g. The pellets obtained were resuspended in complete media before being transferred to a T25 flask and maintained at 37°C in a 5% CO_2 humidified incubator.

2.3. Hypoxia treatment

A Bactron II anaerobic chamber (Shel Labs) was used for hypoxic treatment at <0.1% O_2. Hypoxia treatments were carried out in a Whitley M35 Workstation (Don Whitley Scientific) for treatment at 2% O_2 or cycling hypoxia. This chamber has the ability to provide oxygen concentrations of <0.1% to 21% and can fluctuate between concentrations on the timescale

of hours, as seen in a representative readout of the oxygen concentration over the course of a cyclic hypoxia experiment between <0.1% O_2 and 2% O_2 (Figure 2.3).

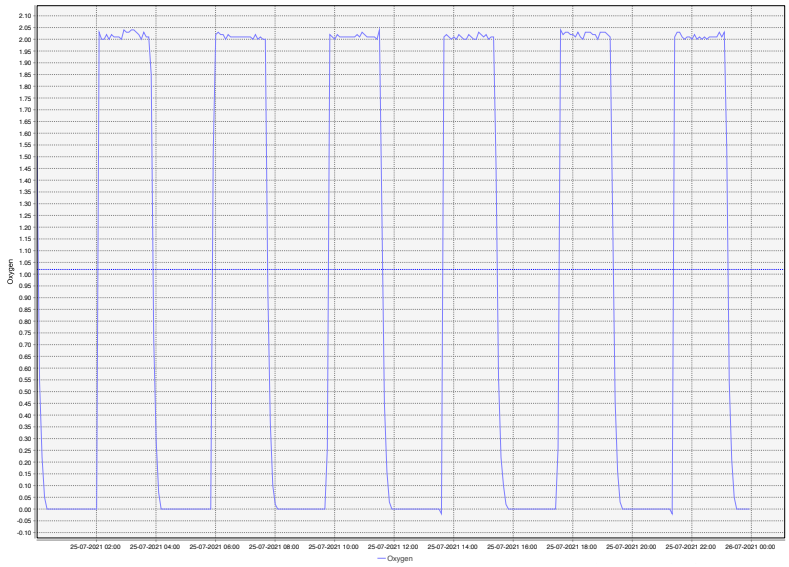


Figure 2.3: Cyclic hypoxia oxygen readout. A representative readout of the oxygen concentration over the course of a cyclic hypoxia experiment between <0.1% O_2 and 2% O_2. Measurement taken from the oxygen probe in the Don Whitley M35 Workstation.

2.4. Irradiation

For Caesium (Cs) irradiation, cells were irradiated at the stated dose (Gy) with a Gamma-Service Medical GmbHGSR D1 irradiator at a rate of 1.5 Gy/min. For FLASH radiotherapy, cells were irradiated with a FLASH-RT linac that could switch between conventional and FLASH radiotherapy. Radiation boxes were used to irradiate cells under hypoxic conditions. These boxes have airtight seals and have been used previously to deliver radiation in hypoxic conditions (Anbalagan et al., 2015) (Figure 2.4).

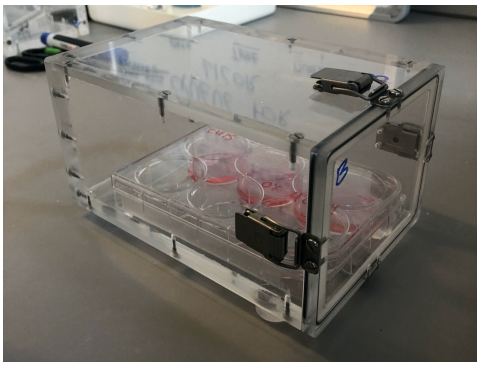


Figure 2.4: Radiation box. Image of a radiation box used to maintain hypoxia while irradiating cells with the Cs irradiator. Boxes are placed into the hypoxic chamber prior to use to ensure equilibration. Normoxic controls were also placed in a box during irradiation.

2.5. Laboratory techniques

2.5.1 Colony Survival Assay

The colony survival assay followed the protocol of Franken et al. (2006) (Franken et al., 2006). The plating efficiency of cell lines was determined such that at least 100 colonies were obtained per well in the control plates. The plating efficiency is the (number of colonies obtained) / (number of cells seeded in the untreated control). The seeded cells were allowed to adhere under normal cell culture conditions for a short period of time before treatment. Post-treatment the colonies were allowed to form untouched under normal cell culture conditions. After 10 days the colonies were stained with crystal violet (0.5% w/v) in 20% ethanol and 50% methanol. A colony was defined to have at least 50 cells. Colonies were counted using a colony counter and finally, the survival fraction was calculated. Survival

fraction is [(number of colonies formed after treatment) / (number of cells seeded x plating efficiency)] x 100. In one repeat, cells were seeded in three wells of a six well plate, and repeated n=3.

Table 2.5.1: The seeding densities and plating efficiencies of the human carcinoma cell lines used for clonogenic assays

Cell Line	Seeding density of cells		Plating efficiency (%)
CAL51	150	6-well plate	66.6
MDA-MB-231	600	6-well plate	15

2.5.2 Cell Lysis

Cells were lysed in UTB. The lysed cells were then sonicated, centrifuged for 10 minutes at 4°C, 12000 g and the supernatant collected. The protein concentration of the supernatant was measured using a Nanodrop One (Thermo Fisher Scientific).

2.5.3 Western Blotting

Protein samples were dissolved in 2X Laemmli buffer supplemented with 0.15 M β-mercaptoethanol and then boiled at 97°C for 10 minutes. The samples were allowed to cool before being loaded onto a pre-cast 4-20% gradient gel (BioRad). The gels were run with 1X running buffer at 100 V. The proteins were then transferred onto a nitrocellulose membrane via the Transfer-Blot Turbo Transfer System (BioRad). The nitrocellulose membrane was blocked with 1:1 TBS and Intercept blocking buffer (LI-COR). Membranes were incubated with their respective primary antibody at 4°C overnight. Membranes were then washed 3x with TBS-T and incubated for 1 hour with their respective secondary antibody at room temperature. The primary and secondary antibodies were made up in the blocking buffer

solution, mentioned above. Membranes were washed again with 3x TBS-T before being imaged by the Odyssey Infrared Imaging Systems (LI-COR). Protein quantification was carried out with ImageJ software.

2.5.4 3-(4,5-dimethylthiazol-2-yl)-2,5-diphenyl-2H-tetrazolium bromide (MTT) assay

A 5 mg/mL stock solution of MTT was made in PBS and filtered through a 0.22 μM Millipore® filter. The stock was stored at 4°C protected from light for a maximum of 4 weeks. Cells were plated in 100 μL of cell line-specific media on a 96 well plate and allowed to settle overnight before being treated as desired. Following treatment, 10 μL of MTT reagent was added to each well and incubated at 37°C for 3 h protected from light. If the treatment involved hypoxia, the MTT incubation was carried out in the chamber. After 3 h, the MTT-containing media was removed and replaced with 100 μL DMSO per well to solubilise crystals. The plate was then incubated for a further 15 min at 37°C protected from light before immediately being read using the MTT programme on the POLARstar Omega plate reader (BMG Labtech) with an absorbance of 570 nm.

2.5.5 RNA extraction and purification

Cells were washed with 2 mL of PBS and then scraped into 1 mL of Trizol (Invitrogen) and stored until RNA extraction at -20°C. For RNA extraction, samples were thawed and 200 μL of chloroform was added, samples were vortexed for 15 s and incubated at room temperature for 2 min before centrifugation at 16200 g for 15 min at 4°C. The supernatant was transferred to a fresh tube and 500 μL of isopropanol was added. The samples were thoroughly mixed by shaking before centrifugation at 16200 g for 10 min at 4°C. The pellet was kept and

resuspended in 1 mL 70% ethanol, then vortexed and centrifuged at 7500 g for 5 min at 4°C. As much supernatant was removed as possible and the residual ethanol on the pellet was left to air dry for approximately 20 min. Once dry, the pellet was resuspended in 60 μL diethylpyrocarbonate (DEPC) water (Thermo Fisher Scientific) and the RNA concentration was measured using the Nanodrop 1000 (Thermo Fisher Scientific). Following this, the samples underwent DNase I treatment to degrade any residual DNA. DNase I (NEB) and DNase I reaction buffer (NEB) were mixed with 10 μg of RNA and then incubated at 37°C for 20 min. The DNase I was then neutralised through adding 1 μL of 0.5 M EDTA before a 10 min incubation at 75°C.

Following the RNA extraction and purification total RNA samples were sent to Novogene for RNA sequencing. The project workflow started with sample quality control to ensure that the samples met the criteria of the RNA-Seq technique. Then, the cDNA library was prepared before an Illumina sequencing was carried out (paired-end 150 base pair, 35 million reads).

2.5.6 cDNA library creation

The Verso enzyme kit (Thermo Fisher Scientific) was used to reverse transcribe RNA into cDNA. The reaction master mix was made up of 5X cDNA synthesis buffer, RNA primer, dNTP mix, RT enhancer, verso enzyme and DEPC water. The RNA sample (1 μg) was combined with the master mix, vortexed and then briefly spun down to ensure even mixing of reagents. cDNA was then generated through placing the samples in a polymerase chain reaction (PCR) machine (Applied Biosystems) with the following schedule: 60 min at 42°C, 2 min at 95°C and then 4°C. Samples were then stored at -20°C until further use.

2.5.7 qPCR

To begin, the cDNA was diluted 1:50 in DEPC water. Master mixes of the chosen primers (Table 2.5.7) were then made of

12.5 μL SYBR green (Applied Biosciences)

2.5 μL forward primer

2.5 μL reverse primer

2.5 μL of DEPC water.

Specifically, the *GLUT-1* master mix was composed of

12.5 μL SYBR green,

0.75 μL forward primer,

0.75 μL reverse primer and

6 μL of DEPC water.

5 μL of the diluted cDNA samples were added to 20 μL of the master mixes in a 96 well plate in which three technical replicated for each gene/primer combination were run. The plate was spun down before being run in a Step One Real-Time PCR System (Thermo Fisher Scientific) with the following schedule:

prep of 20 s at 50°C and 15 min at 95°C,

40 cycles of 15 s at 95°C,

30 s at 60°C and 30 s at 72°C and finally the melting curve of 15 s at 95°C, 1 min at 60°C, 30 s at 95°C and 15 s at 60°C. ΔΔCT was used to quantify the relative fold change of the genes of interest to the endogenous control, *18-S.*

Table 2.5.7: qPCR primers

Gene	Forward/Reverse Sequence	Sequence	Working concentration	Source
18-S	18S-F	TAGAGGGACAAGTGGCGTTC	100 μM	Sigma
	18S-R	CGGACATCTAAGGGCATCAC		
CAIX	CAIX-F	CCTTTGCCAGAGTTGACGAG	100 μM	Sigma
	CAIX-R	GCAACTGCTCATAGGCACTG		
GLUT-1	GLUT1_F1	ATACTCATGACCATCGCGCTAG	4 μM	Primer Blast
	GLUT1_R1	AAAGAAGGCCACAAAGCCAAAG		
EPHA3	EPHA3-F	ATTTTGGCAATGGGCATTTA	100 μM	Sigma
	EPHA3-R	ATGTATGTGGGTCAACATAAGTCC		

2.5.8 Fluorescence activated cell sorting (FACS)

For bromodeoxyuridine (BrdU) incorporation, 20 μM of BrdU was added to cells for an hour in the dark before cells were harvested. Cells were harvested with trypsin and resuspended in fresh media in a 15 mL Falcon tube before being centrifuged at 750 g for 5 min. The supernatant was then removed and cells were fixed in 1 mL of 70% ice-cold ethanol that was added to the pellet dropwise to prevent cell clumping. Cells were fixed for a minimum of 30 min at -20°C. Following fixation, cells were spun at 750 g for 5 min and then resuspended in 1 mL of 2 M HCl and incubated at room temperature for 20 min. After incubation, the HCl was diluted through adding 2 mL of PBS and the tubes were centrifuged again at 750 g for 5 min. The samples were then blocked in PBS containing 2% FBS before being centrifuged at 750 g for 5 min. The pellets were then resuspended in 100 μL of the BrdU primary antibody (BD biosciences), which was prepared in the PBS solution with a 1:50 dilution. The samples were incubated on a shaker overnight at 4°C. 1 mL of PBS was added to the samples following incubation and the samples were centrifuged at 1000 g for 5 min. Once again, the supernatant was removed and the pellets were resuspended in 100 μL of Alexa Fluoro 488 (Invitrogen) secondary antibody, which was diluted 1:200 in the PBS solution. Samples were incubated for

an hour at room temperature before 1 mL of PBS was added to the samples and they were centrifuged at 1000 g for 5 min. The supernatant was removed and finally the pellets were resuspended and incubated at 37°C for 15 min in propidium iodide (PI) solution composed of 1 mL PBS, 20 μL PI (Sigma Aldrich), and 5 μL RNaseA (NEB). Samples were run on a CytoFLEX machine (Beckman Coulter Life Sciences) and the software 'FlowJo' was used to analyse results.

2.5.9 Small interfering RNA gene knockdown (siRNA) transfection

Cells were transfected at 40% confluence in media without antibiotics. A singular transfection sample consisted of one well of a 6-well plate. For each well, solutions A and B were made up. Solution A was composed of 5 μL of oligofectamine reagent (Applied Biosciences) in 15 μL of Opti-MEM I Reduced Serum Media (Thermo Fisher Scientific) without serum and incubated for 10 min room temperature. Solution B was made through adding 10 μL of 20 μM siEPHA3 stock (Dharmacon) to 175 μL of Opti-MEM I Reduced Serum Media. Solutions A (post 10 min incubation) and B were combined and incubated for 20 min room temperature. Cells were seeded in a 6-well plate with 90,000 cells per well using the Opti-MEM I Reduced Serum Media. Following A and B incubation, the combined solution was added to each well with cells targeted for siEPHA3. Mock samples were also prepared alongside siEPHA3 samples, in which no A and B solutions were added to the control well. Cells were then incubated for 6 h at 37°C before changing to media to DMEM with serum. Cells were left overnight. Mock and siEPHA3 samples were collected 24 h, 48 h and 72 h following transfection through scraping the cells into Trizol. These samples were then prepared for qPCR to validate the knockdown.

2.6. Statistical analysis

All experiments are carried out with three, independent biological replicates unless indicated otherwise. Error bars show the standard error of the mean (SEM) of the three, independent biological repeats. The Wilcoxon signed-rank test was used for the comparison of two non-parametric samples. One-way analysis of variance (ANOVA) was used for the comparison of more than two means. Two-way ANOVA was used for the comparison of more than two means when two independent variables were present. For both ANOVA, statistical significance was assumed if $p<0.05$, with the following significance indicators used: * = $p<0.05$, ** = $p<0.01$, *** = $p<0.001$, **** = $p<0.0001$.

CHAPTER 3: The biological response to cyclic hypoxia

Introduction

The response to hypoxia is dependent on the exact nature of the hypoxic conditions to which the cells are exposed. The biological differences between the differing stages of chronic hypoxia, <0.1% O_2 and 2% O_2, have been previously well characterised. For example, factors such as the induction of p53, DDR and UPR and replication stress differ in mild to severe exposure to chronic hypoxia (Hammond et al., 2014, Hompland et al., 2021). Due to the limitations of fluctuating oxygen concentration *in vitro*, the biological response to cyclic hypoxia is less well characterised. Recent work from our laboratory using RKO cells shows that cycling between severe hypoxia (<0.1% O_2) and mild hypoxia (2% O_2) leads to a biological response distinct to chronic hypoxia, whether that be <0.1% O_2 or 2% O_2 (Bader et al., 2021). Due to the aggressive, metastatic nature of TNBC and the role that cyclic hypoxia plays in promoting metastasis, this section aims to characterise and better understand the biological response of TNBC to cyclic hypoxia.

We hypothesised that the responses of the TNBCs to the differing oxygen concentrations would be distinct and investigated this through protein expression analysis, cell cycle dynamic analysis and finally RNA-seq.

3.1. Cyclic hypoxia appears to induce the UPR but not the DDR

MDA-MB-231 cells were exposed to 21% O_2, static 2% O_2, static <0.1% O_2 and cyclic hypoxia. HIF-1α was used as a positive control for hypoxic conditions as it is stabilised in <0.1% O_2 and 2% O_2 and cyclic hypoxia but not 21% O_2 (Wang et al., 1995). The presence of HIF-1α confirms our workstations were truly hypoxic. We noted that the HIF-1α bands detected differ between 2% O_2, <0.1% O_2 and cyclic hypoxia. This could be indicative of post-translational modifications (PTMs), which have been reported for HIF-1α (Daly et al., 2021). The activation of the DDR was measured through the accumulation of phosphorylated KAP1 (serine 824) and RPA phosphorylation at serine 32. KAP1 phosphorylation is ATM dependent and RPA phosphorylation indicates that replication forks have stalled and hence the downstream activation of ATM and ATR has occurred and is ATR dependent (Vassin et al., 2009, Shiloh and Ziv, 2013). After 16 h the DDR was only active in <0.1% O_2 (Figure 3.1 A). This is interesting as it suggests that despite the cyclic conditions including periods of <0.1% O_2 they do not appear sufficient to activate the DDR as seen in static <0.1% O_2. Notably, RKO cells exposed to the same cyclic protocol were found to induce a DDR suggesting some cell line specificity to the response (Bader et al., 2021). GRP78 is an endoplasmic reticulum chaperone and master regulator of the UPR (Li et al., 2008). In addition to the DDR the UPR is also active in <0.1% O_2 (Bolland et al., 2021). Through the increased band intensity of GRP78 in cyclic hypoxia comparative to 21% O_2 and 2% O_2 we infer the UPR is active in cyclic hypoxia (Figure 3.1 A and B).

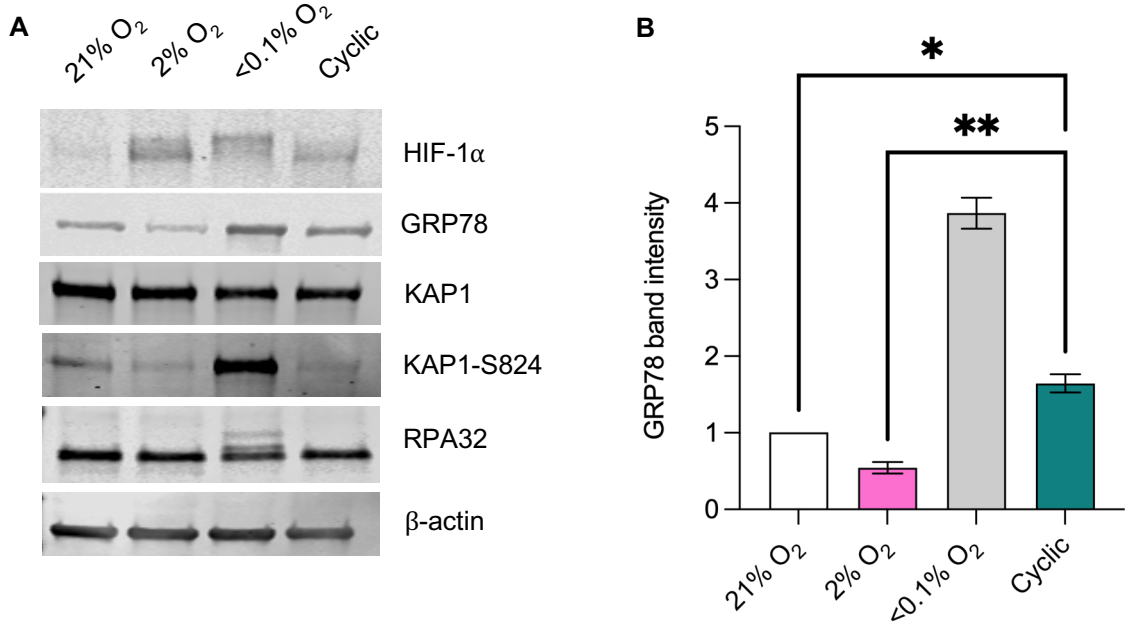


Figure 3.1: Static and cyclic hypoxia elicit different biological responses. (A) MDA-MB-231s were exposed to the indicated treatments for 16 h prior to western blotting. n=3. (B) Quantification of the GRP78 band intensity normalised to 21% O_2. n=3. One-way ANOVA * = $p<0.05$, ** = $p<0.01$.

3.2. Cell cycle dynamics vary between different oxygen conditions

To examine the nature of cell cycle dynamics and DNA replication of breast cancer cells in cyclic hypoxia, comparative to static hypoxia and 21% O_2, we carried out FACS with PI staining and BrdU incorporation. As expected, BrdU incorporation was significantly reduced in cells exposed to <0.1% O_2 (Foskolou et al., 2017). In contrast, MDA-MB-231 (Figure 3.2.1) and CAL51 (Figure 3.2.2) exposed to cyclic conditions continued to incorporate BrdU indicative of ongoing replication. BrdU incorporates in nuclear DNA replication as a thymidine analog, this incorporation therefore highlights the ongoing DNA replication that is occurring in cyclic hypoxia. In addition to the presence of replication in cyclic hypoxia, through the PI staining we determined that cyclic hypoxia induces an S-phase accumulation in the cell cycle for both cell lines. Statistical analysis shows that this accumulation in the S-phase portion of the cell

cycle is significant for cyclic in comparison to chronic <0.1% O_2 and 2% O_2. Together, these data suggest that the cells in S-phase continue to replicate but at a slow speed and therefore take longer to transit this phase of the cell cycle. These data were expected as an S-phase accumulation has previously been reported with this cyclic protocol in RKO cells (Bader et al., 2021).

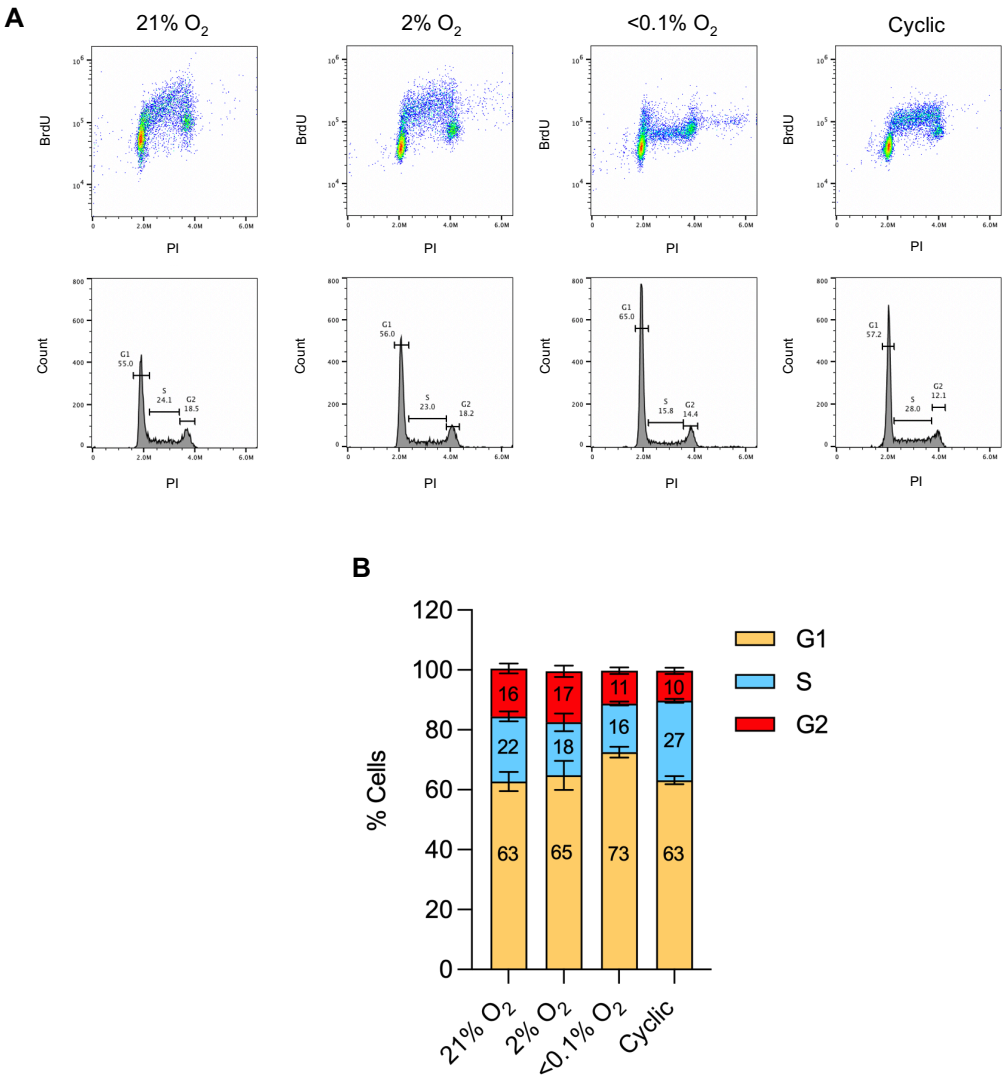


Figure 3.2.1: MDA-MB-231 cell cycle shows distinct profiles in cell proliferation and cycle stage depending on O_2 condition. (A) MDA-MB-231 were subjected to the indicated treatments for 16 h and labelled with BrdU (20 µM) 2 h prior to collection. The cells were stained with PI before analysed by FACS. Representative FACs plots are shown. (B) Quantification of the FACS to show cell cycle distribution. n=3. Two-way ANOVA statistics

show that the S-phase is significantly increased in cyclic hypoxia compared to 2% O_2 ($p<0.05$) and <0.1% O_2 ($p<0.01$). The G1 phase of the cell cycle in <0.1% O_2 is significantly increased compared to cyclic hypoxia ($p<0.05$).

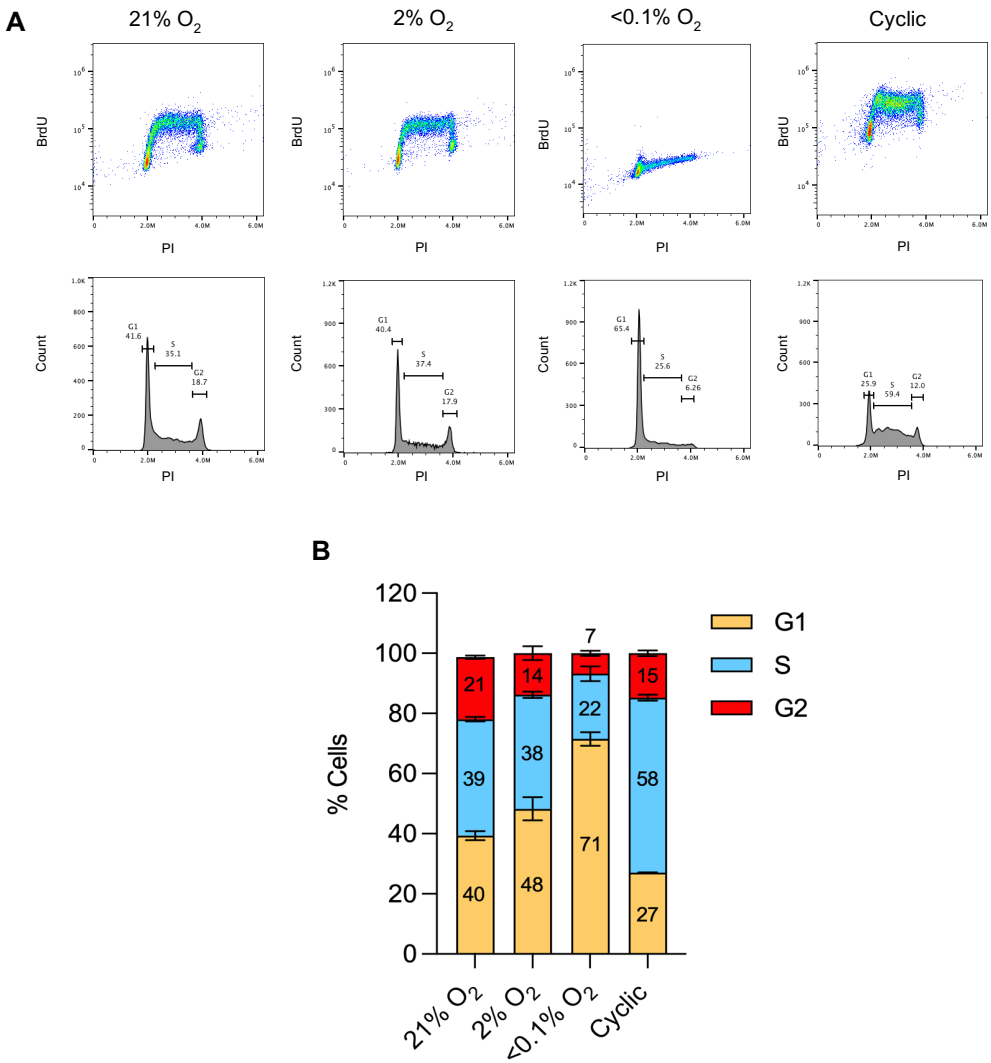


Figure 3.2.2: CAL51 cell cycle shows distinct profiles in cell proliferation and cycle stage depending on O_2 condition. (A) CAL51 were subjected to the indicated treatments for 16 h and labelled with BrdU (20 µM) 2 h prior to collection. The cells were stained with PI before analysed by FACS. Representative FACs plots are shown. (B) Quantification of the FACS to show cell cycle distribution. n=3. Two-way ANOVA statistics shows that the S-phase is significantly increased in cyclic compared to <0.1% O_2 and to 2% O_2 with $p<0.0001$. The G1 phase of the cell cycle in <0.1% O_2 is significantly increased with $p<0.0001$ compared to all other conditions.

3.3. Cyclic hypoxia reduces cell viability in four TNBC cell lines

With the knowledge that the cell cycle response to cyclic hypoxia is distinct to exposure to static hypoxia in both the cell lines tested (MDA-MB-231 and CAL51), we then asked how cyclic hypoxia impacted viability. We first investigated this with the MTT assay. To investigate the cell viability with MTT we used the MDA-MB-231 and CAL51 cell lines as well as three other available breast cancer cell lines, MDA-MB-468 (TNBC), MDA-MB-436 (TNBC) and MCF7 (Luminal A). Our MTT results demonstrate that cyclic hypoxia decreases cell viability of the four TNBC cell lines and has a more profound impact than exposure to <0.1% O_2 and 2% O_2 in MDA-MB-468, MDA-MB-231 and CAL51 (Figure 3.3.1). Intriguingly, this cyclic-induced decrease in cell viability is not seen in the Luminal A MCF7, but due to only one cell line being investigated, no deductions can be made as to whether this viability decrease is TNBC-specific. Measuring cell viability with the MTT assay has limitations (van Tonder et al., 2015). Therefore, we also investigated cell viability with the clonogenic assay. We carried out the clonogenic assay in CAL51 and MDA-MB-231, the cells were exposed to the differing oxygen conditions for 16 h. The CAL51 surviving fractions for the different conditions agree with the MTT data, providing confidence in the MTT results (Figure 3.3.2). In contrast, the MDA-MB-231 clonogenic data did not agree with the MTT assay and instead suggested that exposure to 2% caused a significant loss in viability, inferring that 2% O_2 is toxic (Figure 3.3.3). Not only does this not agree with the MTT data, but it is not in line with previous findings (Gwak et al., 2005). Our hypothesis is that 2% O_2 is not toxic, but in fact these cells have lost their colony forming ability due to increased motility of MDA-MB-231 in hypoxia, as has been reported (Liu et al., 2017, Nagelkerke et al., 2013, Nagelkerke et al., 2011). Therefore, going forward we utilised the CAL51 cell line for clonogenic assays due to its propensity to form colonies.

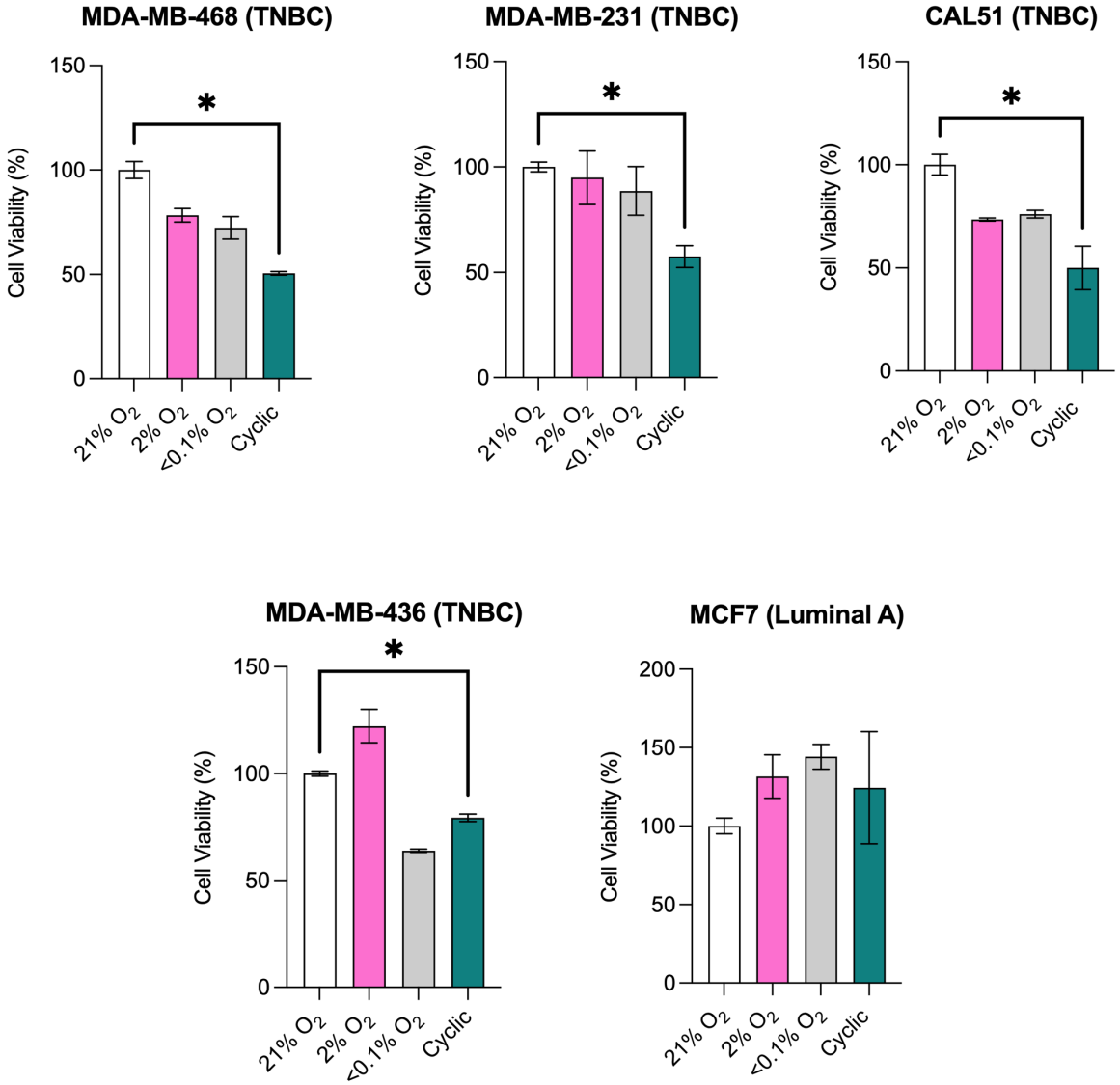


Figure 3.3.1: Cyclic hypoxia leads to decreased cell viability in four TNBC cell lines. CAL51, MDA-MB-468, MDA-MB-231, MDA-MB-436 and MCF7s were subjected to the indicated treatments for 24 h before viability was measured with the MTT assay. n=3. One-way ANOVA, * = $p<0.05$.

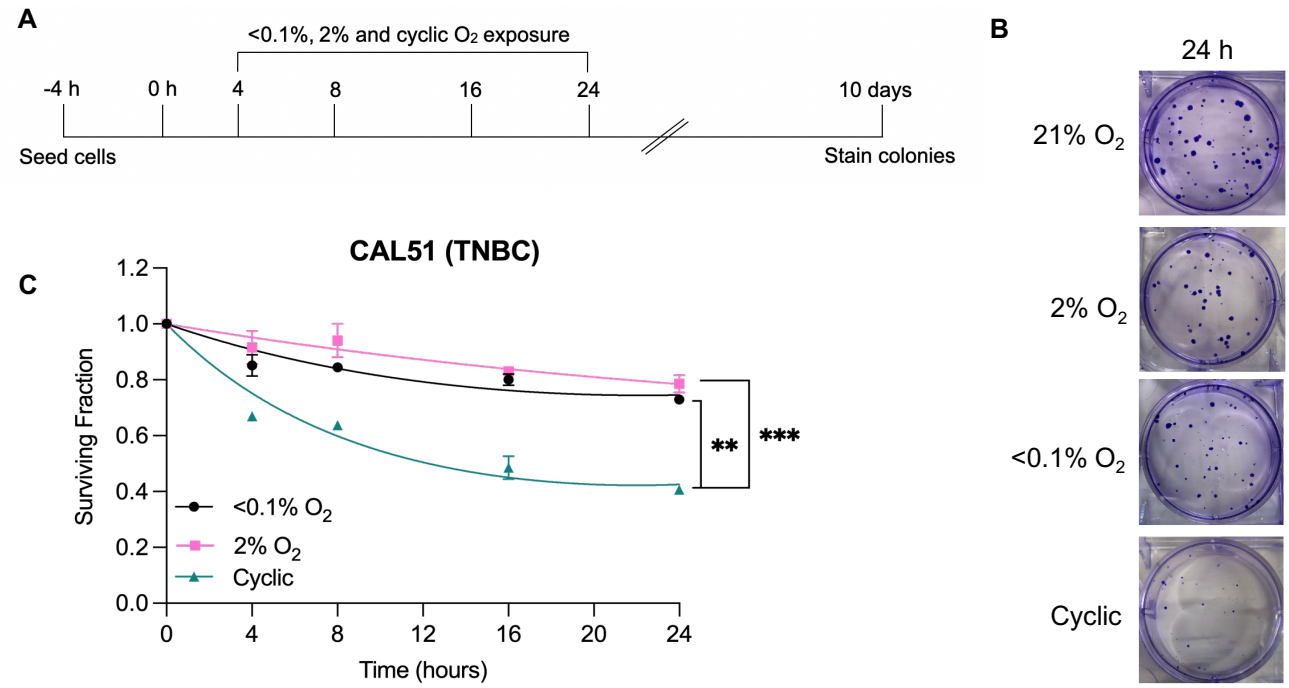


Figure 3.3.2: Colony survival in CAL51 supports the cell viability results determined by MTT assay. (A) Schematic representation of the time course of CAL51 cells treated with static <0.1% O_2, 2% O_2 and cyclic hypoxia (B) representative images (C) Clonogenic survival of CAL51 cells following 24 h treatment. n=3. One-way ANOVA, ** = p<0.01, *** = p< 0.001.

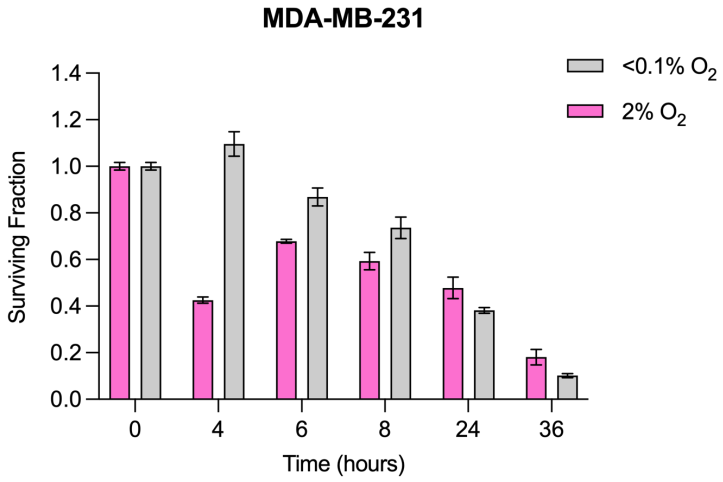


Figure 3.3.3: MDA-MB-231 appear to decrease in cell viability in 2% O_2. Clonogenic survival of MDA-MB-231 cells following a treatment time course in <0.1% O_2 and 2% O_2. Data are shown as a histogram as n=1.

3.4. The oxygen conditions tested induce differential gene expressions

As part of the characterisation of the biological response of breast cancer to cyclic hypoxia, we carried out Illumina sequencing with MDA-MB-231 in 21% O_2, 2% O_2, <0.1% O_2 and cyclic hypoxia. Before undergoing the RNA-seq we carried out qPCRs of two prototypical HIF-1α induced genes *CAIX* and *GLUT-1* with the cDNA generated for the RNA-seq. The expressions of *CAIX* and *GLUT-1* are known to increase in hypoxia (Clavo et al., 1995, Wykoff et al., 2000). As expected, our results show this increase in expression, however, distinct increases occur across the differing hypoxic conditions (Figure 3.4.1). The gene expressions of these two genes support that the hypoxic workstations were providing distinct hypoxic conditions, hence validating that the cells were exposed 2% O_2, <0.1% O_2 and cyclic hypoxia respectively.

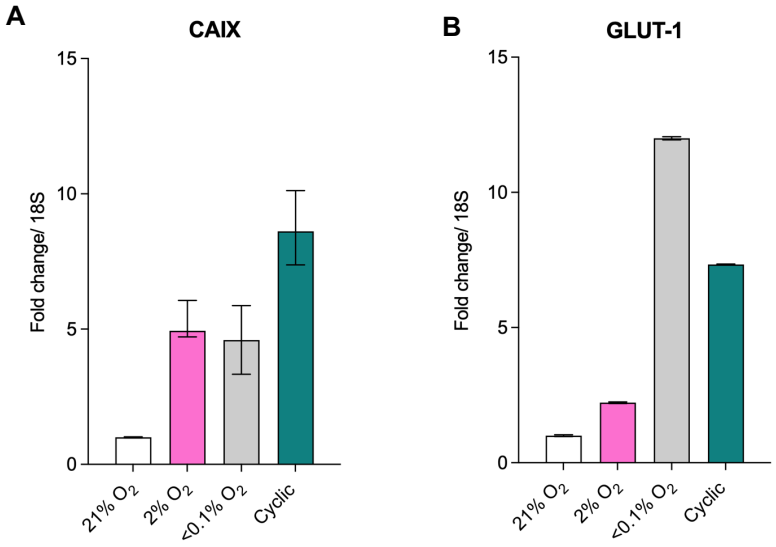


Figure 3.4.1: Gene expression of CAIX and GLUT-1 confirm different hypoxic conditions. MDA-MB-231s were subjected to the indicated treatments for 16 h. Cells then underwent qPCR for the hypoxia inducible genes (A) *CAIX* and (B) *GLUT-1*. Gene expressions are normalised to the housekeeping gene, *18-S*. n=1

In addition to the qPCR validation, a Pearson correlation coefficient analysis of the RNA-seq data verifies repeatability within our experiment. The Pearson correlation coefficient measures correlation of the gene expression levels between samples and therefore plays an important role in the verification of sample repeats. The closer the correlation coefficient is to 1, the higher the similarity the samples have. The square of the Pearson correlation coefficient should be greater than 0.92 in conditions that show high repeatability. The Pearson correlation coefficient for our RNA-seq data shows values of greater than 0.92 within sample repeats and therefore verifies repeatability within our experiment (Figure 3.4.2).

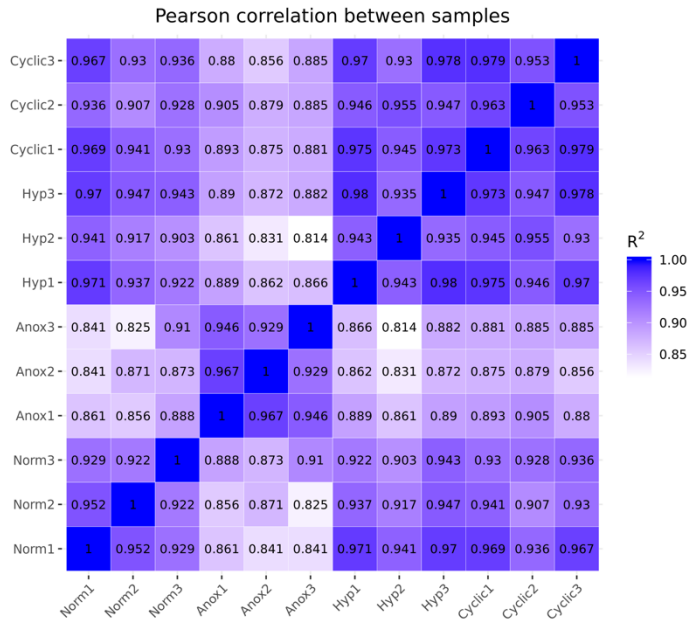


Figure 3.4.2: Pearson correlation coefficient of gene expression levels between samples supports repeat validity. MDA-MB-231 cells were subjected to the indicated treatments for 16 h before RNA-seq. Norm' = 21% O_2, 'Anox' = <0.1% O_2, 'Hyp' = 2% O_2. The closer correlation coefficient is to 1, the higher similarity the samples have. The square of the Pearson correlation coefficient should be greater than 0.92 to support repeat validity.

Differential gene expression analysis across our four conditions can be seen in the cluster heatmap (Figure 3.4.3 A). Despite all three types of hypoxia leading to an increase in HIF-mediated signalling, it can be seen that clear differences in gene expression were determined. Overall, despite unique clustering within the heatmap, the most similar upregulation and downregulation gene expression patterns emerge between 2% O_2 and cyclic hypoxia. The heatmap shows that <0.1% O_2 has an overall contrasting gene expression pattern to 2% O_2 and cyclic hypoxia. In <0.1% O_2 the upregulation and downregulation of genes are predominantly reverse of the upregulated and downregulated gene clusters seen in 2% O_2 and cyclic hypoxia. The distinct response of MDA-MB-231s to each hypoxic condition is further highlighted through the co-expression Venn diagram in which each condition holds its own set of uniquely expressed genes (Figure 3.4.3 B).

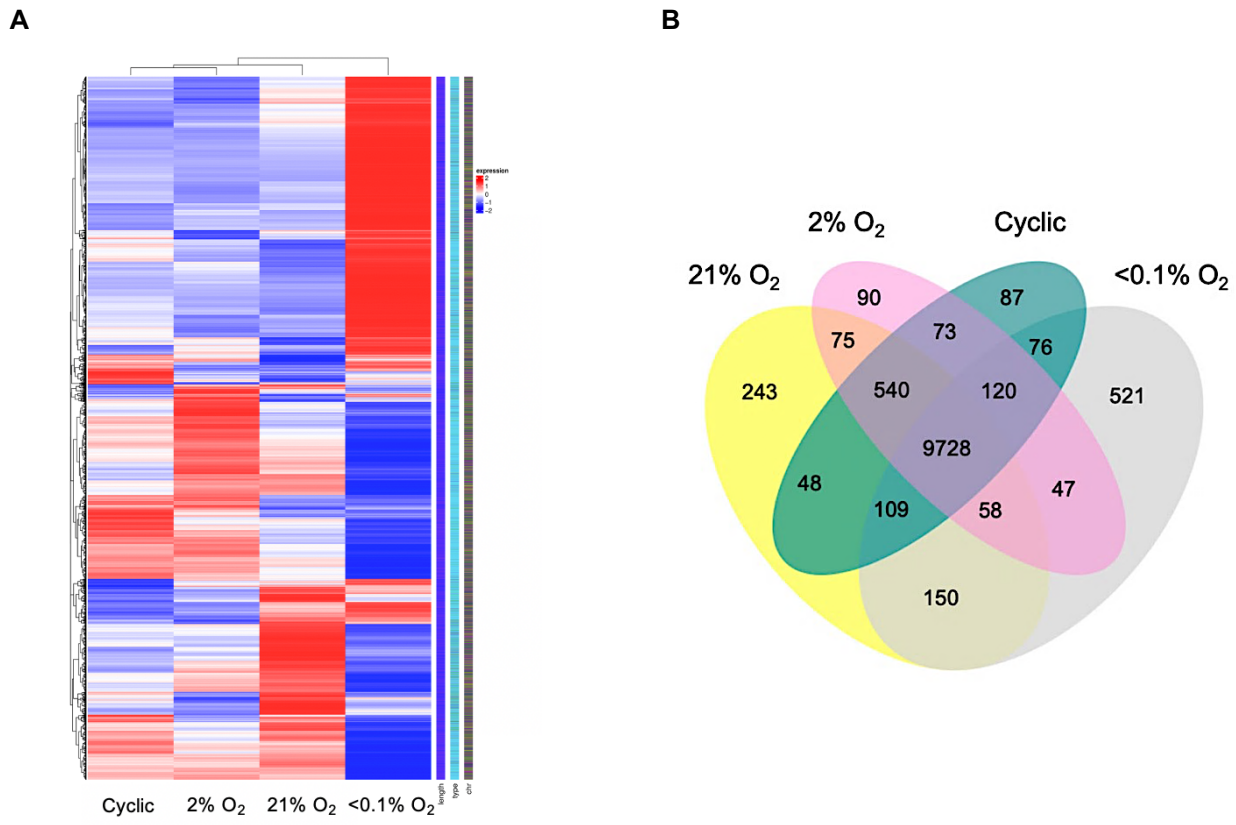


Figure 3.4.3: Differential gene expression profiles occur in response to the varied hypoxic conditions. MDA-MB-231 cells were subjected to the indicated treatments for 16 h before undergoing RNA-seq. (A) Cluster analysis of differentially expressed genes. (B) Co-expression Venn diagram of overlapping and uniquely expressed genes.

The overall distribution of these differentially expressed genes can be further broken down and explored with volcano plots. Volcano plots present the number and distribution of genes with significantly increased or decreased expression in the different hypoxic conditions compared to 21% O_2. In 2% O_2, 543 genes significantly increase in expression and 943 genes significantly decrease in expression compared to 21% O_2 (Figure 3.4.4 A). In <0.1% O_2, 3237 genes significantly increase in expression and 3470 genes significantly decrease in expression compared to 21% O_2 (Figure 3.4.4 B). In cyclic hypoxia, 938 genes significantly increase in expression and 1087 genes significantly decrease in expression compared to 21% O_2 (Figure

3.4.4 C). Despite differences in gene distributions, some of the most upregulated and downregulated genes in cyclic hypoxia, 2% O_2 and <0.1% O_2 comparative to 21% O_2 are overlapping (indicated on Figure 3.4.4). For example, *PPFIA4*, a member of the liprin-α gene family, is one of the most significantly upregulated genes in both cyclic hypoxia and 2% O_2 comparative to 21% O_2, while *NMRAL2P* is one of their most downregulated genes. Furthermore, comparative to 21% O_2, *EGLN3* (*PHD3*), is one of the most upregulated genes in <0.1% O_2 and cyclic hypoxia. It is interesting to see the stark number of downregulated genes in <0.1% O_2 as highlighted in both the cluster heatmap (Figure 3.4.3 A) and the volcano plots (Figure 3.4.4). A number of genes and processes are repressed in severe hypoxia, such as DNA repair and transcription (Hammond and Giaccia, 2005, Kumareswaran et al., 2012). The volcano plots support the repressive nature of <0.1% O_2 (Figure 3.4.4 B). Despite cyclic hypoxia having <0.1% O_2 within its protocol it does not result in the same repression of genes as seen in static <0.1% O_2 (Figure 3.4.4 C).

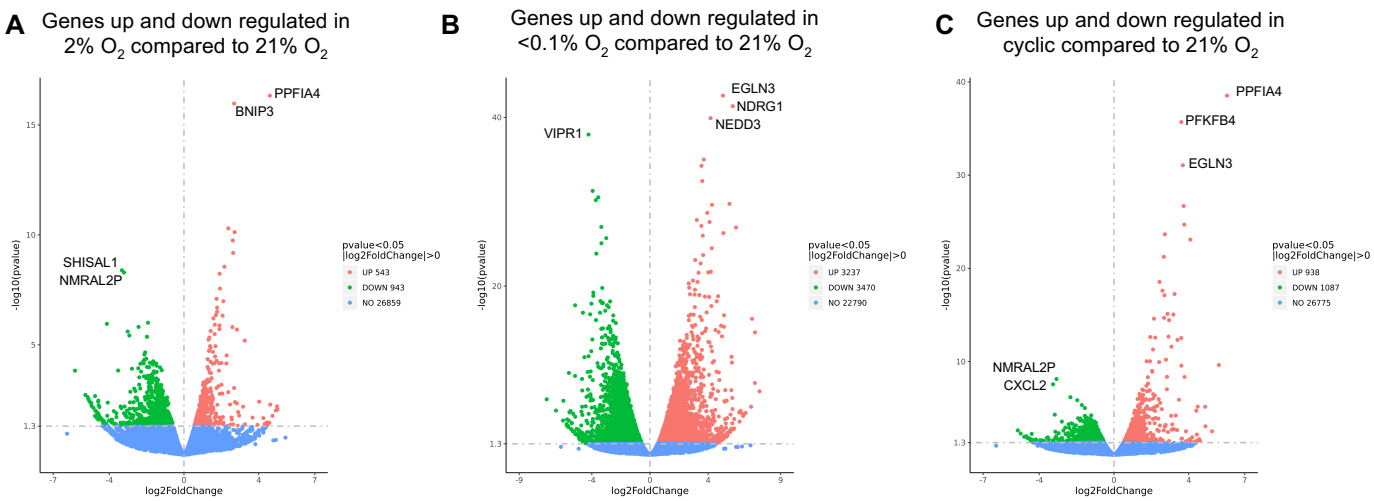


Figure 3.4.4: The distribution of differentially expressed genes in 2% O_2, <0.1% O_2 and cyclic hypoxia comparative to 21% O_2. MDA-MB-231 were subjected to the indicated treatments for 16 h before undergoing RNA-seq. The individual points on the graph represent genes. The most upregulated and downregulated genes between comparative conditions have been labelled. (A) Blue dots indicate no significant difference in gene expression between 2% O_2 and 21% O_2. Red dots indicate the gene has significantly increased expression in 2% O_2 compared to 21% O_2. Green dots indicate the gene has significantly decreased expression in 2% O_2 compared to 21% O_2. (B) Blue dots indicate no significant difference in gene expression between <0.1% O_2 and 21% O_2. Red dots indicate the gene has significantly increased expression in <0.1% O_2 compared to 21% O_2. Green dots indicate the gene has significantly decreased expression in <0.1% O_2 compared to 21% O_2. (C) Blue dots indicate no significant difference in gene expression between cyclic hypoxia and 21% O_2. Red dots indicate the gene has significantly increased expression in cyclic hypoxia compared to 21% O_2. Green dots indicate the gene has significantly decreased expression in cyclic hypoxia compared to 21% O_2.

We wanted to explore the impact of the different hypoxic conditions on HIF-1α mediated transcription and see if the distinct hypoxic conditions led to differential HIF-1α mediated gene responses. Through statistical analysis of our RNA-seq log2fold changes in expression of

genes transcriptionally mediated by HIF-1α, we determined that the HIF-1α mediated response was distinct for a selection of genes between <0.1% O_2, 2% O_2 and cyclic hypoxia (Figure 3.4.5).

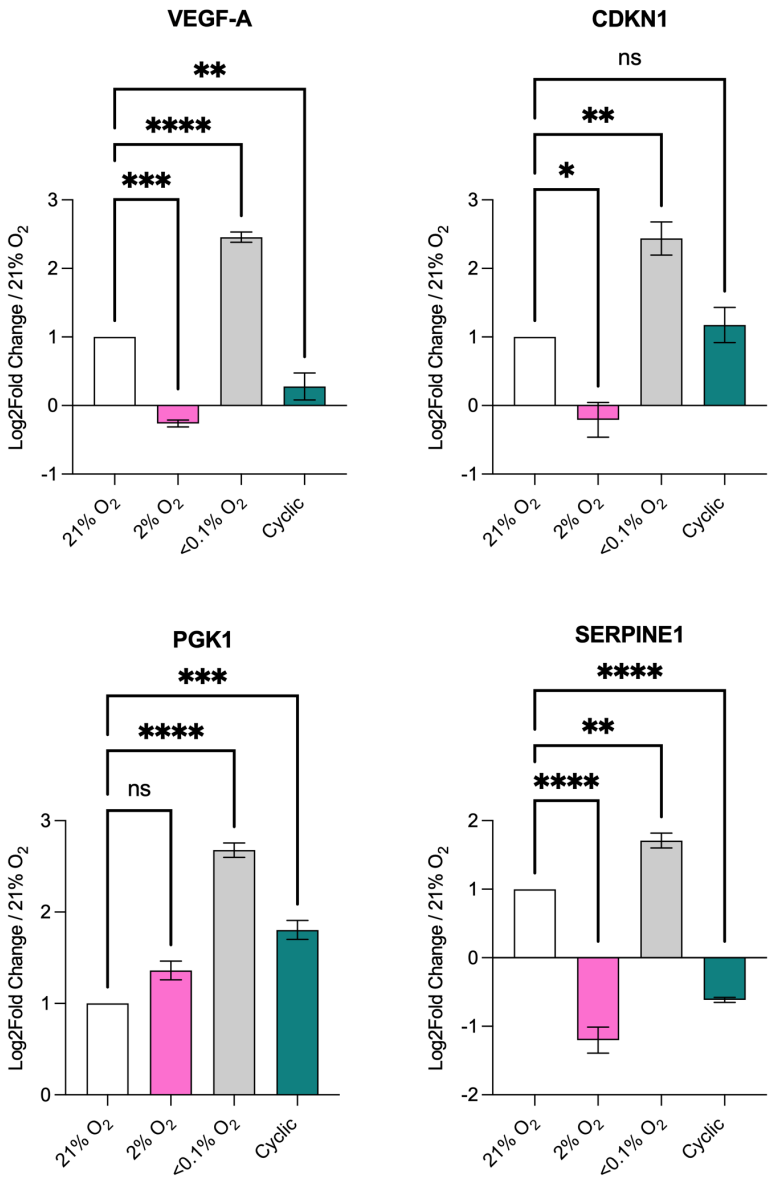


Figure 3.4.5: Differential gene expression of four HIF-1α mediated genes in our different hypoxic conditions. MDA-MB-231 cells were subjected to the indicated treatments for 16 h before undergoing RNA-seq. The RNA-seq gene expression data of HIF-1α mediated genes were compared between hypoxic conditions. n=3. One-way ANOVA. * = p<0.05, ** = p<0.01, *** = p<0.001, **** = p<0.0001.

3.5. Expression analysis of genes in the Buffa hypoxia signature indicates the signature cannot distinguish between the different oxygen conditions

Our RNA-seq differential gene expression data supports that the response to hypoxia is dependent on the exact nature of the hypoxic conditions. To date, efforts to measure hypoxia in patient tumours is limited and preclinical studies often rely on well-validated hypoxia signatures. One of the most widely used of these signatures is the Buffa hypoxia signature, defined in 2010, which includes upregulated as well as repressed genes (Buffa et al., 2010). The Buffa hypoxia signature is largely composed of HIF-1 targets and therefore reports on a wide range of hypoxic conditions including mild chronic hypoxia, severe chronic hypoxia and cyclic hypoxia. Having observed a difference in expression levels of some HIF-1α mediated genes in the differing hypoxic conditions (Figure 3.4.5), we wanted to investigate the difference in expression of genes within the Buffa hypoxia signature in the differing hypoxic conditions. We first looked at the log2fold changes in our RNA-seq gene expressions in the three hypoxic conditions for the top-ranked 15 genes within the Buffa hypoxia signature. We determined that the gene expression of 6 of the 15 genes (*ENO1*, *LDHA*, *TPI1*, *PGAM1*, *ALDOA* and *MIF*) has overlapping gene expression between 2% O_2, <0.1% O_2 and cyclic hypoxia (Figure 3.5.1). The average from the mean fold changes for each gene of the 15 top-ranked genes of the Buffa hypoxia signature was then calculated for each hypoxic condition, and normalised to 21% O_2, using raw RNA-sequencing read numbers. We see that overall the three hypoxic conditions have significantly increased Buffa hypoxia expression compared to 21% O_2, showing that these MDA-MB-231 hypoxic samples correlate with the Buffa hypoxia signature (Figure 3.5.2). This expression analysis of the 15 top-ranked genes in the Buffa

hypoxia signature indicates that the Buffa hypoxia signature cannot distinguish between <0.1% O_2, 2% O_2 and cyclic hypoxia.

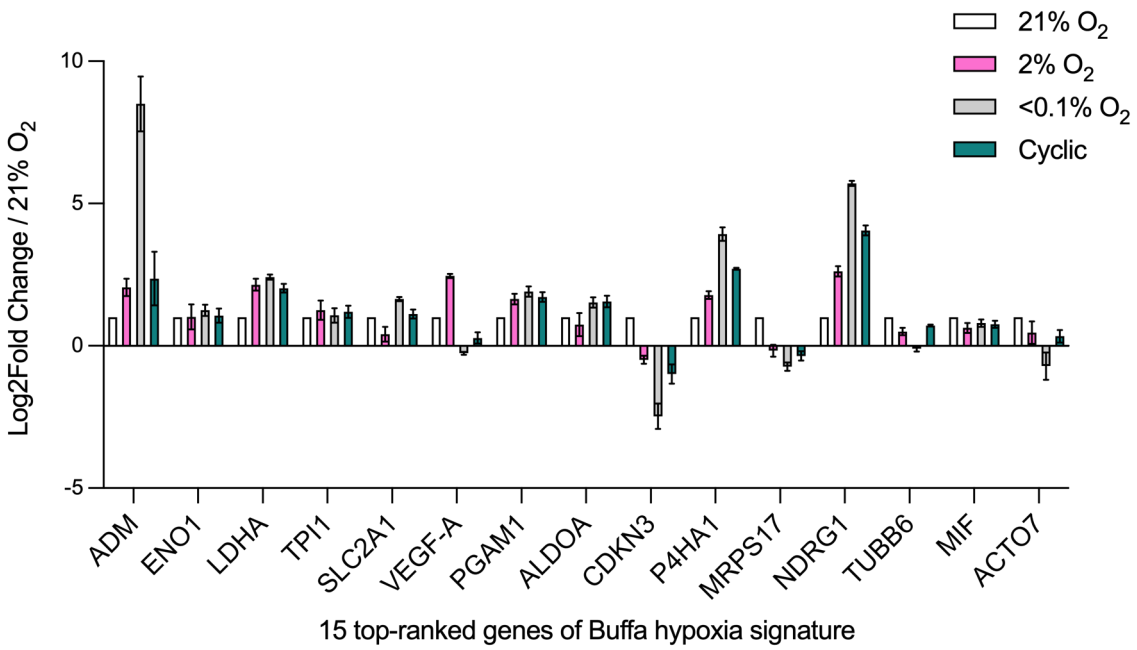


Figure 3.5.1: Differential expression of the 15 top-ranked genes from the Buffa hypoxia signature in our range of hypoxia conditions. MDA-MB-231 cells were subjected to the indicated treatments for 16 h before undergoing RNA-seq. The RNA-seq gene expression data of the genes within the Buffa hypoxia signature were compared between hypoxic conditions. n=3.

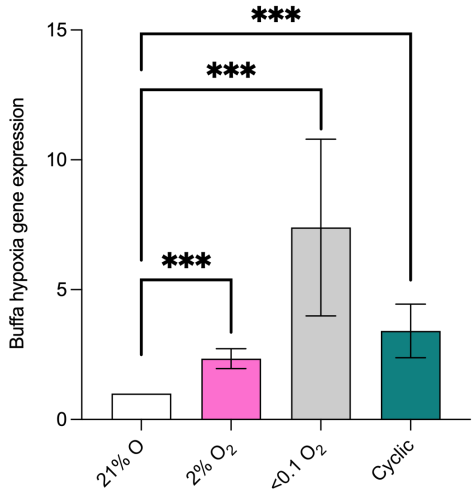


Figure 3.5.2: The expression of the Buffa hypoxia gene signature in MDA-MB-231 cells exposed to 16 h of 21% O_2, 2% O_2, <0.1% O_2 and cyclic hypoxia. The average from the mean fold changes for each gene of the 15 top-ranked genes of the Buffa common hypoxia metagene was calculated for each condition, normalised to 21% O_2, using raw RNA-sequencing read numbers. n=3. The Wilcoxon signed-rank test was used *** = p<0.001.

3.6. The differing oxygen conditions lead to distinct upregulation in gene ontologies

Gene ontology (GO) is a major bioinformatics classification system to unify the presentation of gene properties across all species. It includes three main branches: cellular component, molecular function and biological process. Following on from differential gene expression analysis, it is unsurprising to see that, comparative to 21% O_2, the most enriched gene ontologies for each hypoxic condition differ (Figure 3.6.1). Despite differences, 2% O_2 and cyclic hypoxia are both heavily metabolic reprogramming focused. Nonetheless, they differ in the specific process and order of processes which are upregulated regarding metabolism and the shift to glycolysis. In addition to enriched metabolic reprogramming, cyclic hypoxia has

two processes which are uniquely upregulated in this condition alone. The first is oxidoreductase activity inferring an increase of redox reactions in cyclic hypoxia. The second is angiogenesis (Figure 3.6.1 C). The most enriched GOs in <0.1% O_2 are UPR related. Examples of the most upregulated UPR processes include response to topologically incorrect protein; response to unfolded protein; response to endoplasmic reticulum stress; cellular response to topologically incorrect protein; cellular response to unfolded protein (Figure 3.6.1 B).

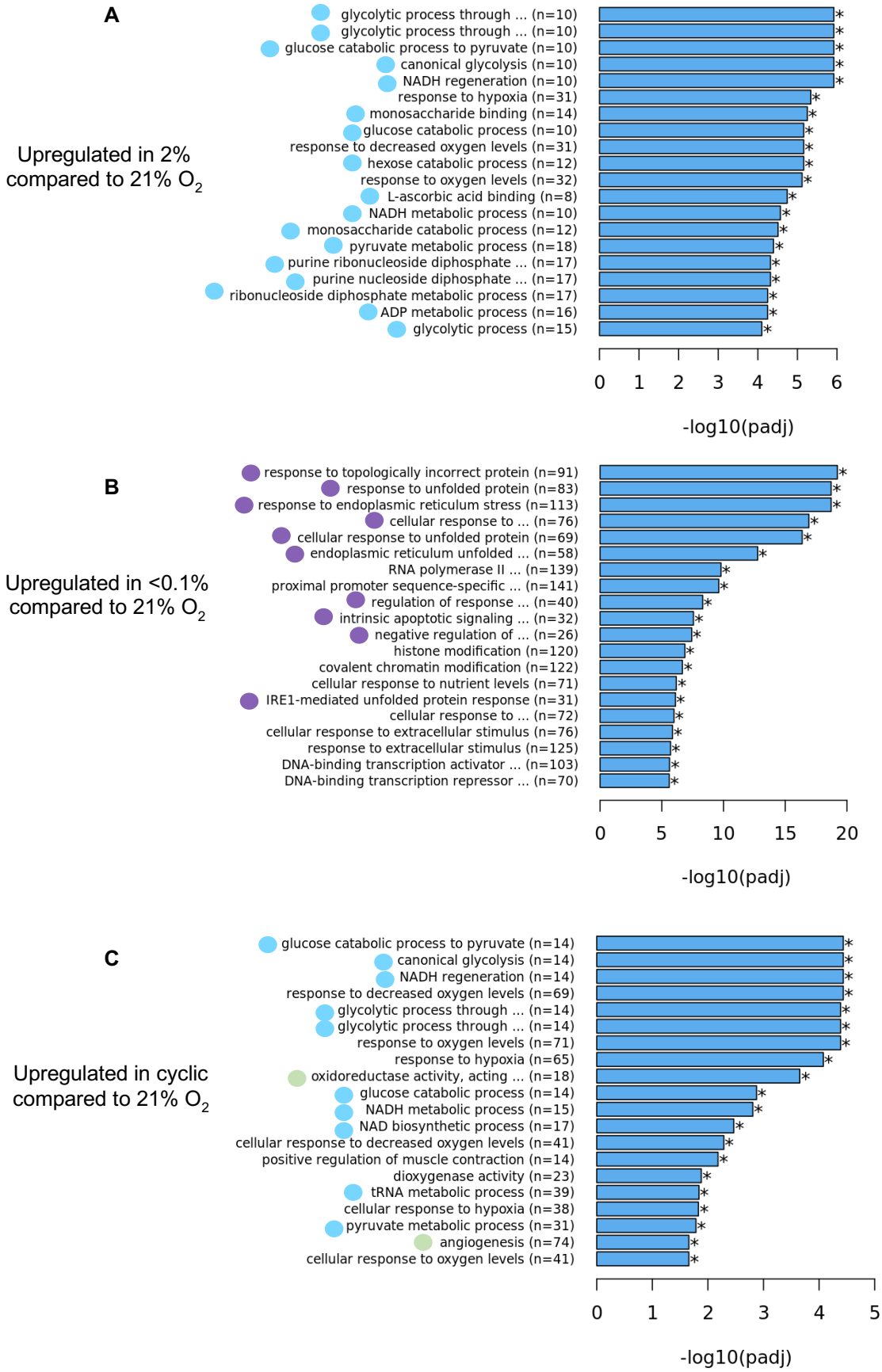


Figure 3.6.1: Distinct gene ontologies are enriched dependent on the hypoxic conditions, with cyclic hypoxia and 2% O_2 enriching metabolic reprogramming and <0.1% O_2 enriching

the UPR. MDA-MB-231 cells were subjected to the indicated treatments for 16 h before undergoing RNA-seq. Metabolic reprogramming processes are highlighted with a blue dot. UPR related processes are highlighted with a purple dot. Enriched processes unique to cyclic hypoxia and discussed in this thesis are highlighted with a green dot. Abbreviations '…' in the figures shall now be stated in order of succession (A) glycolytic process through fructose-6-phosphate; glycolytic process through glucose-6-phosphate; purine ribonucleoside diphosphate metabolic process; purine nucleoside diphosphate metabolic process. (B) cellular response to topologically incorrect protein; endoplasmic reticulum unfolded protein response; RNA polymerase II proximal promoter sequence-specific DNA binding; proximal promoter sequence-specific DNA binding; regulation of response to endoplasmic reticulum stress; intrinsic apoptotic signalling pathway in response to endoplasmic reticulum stress; negative regulation of response to endoplasmic reticulum stress; cellular response to steroid hormone stimulus; DNA-binding transcription activator activity, RNA polymerase II-specific; DNA-binding transcription repressor activity, RNA polymerase II-specific. (C) glycolytic process through fructose-6-phosphate; glycolytic process through glucose-6-phosphate; oxidoreductase activity, acting on paired donors, with incorporation or reduction of molecular oxygen, 2-oxoglutarate as one donor, and incorporation of one atom each of oxygen into both donors. 'n' refers to the number of genes enriched in the indicated process; * = $p<0.5$, shows significance of the enriched process. n=3.

It should be noted that when looking specifically at the cellular component GO (rather than combined with molecular function and biological process as in Figure 3.6.1), the UPR related endoplasmic reticulum chaperone complex is most upregulated cellular component process in cyclic hypoxia comparative to 21% O_2 (Figure 3.6.2 C). This complements the GRP78 protein expression increase in cyclic hypoxia (Figure 3.1) and further supports that the UPR is activated in cyclic hypoxia.

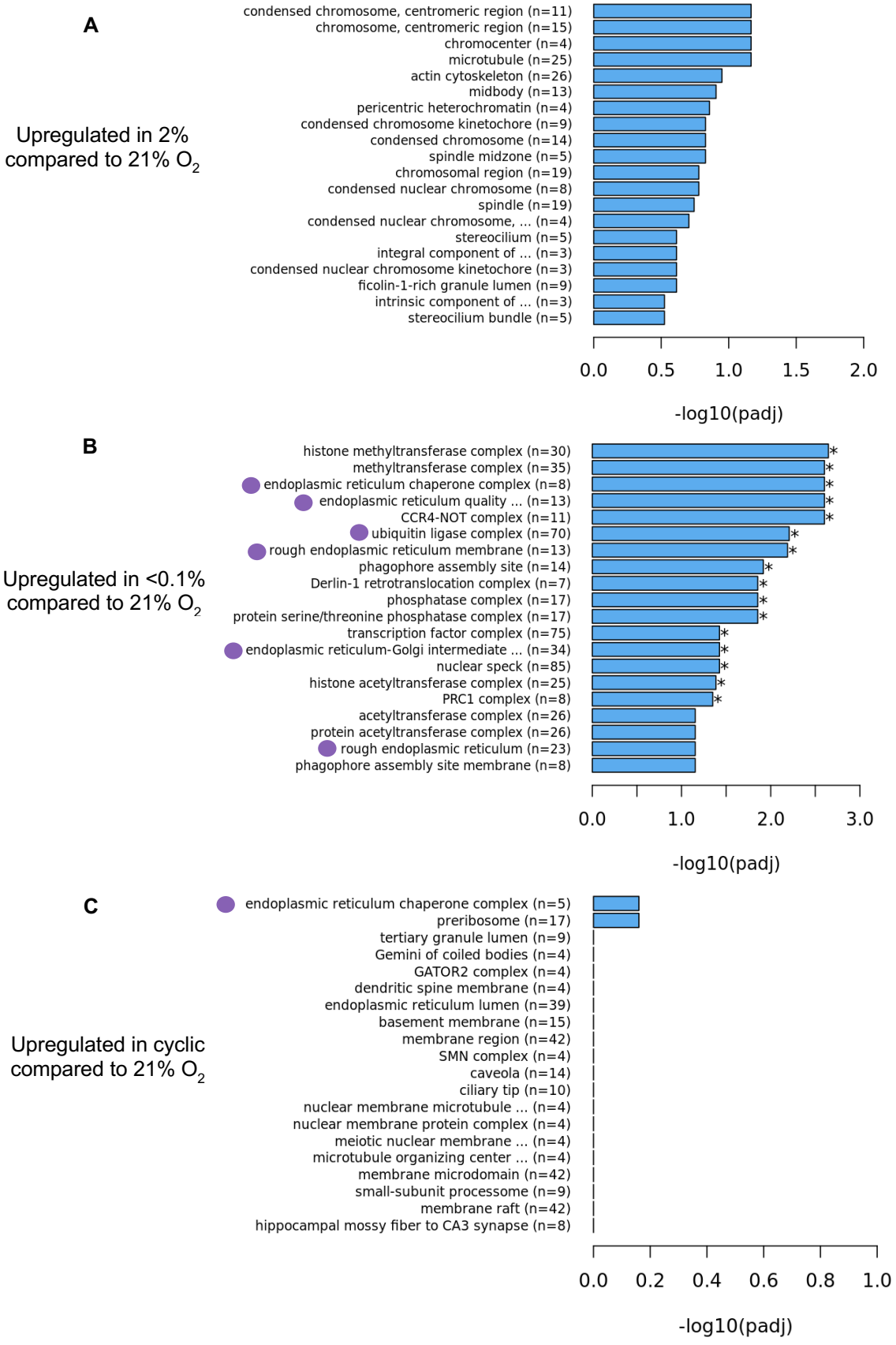


Figure 3.6.2: The cellular component of the GO highlights the induction of UPR in cyclic hypoxia. MDA-MB-231 cells were subjected to the indicated treatments for 16 h before

undergoing RNA-seq. UPR related cellular components are highlighted with a purple dot. Abbreviations '…' in the figures shall now be stated in order of succession (A) condensed nuclear chromosome, centromeric region; integral component of presynaptic active zone membrane; intrinsic component of presynaptic active zone membrane. (B) endoplasmic reticulum quality control compartment; endoplasmic reticulum-Golgi intermediate compartment. (C) nuclear membrane microtubule tethering complex; meiotic nuclear membrane microtubule tethering complex; microtubule organizing centre attachment site. 'n' refers to the number of genes enriched in the indicated process; * = $p<0.5$, shows significance of the enriched process. n=3.

3.7. Cyclic hypoxia is most relevant to breast cancer

The disease ontology (DO) highlights where differential gene expression patterns are significantly relevant to human disease. Cyclic hypoxia is the only condition in which, comparative to 21% O_2, cancer-related gene enrichment is significant in breast cancer, nervous system cancer, thoracic cancer, organ system benign neoplasm, kidney cancer and urinary system cancer (Figure 3.7). Breast cancer is also seen to be one of the cancers most enriched in 2% O_2, but this enrichment is not significant. 32 genes (n=32) were identified leading to the enrichment of breast cancer in 2% O_2 (Figure 3.7 A), in contrast, 54 genes (n=54) were identified leading to the significant enrichment of breast cancer in cyclic hypoxia (Figure 3.7 C). There are 28 overlapping genes between the 34 genes enriched in breast cancer in 2% O_2 and 54 genes enriched in cyclic hypoxia.

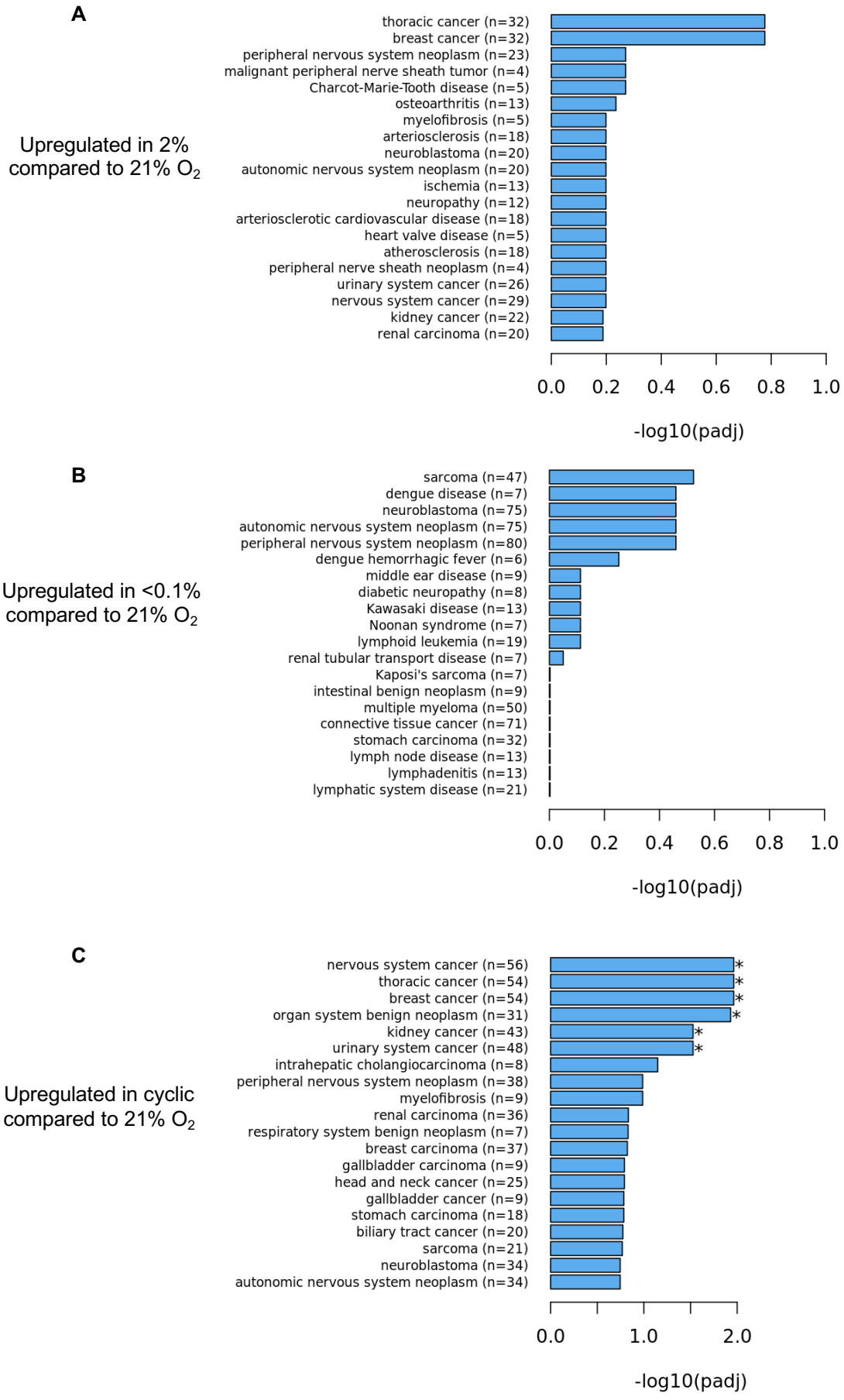


Figure 3.7: Cyclic hypoxia is the only condition in which, comparative to 21% O_2, cancer-related gene enrichment is significant in breast cancer. MDA-MB-231 cells were subjected

to the indicated treatments for 16 h before undergoing RNA-seq. ‘n’ refers to the number of genes enriched in the indicated process; * = p<0.5, shows significance of the enriched process. n=3

Discussion

Due to the aggressive, metastatic nature of TNBC and the role that cyclic hypoxia plays in these processes, this chapter aimed to characterise and better understand the biological response of TNBC to cyclic hypoxia. Our results show that the response to hypoxia is dependent on the exact nature of the hypoxic conditions in which the cells are exposed, with distinct biological responses between 21% O_2, 2% O_2, <0.1% O_2 and cyclic hypoxia.

We first confirmed the three hypoxic conditions through the presence of HIF-1α on a western blot. We saw that despite all the hypoxic conditions leading to HIF-1α accumulation they each possessed differing patterns of HIF-1α bands. These differing bands could be indicative of differing PTMs across 2% O_2, <0.1% O_2 and cyclic hypoxia. Differing HIF-1α PTMs result in differing stabilisation, localisation and ability to bind and form protein complexes (Albanese et al., 2020, Daly et al., 2021). In addition to this we saw a <0.1% O_2 specific induction of the DDR. It was interesting to see that despite cyclic hypoxia having periods of <0.1% O_2 the DDR is not induced. This was in contrast to findings in RKO cells in the same cyclic hypoxia protocol (Bader et al., 2021). Therefore, it is important in the future to consider different timepoints and more DDR markers to see if DDR induction does occur but is just not seen at the 16 h timepoint with the DDR markers chosen. In contrast to DDR induction, we did see induction of the UPR in cyclic hypoxia through the increased expression of GRP78 compared to 21% O_2 and 2% O_2.

Our results support a cyclic hypoxia specific response in cell cycle dynamics compared to 21% O_2, 2% O_2 and <0.1% O_2, in which an S-phase accumulation occurs and cells continue to

synthesise DNA. With the knowledge that the cell cycle response to cyclic hypoxia is distinct, we went on to measure cell viability in response to the different hypoxic conditions. We saw that cyclic hypoxia is a challenging environment for TNBC cell lines and results in the greatest decrease in cell viability of three out of four TNBC cell lines. Our results highlight the fate of cells in cyclic hypoxia. A limitation of the MTT assay is that the conversion of MTT to insoluble formazan crystals depends on the cellular metabolic rate and number of mitochondria (van Tonder et al., 2015). Therefore, the decrease in viability observed in the hypoxic conditions may be due to the metabolic shift and decreased mitochondrial function of cells in hypoxia (Semenza, 2010b, Fuhrmann et al., 2013). While we can infer a loss of viability in the conditions tested by the MTT assay, it is also possible that the cells may eventually recover. Conversely, the colony survival assay shows a definitive loss of viability and confirms that the cells no longer have the ability to replicate. The colony survival assay does not however tell us why the cells are unable to replicate. There are several possible outcomes for the cell fate, including apoptosis, senescence, necrosis, and mitotic catastrophe. Further experiments are therefore required to determine the cell fate following exposure to cyclic hypoxia.

The differential gene expression analysis of the RNA-seq data shows distinct responses to each hypoxic condition. Most profoundly, each hypoxic condition has its own specific set of uniquely expressed genes. In addition to this, the GO highlight cyclic hypoxia-specific enriched events of oxidoreductase activity and angiogenesis as well as cyclic hypoxia induction of the UPR and metabolic reprogramming. The UPR activation in cyclic hypoxia is further supported by the GRP78 increase in expression in cyclic hypoxia. Despite the distinct responses to the differing hypoxic conditions, our results indicate that the Buffa hypoxia signature is unable to distinguish between hypoxic conditions. This highlights the need for hypoxia-specific

signatures. For example, our results show that a cyclic hypoxia signature would differ from a chronic hypoxia signature and therefore could act to identify a subset of patients with the poorest prognosis or who could benefit from specific therapies, for example those that modify the S-phase of the cell cycle.

Finally, our results suggest that there is a need for hypoxia-specific signatures as the Buffa hypoxia signature cannot differentiate between different oxygen conditions. Despite the Buffa hypoxia signature being derived from breast cancer patient samples (Buffa et al., 2010), it was surprising to see that our DO results indicate that cyclic hypoxia is the only of the hypoxic conditions to have a significant enrichment of genes related to breast cancer. Considering that our results were derived from a TNBC cell line, it is possible that cyclic hypoxia is the most relevant form of hypoxia in TNBC. This is an example of where a cyclic-specific hypoxia signature could be applied, and the distinct biological response to cyclic hypoxia could be harnessed for therapeutic development. Further RNA-seq analyses with a greater number of samples and breast cancer subtypes would be required to validate this.

CHAPTER 4: The therapeutic response to cyclic hypoxia

Introduction

Characterisation of the biological response of breast cancer to cyclic hypoxia indicates that cyclic hypoxia has a greater impact on TNBC cell viability compared with exposure to static hypoxia levels. The literature reports that cyclic hypoxia leads to a more aggressive, metastatic and resistant cancer phenotype, this infers that cyclic hypoxia leads to a selection pressure on cells (Daneau et al., 2010, O'Connor et al., 2019, Ron et al., 2019, Yasui et al., 2010). Therefore, we hypothesised that cells that survive cyclic hypoxia are the most malignant/aggressive. The RNA-seq data presented in chapter 3 demonstrates the distinct differences in gene expression in the types of hypoxia investigated. Based on these differences and the supporting literature we hypothesised that response to therapy would also be markedly different.

The RNA-seq differential gene expression data highlighted that there are 87 genes that are unique to the cyclic hypoxia conditions. One of the most significantly upregulated cyclic hypoxia-specific genes was *EPHA3* which encodes the receptor EphA3. The Eph receptors constitute the largest sub-group within the receptor tyrosine kinase family. Eph receptors interact with ephrins; ephrins are cell mebrane bound ligands. Cell communication mediated by Eph-ephrin control cell interactions such as attachment and detachment, as well as motility and EMT. In the context of tumour development, the Eph receptors, such as EphA3, modulate cell adhesion as well as metastasis, invasion, angiogenesis and tumour growth (Janes et al., 2008, Pasquale, 2008). In addition to tumour promoting properties, EphA3 has also been

shown to play a role in radiotherapy resistance (Kim et al., 2018). *EPHA3* is one of the contributing genes leading to the significant enrichment of several cyclic-specific GOs in our RNA-seq dataset, including: cell-substrate adhesion, angiogenesis, peptidyl-tyrosine modification, and cell junction organisation.

Here, we investigated the impact of DNA-damaging therapies in cyclic hypoxia compared to chronic hypoxia using radiation as an exemplar (Hall and Giaccia, 2011). In addition to investigating the cyclic hypoxia response to radiotherapy with Cs irradiation, we also investigated the response to FLASH radiotherapy.

4.1 The role of EphA3 in cyclic hypoxia

As already discussed, *EPHA3* has roles in cancer promotion and was one of the most upregulated cyclic hypoxia-specific genes identified within our RNA-seq. We first wanted to validate the RNA-seq through carrying out qPCR for *EPHA3* in MDA-MB-231 (Figure 4.1.1 A). Due to the availability of samples treated in the same conditions, we also did the qPCR with the PSN1 cell line and saw a cyclic-specific EPHA3 induction (Figure 4.1.1 B).

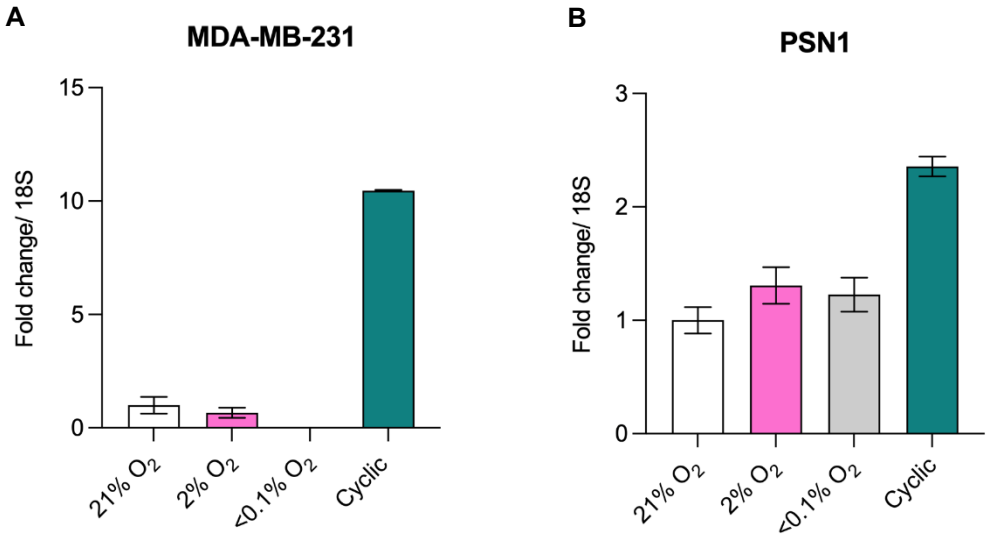


Figure 4.1.1: Cyclic-specific induction of *EPHA3* in the RNA-seq was validated with qPCR. (A) MDA-MB-231 and (B) PSN1 cells were subjected to the indicated treatments for 16 h. Cells then underwent qPCR for *EPHA3*. *EPHA3* gene expressions are normalised to the housekeeping gene, 18-S. n=1.

Next, we investigated the knockdown of *EPHA3* with siRNA, with the aim of investigating the impact of siEPHA3 on cell viability and radiosensitivity in cyclic hypoxia via the clonogenic assay. We therefore chose to use CAL51 due to their propensity to form colonies. We treated CAL51 with 20 µM siEPHA3 and used qPCR to validate the knockdown. Unfortunately, no

significant reduction on *EPHA3* mRNA was observed (Figure 4.1.2). Due to time constraints of this project, we were unable to further optimise this experiment.

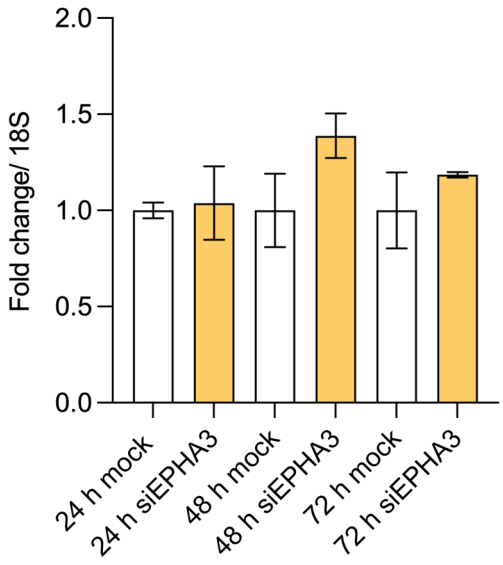


Figure 4.1.2: No significant reduction on *EPHA3* mRNA is observed. CAL51 cells were treated with siEPHA3 or mock over a 72 h time course at 21% O_2. *EPHA3* gene expressions are normalised to the housekeeping gene, 18-S. n=2.

4.2. Cyclic hypoxia leads to increased radioresistance compared to 2% O_2 but increased radiosensitivity compared to <0.1% O_2

The concentration of oxygen present at the exact moment irradiation is carried out determines the tumour cell radiation efficacy. This is called the oxygen enhancement ratio (OER). The definition of the OER is the dose ratio required to produce the equivalent biological response from severe hypoxic to well-oxygenated conditions. When using gamma ray sources, such as a Cs irradiator, the OER between tumour cells in anoxia and well-oxygenated conditions is between 2.5 and 3.0. When cells are subjected to radiation, free radicals form, which are highly reactive and cause DNA damage. This damage is repairable, however, in the

presence of oxygen these free radicals can react with oxygen and form peroxyl radicals. Peroxyl radicals cause permanent fixed DNA damage. Therefore, irradiated cells with less oxygen have decreased overall damage as the damage that occurs can be repaired. As the oxygen tension increases from <0.1% O_2 to 0.5% O_2 a rapid change in radiosensitivity occurs. The oxygen tension at which the OER is halfway between well-oxygenated cells and <0.1% O_2 cells is 0.5% O_2. This profound impact on radiosensitivity through such a small change in oxygen tension highlights the importance of oxygen at the time of irradiation (Hall and Giaccia, 2011). We therefore first wanted to ensure that the radiation boxes we use to carry out hypoxic irradiation were airtight and no reoxygenation occurred (Figure 2.4). We determined the OER between <0.1% O_2 and 21% O_2, and 2% O_2 and 21% O_2, through calculating the ratio between their respective doses (Gy) at the 10% surviving fraction. The OER between <0.1% O_2 and 21% O_2 was calculated to be 2.05 (Figure 4.2.1 A). This suggests that our radiation boxes are airtight and reoxygenation does not occur. The OER between 2% O_2 and 21% O_2 was calculated to be 1.13 (Figure 4.2.1 B).

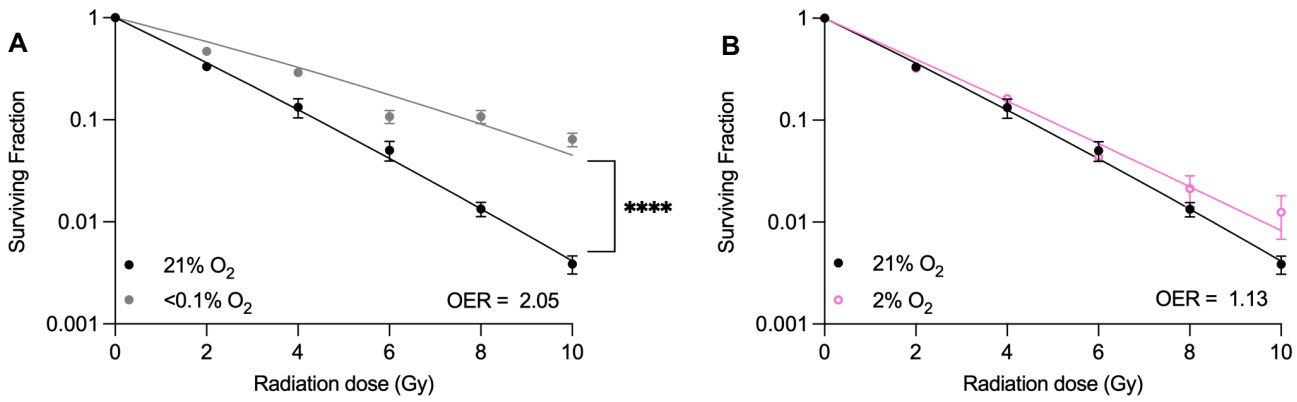


Figure 4.2.1: An OER of 2.05 between 21% O_2 and <0.1% O_2 provides confidence in our radiation boxes being airtight. CAL51 were subjected to the indicated treatments for 16 h before irradiation. n=3. (A) The OER was calculated from the dose ratio between 21% O_2 and <0.1% O_2. n=3. Two-way ANOVA. **** = p <0.0001. (B) The OER was calculated from the dose ratio between 21% O_2 and 2% O_2. n=3. Two-way ANOVA showed no significance between 2% O_2 and 21% O_2 dose response curves.

Following validation that the radiation boxes maintained hypoxia, we investigated the response of cyclic hypoxia exposed CAL51 to a range of radiation doses (Gy) compared to chronic hypoxia. Our experimental design ensured that the conditions being compared were irradiated at the same level of oxygen therefore ruling out the oxygen effect at the time of radiation. Cells exposed to cyclic hypoxia and then irradiated at <0.1% O_2 were more sensitive compared to those irradiated in constant <0.1% O_2 (Figure 4.2.2 A). The opposite was true for cells exposed to cyclic hypoxia and then irradiated at 2% O_2, these were more radioresistant compared to cells irradiated in constant 2% O_2 (Figure 4.2.2 B).

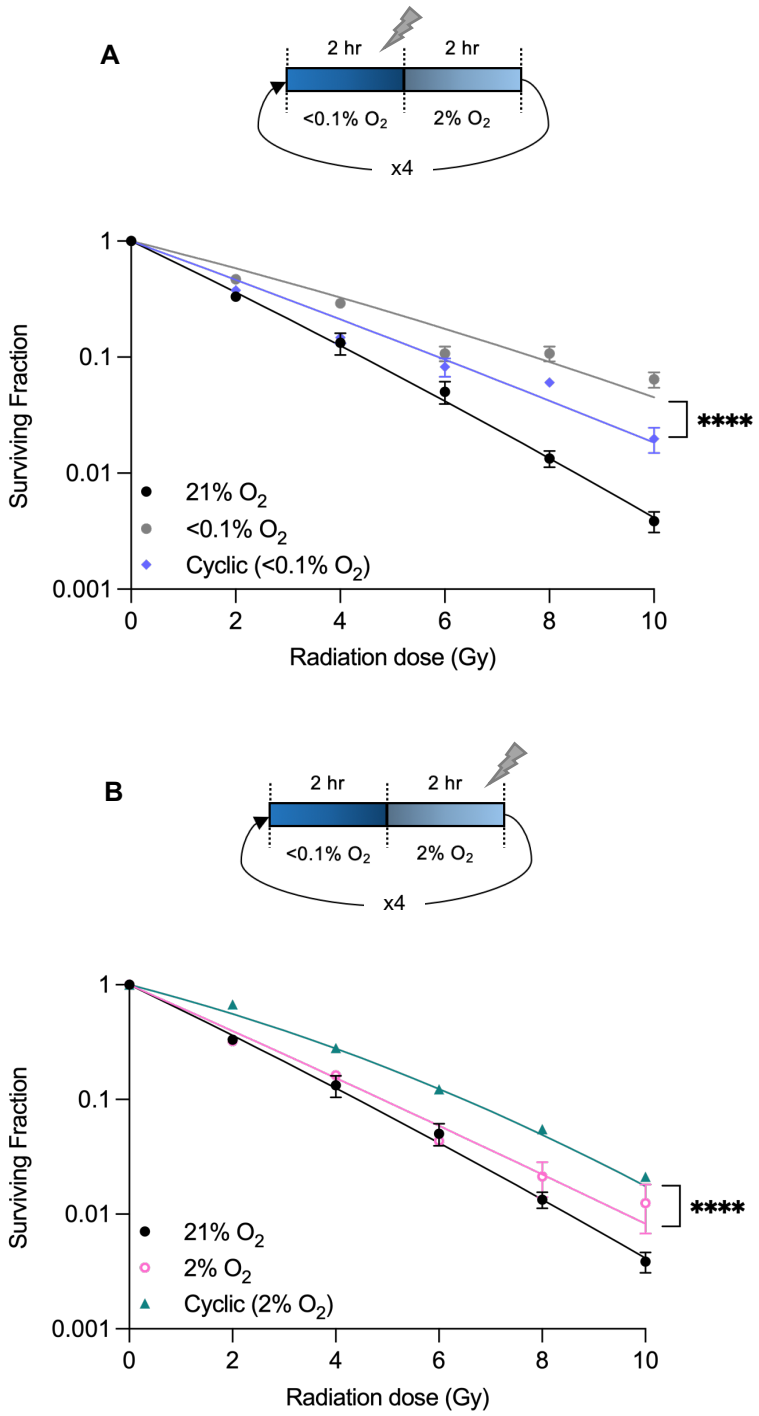


Figure 4.2.2: Cyclic hypoxia induces a distinct radioresistance response to 2% O_2 and <0.1% O_2. CAL51 were subjected to the indicated treatments for 16 h before irradiation and colony formation (A) Irradiation took place at the end of <0.1% O_2 portion of cyclic hypoxia in the 4th cycle. n=3. Two-way ANOVA **** = p <0.0001. (B) Irradiation took place at the end of 2% O_2 portion of cyclic hypoxia in the 4th cycle. n=3. Two-way ANOVA **** = p <0.0001.

4.3. FLASH

With the knowledge that cyclic hypoxia leads to a distinct radiation response to 2% O_2 and <0.1% O_2 with Cs irradiation, we were intrigued to investigate the response of cyclic hypoxia exposed cells to FLASH radiotherapy. Before beginning the FLASH experiments, method optimisation was required. Due to the FLASH protocol requiring cells to be irradiated horizontally we were unable to use the same methodology as the vertical Cs irradiation in which radiation boxes maintain the hypoxic environment (Figure 2.4). We hypothesised that through wrapping sealed T12.5 flasks in tight parafilm seal, we could maintain the hypoxic environment to the same extent as the radiation boxes. If this held true, then the surviving fraction of colonies would show the same radioresistance to those irradiated in the radiation box. Our results supported this hypothesis (Figure 4.3.1). Therefore, going forward FLASH was carried out with cells in sealed T12.5 flasks wrapped in parafilm to maintain hypoxia.

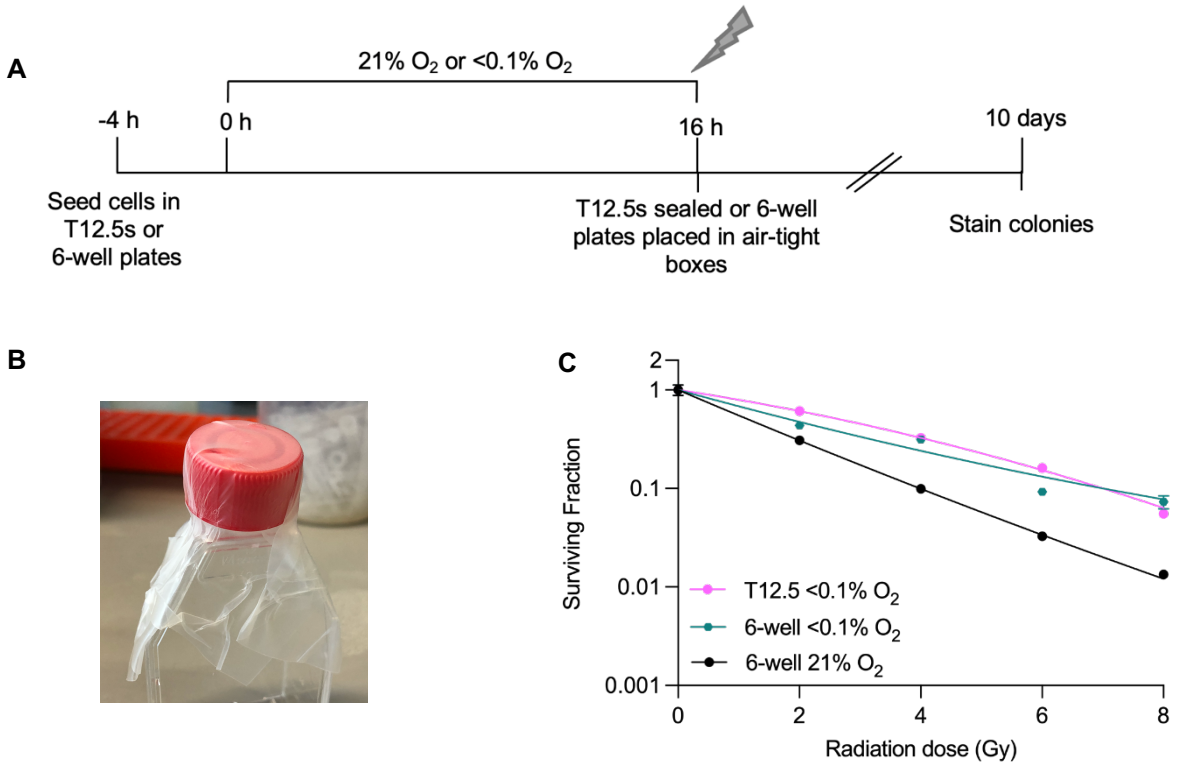


Figure 4.3.1: Preliminary experiment to determine if T12.5s can maintain hypoxia during irradiation. CAL51 were subjected to 16 h in the indicated treatments before irradiation (A) Schematic of the experimental set up. (B) T12.5 flasks were sealed (lids on tightly) and then wrapped in parafilm in the hypoxia chamber and then transported to the irradiator. (C) Colony survival curve comparison between cells irradiated in a 6-well plate under 21% O_2 (black line), cells irradiated in a 6-well plate in the radiation box to maintain <0.1% O_2 (green line) and cells irradiated in a parafilm-wrapped T12.5 to maintain <0.1% O_2 (pink line). n=1.

Previous studies show that radiosensitivity of cells in <0.1% O_2 exposed to the same dose of FLASH and Conv should result in the same survival (Cygler et al., 1994, Zackrisson et al., 1991). In contrast, in mild hypoxia cells exposed to FLASH should be significantly less radiosensitive compared to the same Conv dose above 15 Gy, with the difference in radiosensitivity emerging above 5 Gy (Adrian et al., 2020). Although our data is too preliminary to draw firm conclusions (n=2), it is supportive of these reports. Specifically, the surviving fraction of cells

in <0.1% O_2 at 8 Gy and 12 Gy FLASH do not differ to 8 Gy and 12 Gy Conv, respectively. Conversely, the surviving fraction of cells in 2% O_2 at 12 Gy FLASH is greater than cells at 12 Gy Conv (Figure 4.3.2). Considering the literature with the 2% O_2 results, we hypothesise that cells exposed to 2% O_2 would have a significant increase in the FLASH surviving fraction compared to Conv at 15 Gy. More repeats are required to confirm these results.

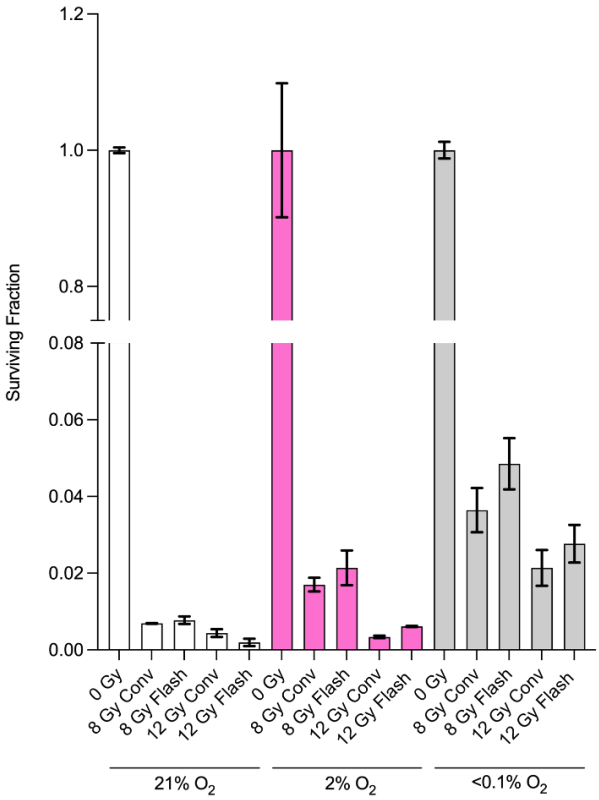


Figure 4.3.2: FLASH versus Conv radioresistance across 21% O_2, 2% O_2 and <0.1% O_2. Colony survival fraction of CAL51 cells exposed to 3 h 21% O_2, 2% O_2 or <0.1% O_2 prior to irradiation with conventional or FLASH radiotherapy. The surviving fraction is calculated from three flasks per condition, n=2.

With confidence in our FLASH experimental conditions, we investigated the response in cyclic hypoxia to FLASH compared to chronic <0.1% O_2. Our experimental design ensured that the conditions being compared were irradiated at the same level of oxygen therefore ruling out

the oxygen effect at the time of radiation. The surviving fraction of cells in <0.1% O_2 at 8 Gy and 12 Gy FLASH do not differ to 8 Gy and 12 Gy Conv, respectively (Figure 4.3.3). This is an experimental repeat to the Figure 4.3.2 data and is therefore supportive of the Figure 4.3.2 data. Cyclic hypoxia treated CAL51 irradiated at <0.1% O_2, suggest that the surviving fraction of cells at 8 Gy and 12 Gy FLASH is greater than 8 Gy and 12 Gy Conv (Figure 4.3.3). More repeats are required to confirm these results.

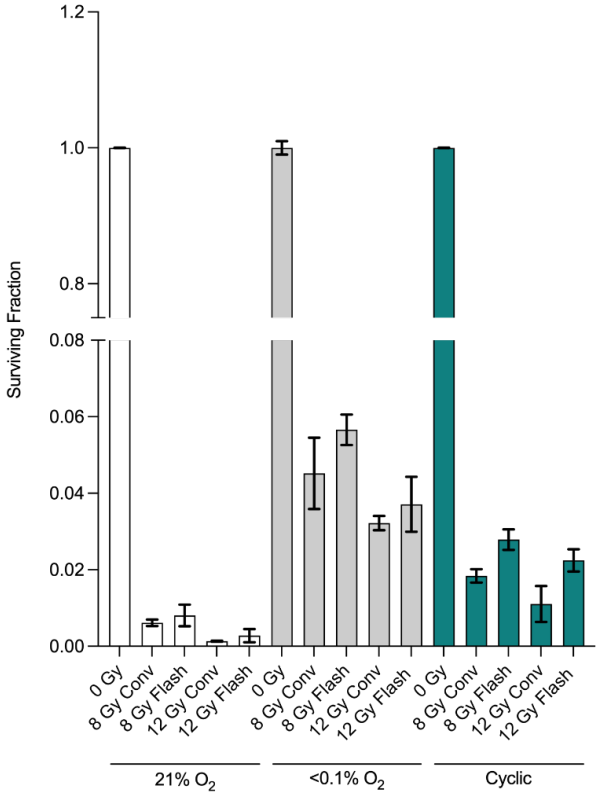


Figure 4.3.3. Cyclic hypoxia may induce differing radiosensitivity responses to FLASH compared to Conv. Colony survival fraction of CAL51 cells exposed to 6 h 21% O_2, <0.1% O_2 or cyclic hypoxia prior to irradiation. Irradiation took place at the end of the <0.1% O_2 portion of cyclic hypoxia in the 2nd cycle. The surviving fraction is calculated from three flasks per condition. n=1.

Discussion

The RNA-seq data presented in chapter 3 demonstrated numerous changes in gene expression in response to our range of hypoxic conditions. We hypothesised that some of these changes in gene expression could impact the response to DNA damaging therapies. *EPHA3* was selected as a candidate for further investigation. *EPHA3* encodes the receptor EphA3 which has been shown to promote tumour development as well as radiotherapy resistance (Janes et al., 2008, Pasquale, 2008, Kim et al., 2016). We therefore wanted to investigate the viability and radiosensitivity of CAL51 treated with siEPHA3. Unfortunately, our results showed no significant reduction on *EPHA3* mRNA. The siEPHA3 we used was not previously validated, however, was a smart pool. A smart pool combines four siRNAs specific to the target gene in a single reagent pool. These pooled siRNAs improve the prospect of effective gene silencing. As we did not see gene silencing there is potential that 20 μM siEPHA3 may be insufficient to knockdown *EPHA3* mRNA. This experiment should therefore be optimised with a higher concentration of siEPHA3. Previous reports have identified *EPHA3* as a HIF-1α target gene in mesenchymal stem cells (Martin-Rendon et al., 2007, To et al., 2014). Ours is the first report of *EPHA3* being induced in response to hypoxia in TNBC. Interestingly, our finding that *EPHA3* induction is restricted to cyclic conditions suggests that it may not be solely HIF-1α regulated or that this is an example of a stress specific HIF-1α effect.

We used Cs irradiation as a DNA-damaging technique to determine the response of cyclic hypoxia exposed TNBC cells to DNA-damaging therapies. Our results show that cyclic hypoxia exposed cells irradiated at 2% O_2 are more radioresistant than cells irradiated following static

2% O_2 treatment for the same amount of time. Conversely, we saw that cyclic hypoxia exposed cells irradiated at <0.1% O_2 were less radioresistant than cells irradiated following static <0.1% O_2 treatment for the same amount of time. We irradiated the cells at the end of the respective <0.1% O_2 or 2% O_2 portion of the cyclic protocol to allow for the residual oxygen in the plates from the previous concentration to have been fully displaced. Nonetheless, these results infer that potentially the oxygen concentrations at which we irradiated the cells in cyclic hypoxia are not the actual concentration of oxygen within the media/cells. Small differences in oxygen concentration can largely impact radiosensitivity, highlighted by 0.5% O_2 being the halfway point between the OER of 21% O_2 and <0.1% O_2 (Hall and Giaccia, 2011). It is possible that a small difference in the oxygen concentration between cyclic <0.1% O_2 and static <0.1% O_2, likely between 0.5% O_2 and <0.1% O_2, contributed to the increased radiosensitivity of cells irradiated in cyclic hypoxia (<0.1% O_2) compared to static <0.1% O_2. To investigate this further, it would be necessary to measure the oxygen concentration of the media in a cyclic hypoxia treated plate at the end of a <0.1% O_2 cycle segment with an oxygen probe (for example, OxyLite, from Oxford Optronics, Oxford, UK).

The FLASH results support the notion that the cyclic hypoxia exposed cells irradiated at <0.1% O_2 are not at true <0.1% O_2. Based on the oxygen depletion hypothesis, when cells are irradiated at <0.1% O_2 there should not be a difference in the surviving fraction of FLASH compared to Conv, as seen in our FLASH versus Conv results at static <0.1% O_2 (Abolfath et al., 2020, Adrian et al., 2020, Zackrisson et al., 1991, Cygler et al., 1994). It would therefore be predicted that cells irradiated in the <0.1% O_2 portion of cyclic hypoxia would have the same response. Our results indicate that cyclic hypoxia may have a decreased radiosensitivity to FLASH radiotherapy compared to Conv radiotherapy, inferring an oxygen concentration in

the T12.5 flask above <0.1% O_2. It must however be acknowledged that this cyclic hypoxia FLASH data is only n=1 and therefore no conclusions can be made until further repeats are carried out. In addition to this, it cannot be ruled out that there are biological mechanisms at play leading to the distinct radiotherapy response that we see in cyclic hypoxia, discussed in the next section.

CHAPTER 5: Discussion

Hypoxia in breast cancer has been linked to metastasis and therapy resistance and ultimately poor patient prognosis. More specifically, TNBC has the worst prognosis of all breast cancers and is the most metastatic, often leading to bone, brain and lung metastases (Chen et al., 2014, Loibl et al., 2021). The role of hypoxia in metastasis has been well characterised, nonetheless, the heterogenous nature of hypoxia is often overlooked with characterisation referring specifically to chronic hypoxia (Bader et al., 2020, Rankin and Giaccia, 2016). An array of studies show that cyclic hypoxia is commonplace within tumours and is associated with the most aggressive diseases (Cao et al., 2005, Hillestad et al., 2020, O'Connor et al., 2019, Ron et al., 2019, Yasui et al., 2010). This project had two main aims. The first was to characterise the biological response of TNBC to cyclic hypoxia comparative to 21% O_2 and static 2% O_2 and <0.1% O_2. The second aim was to understand the impact of DNA-damaging therapies in cyclic hypoxia compared to chronic hypoxia, using radiation as an exemplar DNA-damaging agent. Overall, we have shown that the response of TNBC to cyclic hypoxia is distinct to the response in static 2% O_2, <0.1% O_2 and 21% O_2. This distinct response is most prominent in the differing cell cycle dynamics, viability and gene expression patterns.

We first noticed that HIF-1α protein expression consistently had different banding across the different hypoxic conditions in our western blot analysis. These alternative banding patterns could be due to differing PTMs across <0.1% O_2, 2% O_2 and cyclic hypoxia. Through RNA-seq expression analysis of HIF-1α target genes, we saw that some genes under HIF-1α mediated transcription have significantly different levels of gene expression between the hypoxic conditions. More work is required to determine what explains the differing expression of HIF-

1α targets in the different hypoxic conditions, but there are a few possible explanations. The transcriptional activity and stability of HIF-1α is regulated by PTMs and biomolecular interactions. One possible explanation is that differing HIF-1α PTMs across the three hypoxic conditions may result in distinct HIF-1α mediated transcription of specific target genes. For example, *VEGF-A* is a HIF-1α target gene that has a largely increased log2fold expression in <0.1% O_2, slightly log2fold increase in expression in cyclic hypoxia and decreased log2fold expression in 2% O_2. It was interesting to see that previous studies have shown lysine-specific demethylase 1 (LSD1) demethylates HIF-1α at lysine 391 and that this demethylation event facilitates HIF-1 binding to the *VEGF* promoter (Kim et al., 2016, Lee et al., 2017). LSD1 is therefore an example of a protein that modifies HIF-1α which is also regulated in an oxygen dependent manner (Yang et al., 2017). Additionally, we see DDR induction in <0.1% O_2 alone. The DDR could be playing a role in <0.1% O_2 specific PTMs of HIF-1α. Previous studies have shown that ATM and ATR stabilise HIF-1α and that ATM phosphorylates HIF-1α at S696. This S696 phosphorylation is proposed to increase HIF-1α stability and subsequent transcriptional activity (Cam et al., 2010, Pires et al., 2012).

Aside from PTMs, a second possible explanation for the different expression of some HIF-1α target genes is differing HIF-1α binding partner interactions across the three hypoxic conditions. HIF-1α binding partners regulate transactivation through acting as co-activators or co-repressors (Semenza, 2017). Examples of co-activators include: signal transducer and activator of transcription 3 (STAT3) which binds to HIF1 target gene promoters and recruits p300/CBP and RNA polymerase II (Pawlus et al., 2014); mucin 1 (MUC1) which stabilises the p300/HIF-1α interaction (Kuo et al., 2015); and, transcriptional co-activator with PDZ-binding motif (TAZ) which increases HIF binding to HREs (Xiang et al., 2015). Examples of co-repressors

include: minichromosome maintenance complex component 7 (MCM7) which inhibits transactivation through hydroxylation (Hubbi et al., 2011); and, Sirtuin 1 (SIRT1) which prevents p300/HIF-1α binding through deacetylating HIF-1α on K674 (Lim et al., 2010). A large number of binding proteins are regulated by O_2 tension. For example, a recent study has shown that HIF-1α has 97 binding proteins significantly upregulated at 1% O_2 (Daly et al., 2021). Previous studies have shown that STAT3 is essential for maximal *VEGF* expression (Gray et al., 2005, Sánchez-Elsner et al., 2001). Potentially, STAT3 co-activation is specific to <0.1% O_2 and not 2% O_2 and cyclic hypoxia leading to a <0.1% O_2 *VEGF-A* expression increase.

Cyclic hypoxia appears to be a challenging environment for TNBC cell lines that decreases cell viability compared to chronic hypoxia. Our results highlight the fate of cells in cyclic hypoxia. A limitation of the MTT assay is that while we can infer a loss of viability in the conditions tested as it is also possible that the cells eventually recovered and went on to divide. In contrast, the colony survival assay shows a definitive loss of viability, such that the cells no longer have the ability to replicate. The colony survival assay does not however tell us why the cells are unable to replicate and there are several possible scenarios including apoptosis, senescence, necrosis and mitotic catastrophe. Moreover, p53 is a major determinant of cell fate after hypoxia (Hammond et al., 2002, Zhou et al., 2015). Of the cell lines tested, only the CAL51 have wild type p53 and therefore cell fate is likely to be different in these cells compared to the others investigated. Our previous studies demonstrated that in RKO cells (wild type p53) p53 accumulated in response to cyclic hypoxia, but this did not appear to lead to apoptosis. Instead, in the RKO cell line the biological response to cyclic hypoxia was suggestive of increased senescence although this was not formally proved (Bader et al., 2021). It is therefore possible that in the CAL51 cells cyclic hypoxia leads to p53-mediated

senescence. In order to investigate this, it would be necessary to first investigate markers of the DDR in CAL51 cells exposed to hypoxia (the data shown in Figure 3.1 is in MDA-MB-231 cells).

RKO cells undergo replication catastrophe following exposure to cyclic hypoxia (Bader et al., 2021). Replication catastrophe is characterised by the presence of replication stress and an accumulation of S-phase specific DNA damage (Toledo et al., 2013). Our results show that S-phase accumulation is occurring in cyclic hypoxia, however our protein expression analysis indicated a lack of DDR induction in MDA-MB-231 cells and hence a lack of replication stress and consequent catastrophe. However, our analysis into the DDR induction only focused on one TNBC cell line and two markers at one timepoint. It is possible that if we looked at more DDR markers over a greater timecourse in all the cell lines and particularly CAL51, a DDR would be observed. The many questions surrounding our cell fate hypothesis highlights the importance to carry out a greater investigation into the DDR activation in cyclic hypoxia. Additionally, the cell fate could further be examined through the use of apoptosis or senescence assays.

While p53 is a major determinant of cell fate in response to cellular stress, the majority of cancer cells have lost wild type p53 and so these pathways are less relevant (Mantovani et al., 2019). It is however, possible that cyclic hypoxia could lead to senescence in the absence of p53 as previous reports indicate that a p16-mediated senescent phenotype occurs in cells which are p53 deficient (Alcorta et al., 1996, Huschtscha and Reddel, 1999, Leong et al., 2009, Mirzayans et al., 2010, Stein et al., 1999). We therefore hypothesise if these cyclic hypoxia exposed p53 mutant cells are undergoing replication catastrophe their cell fate will be p16-

mediated senescence rather than the p53-mediated senescence we would see in CAL51. In order to investigate this, we would begin by exposing our cells to cyclic hypoxia and carrying out assays for senescence associated β-gal expression. In addition, as DNA damage is a key predictor of senescence, we would investigate the presence of DNA damage using the 53BP1 foci assay in cyclic hypoxia.

Our data demonstrate that exposure to cyclic hypoxia prior to irradiation impacts radiosensitivity and that this is likely linked to changes in cell cycle progression. Cyclic hypoxia induces an S-phase accumulation in MDA-MB-231 and CAL51. This S-phase accumulation is significant and unique to cyclic hypoxia. The S-phase portion of the cell cycle is linked to increased radioresistance (Pawlik and Keyomarsi, 2004). Cell survival data from synchronised Chinese hamster cells showed that cells are least sensitive to irradiation during S-phase, and increasing sensitivity then occurs in G1 followed by mitosis and the G2 phase of the cell cycle (Sinclair and Morton, 1963, Sinclair and Morton, 1965, Sinclair and Morton, 1966). S-phase-induced radioresistance is believed to be due to an increase in DNA synthesis and a subsequent increase in DNA repair enzymes. These repair enzymes therefore act to repair damage induced through radiation (Leadon, 1996). In addition to this, during S-phase there are increased intracellular levels of glutathione. Glutathione is a free radical scavenger, which has a protective role against the radicals that induce radiation-specific damage (Hanot et al., 2012, Shimizu et al., 1998). Our results highlight that cells exposed to cyclic hypoxia and irradiated at 2% O_2 have an increased radioresistance compared to cells exposed to static 2% O_2. We hypothesise that this difference in radiosensitivity between cells in cyclic hypoxia irradiated at 2% O_2 and cells in static 2% O_2 is due to the S-phase induced radioresistance in the cyclic exposed cells.

Our protein expression analysis and RNA-seq results point toward UPR induction in cyclic hypoxia. This is highly relevant to this project as a signature reflecting the IRE1/XBP1 branch of the UPR has previously been associated with aggressive TNBC. Through genome-wide mapping, XBP1 has been shown to play a role in driving TNBC tumorigenicity. XPB1 assembles with HIF-1α to form a transcriptional complex that regulates HIF-1α target gene expression through recruiting RNA polymerase II. The gene expression signature of XBP1 was correlated with hypoxic signatures that drive poor patient prognosis (Chen et al., 2014). It would be interesting to compare the expression of genes within the IRE1/XBP1 signature and HIF-1α targets upregulated by the signature in cyclic hypoxia compared to <0.1% O_2. This comparison would determine if the IRE1/XBP1 signature is more relevant to a specific form of hypoxia. Our results suggest that hypoxia signatures cannot be used to differentiate between mild hypoxia, severe hypoxia or acute hypoxia. It would be highly relevant and beneficial to try and determine more specific hypoxia signatures. For example, a cyclic-specific signature could identify a subset of patients with the poorest prognosis or who could benefit from specific therapies, for example those that modify the cell cycle.

Therapeutic potential for cyclic hypoxia

Cyclic hypoxia leads to an S-phase accumulation that is not seen in other hypoxic conditions. Therefore, this presents a mechanism to target cells in cyclic hypoxia. The use of ATR, Chk1 and CDK2 inhibitors have been shown to decrease the S-phase population in cyclic hypoxia (Bader et al., 2021). In addition to this, agents such as palbociclib or abemaciclib, that inhibit CDK4/6 involved in G1/S transition, could be used to prevent S-phase accumulation. These

CDK4/6 inhibitors have already been shown to decrease radioresistance in chronic hypoxia exposed head and neck squamous cell carcinoma and hence the impact in cyclic hypoxia would be interesting to investigate (Göttgens et al., 2019). In the future, it would therefore be interesting to investigate the sensitivity of cells to CDK4/6i in cyclic hypoxia, using static conditions (<0.1 O_2 and 2% O_2) as a comparator. In addition to this, if further experiments determine our TNBC cells are undergoing replication catastrophe, replication catastrophe is the signal that leads to APOBEC3B induction (Bader et al., 2021). Therefore, one could not only target the potential radioresistant response in cyclic hypoxia through decreasing the S-phase accumulation but potentially, could also counteract genomic instability seen in cyclic hypoxia that stems for the S-phase accumulation of the cell cycle.

Future Directions

There are three main follow up experiments to carry out from this project. The first is to determine whether the DDR is activated in TNBC cyclic hypoxia exposed cells. The second is to determine the pO_2 in the media of cells at the time of cyclic hypoxia <0.1% O_2 irradiation. The third is to optimise the siEPHA3 and determine whether knockdown of *EPHA3* sensitises cells to radiotherapy.

We chose to study the response of cyclic hypoxia exposed TNBC cells to radiation with the outlook that radiation is an easily controlled DNA damaging agent and therefore our results would translate to other forms of DNA damaging therapy. However, we found that cyclic hypoxia complicates the use of radiotherapy as a representative DNA damaging agent due to uncertainty of pO_2 in the media of cells at the time of cyclic hypoxia <0.1% O_2 irradiation.

Therefore, it is important to consider the use of chemical DNA damaging therapies, such as doxorubicin, cisplatin and paclitaxel, in the future as they may be more straightforward and relevant to characterise the therapeutic response of TNBC to cyclic hypoxia.

REFERENCES

ABOLFATH, R., GROSSHANS, D. & MOHAN, R. 2020. Oxygen depletion in FLASH ultra-high-dose-rate radiotherapy: A molecular dynamics simulation. *Med Phys,* 47**,** 6551-6561.

ADRIAN, G., KONRADSSON, E., LEMPART, M., BÄCK, S., CEBERG, C. & PETERSSON, K. 2020. The FLASH effect depends on oxygen concentration. *Br J Radiol,* 93**,** 20190702.

ALBANESE, A., DALY, L. A., MENNERICH, D., KIETZMANN, T. & SÉE, V. 2020. The Role of Hypoxia-Inducible Factor Post-Translational Modifications in Regulating Its Localisation, Stability, and Activity. *Int J Mol Sci,* 22.

ALCORTA, D. A., XIONG, Y., PHELPS, D., HANNON, G., BEACH, D. & BARRETT, J. C. 1996. Involvement of the cyclin-dependent kinase inhibitor p16 (INK4a) in replicative senescence of normal human fibroblasts. *Proceedings of the National Academy of Sciences,* 93**,** 13742-13747.

ALEXANDROV, L. B., NIK-ZAINAL, S., WEDGE, D. C., APARICIO, S. A., BEHJATI, S., BIANKIN, A. V., BIGNELL, G. R., BOLLI, N., BORG, A., BØRRESEN-DALE, A. L., BOYAULT, S., BURKHARDT, B., BUTLER, A. P., CALDAS, C., DAVIES, H. R., DESMEDT, C., EILS, R., EYFJÖRD, J. E., FOEKENS, J. A., GREAVES, M., HOSODA, F., HUTTER, B., ILICIC, T., IMBEAUD, S., IMIELINSKI, M., JÄGER, N., JONES, D. T., JONES, D., KNAPPSKOG, S., KOOL, M., LAKHANI, S. R., LÓPEZ-OTÍN, C., MARTIN, S., MUNSHI, N. C., NAKAMURA, H., NORTHCOTT, P. A., PAJIC, M., PAPAEMMANUIL, E., PARADISO, A., PEARSON, J. V., PUENTE, X. S., RAINE, K., RAMAKRISHNA, M., RICHARDSON, A. L., RICHTER, J., ROSENSTIEL, P., SCHLESNER, M., SCHUMACHER, T. N., SPAN, P. N., TEAGUE, J. W., TOTOKI, Y., TUTT, A. N., VALDÉS-MAS, R., VAN BUUREN, M. M., VAN 'T VEER, L., VINCENT-SALOMON, A., WADDELL, N., YATES, L. R., ZUCMAN-ROSSI, J., FUTREAL, P. A., MCDERMOTT, U., LICHTER, P., MEYERSON, M., GRIMMOND, S. M., SIEBERT, R., CAMPO, E., SHIBATA, T., PFISTER, S. M., CAMPBELL, P. J. & STRATTON, M. R. 2013. Signatures of mutational processes in human cancer. *Nature,* 500**,** 415-21.

AMIN, A., KARPOWICZ, P. A., CAREY, T. E., ARBISER, J., NAHTA, R., CHEN, Z. G., DONG, J. T., KUCUK, O., KHAN, G. N., HUANG, G. S., MI, S., LEE, H. Y., REICHRATH, J., HONOKI, K., GEORGAKILAS, A. G., AMEDEI, A., AMIN, A., HELFERICH, B., BOOSANI, C. S., CIRIOLO, M. R., CHEN, S., MOHAMMED, S. I., AZMI, A. S., KEITH, W. N., BHAKTA, D., HALICKA, D., NICCOLAI, E., FUJII, H., AQUILANO, K., ASHRAF, S. S., NOWSHEEN, S., YANG, X., BILSLAND, A. & SHIN, D. M. 2015. Evasion of anti-growth signaling: A key step in tumorigenesis and potential target for treatment and prophylaxis by natural compounds. *Semin Cancer Biol,* 35 Suppl**,** S55-s77.

ANBALAGAN, S., BIASOLI, D., LESZCZYNSKA, K. B., MUKHERJEE, S. & HAMMOND, E. M. 2015. In Vitro Radiosensitization of Esophageal Cancer Cells with the Aminopeptidase Inhibitor CHR-2797. *Radiat Res,* 184**,** 259-65.

BADER, S. B., DEWHIRST, M. W. & HAMMOND, E. M. 2020. Cyclic Hypoxia: An Update on Its Characteristics, Methods to Measure It and Biological Implications in Cancer. *Cancers (Basel),* 13.

BADER, S. B., MA, T. S., SIMPSON, C. J., LIANG, J., MAEZONO, S. E. B., OLCINA, M. M., BUFFA, F. M. & HAMMOND, E. M. 2021. Replication catastrophe induced by cyclic hypoxia leads to increased APOBEC3B activity. *Nucleic Acids Res,* 49**,** 7492-7506.

BAGHBAN, R., ROSHANGAR, L., JAHANBAN-ESFAHLAN, R., SEIDI, K., EBRAHIMI-KALAN, A., JAYMAND, M., KOLAHIAN, S., JAVAHERI, T. & ZARE, P. 2020. Tumor microenvironment

complexity and therapeutic implications at a glance. *Cell Communication and Signaling,* 18**,** 59.

BARTOSZEWSKA, S. & COLLAWN, J. F. 2020. Unfolded protein response (UPR) integrated signaling networks determine cell fate during hypoxia. *Cell Mol Biol Lett,* 25**,** 18.

BENCOKOVA, Z., KAUFMANN, M. R., PIRES, I. M., LECANE, P. S., GIACCIA, A. J. & HAMMOND, E. M. 2009. ATM activation and signaling under hypoxic conditions. *Mol Cell Biol,* 29**,** 526-37.

BERNARDI, R. & GIANNI, L. 2014. Hallmarks of triple negative breast cancer emerging at last? *Cell research,* 24**,** 904-905.

BHOO-PATHY, N., VERKOOIJEN, H. M., WONG, F. Y., PIGNOL, J. P., KWONG, A., TAN, E. Y., AISHAH TAIB, N., NEI, W. L., HO, G. F., TAN, B., CHAN, P., LEE, S. C., HARTMAN, M., YIP, C. H. & DENT, R. 2015. Prognostic role of adjuvant radiotherapy in triple-negative breast cancer: A historical cohort study. *Int J Cancer,* 137**,** 2504-12.

BINDRA, R. S. & GLAZER, P. M. 2007. Repression of RAD51 gene expression by E2F4/p130 complexes in hypoxia. *Oncogene,* 26**,** 2048-2057.

BLACKFORD, A. N. & JACKSON, S. P. 2017. ATM, ATR, and DNA-PK: The Trinity at the Heart of the DNA Damage Response. *Mol Cell,* 66**,** 801-817.

BOLLAND, H., MA, T. S., RAMLEE, S., RAMADAN, K. & HAMMOND, E. M. 2021. Links between the unfolded protein response and the DNA damage response in hypoxia: a systematic review. *Biochem Soc Trans,* 49**,** 1251-1263.

BRAUN, R. D., LANZEN, J. L. & DEWHIRST, M. W. 1999. Fourier analysis of fluctuations of oxygen tension and blood flow in R3230Ac tumors and muscle in rats. *Am J Physiol,* 277**,** H551-68.

BRAY, F., LAVERSANNE, M., WEIDERPASS, E. & SOERJOMATARAM, I. 2021. The ever-increasing importance of cancer as a leading cause of premature death worldwide. *Cancer,* 127**,** 3029-3030.

BROWN, J. M. & WILSON, W. R. 2004. Exploiting tumour hypoxia in cancer treatment. *Nat Rev Cancer,* 4**,** 437-47.

BUFFA, F. M., HARRIS, A. L., WEST, C. M. & MILLER, C. J. 2010. Large meta-analysis of multiple cancers reveals a common, compact and highly prognostic hypoxia metagene. *Br J Cancer,* 102**,** 428-35.

CAIADO, F., SILVA-SANTOS, B. & NORELL, H. 2016. Intra-tumour heterogeneity – going beyond genetics. *The FEBS Journal,* 283**,** 2245-2258.

CAM, H., EASTON, J. B., HIGH, A. & HOUGHTON, P. J. 2010. mTORC1 signaling under hypoxic conditions is controlled by ATM-dependent phosphorylation of HIF-1α. *Mol Cell,* 40**,** 509-20.

CAO, X., ZHANG, R., ESIPOVA, T. V., ALLU, S. R., ASHRAF, R., RAHMAN, M., GUNN, J. R., BRUZA, P., GLADSTONE, D. J., WILLIAMS, B. B., SWARTZ, H. M., HOOPES, P. J., VINOGRADOV, S. A. & POGUE, B. W. 2021. Quantification of Oxygen Depletion During FLASH Irradiation In Vitro and In Vivo. *Int J Radiat Oncol Biol Phys*.

CAO, Y., LI, C. Y., MOELLER, B. J., YU, D., ZHAO, Y., DREHER, M. R., SHAN, S. & DEWHIRST, M. W. 2005. Observation of incipient tumor angiogenesis that is independent of hypoxia and hypoxia inducible factor-1 activation. *Cancer Res,* 65**,** 5498-505.

CASWELL, D. R. & SWANTON, C. 2017. The role of tumour heterogeneity and clonal cooperativity in metastasis, immune evasion and clinical outcome. *BMC Medicine,* 15**,** 133.

CHEE, N. T., LOHSE, I. & BROTHERS, S. P. 2019. mRNA-to-protein translation in hypoxia. *Mol Cancer,* 18**,** 49.

CHEN, A., SCENEAY, J., GÖDDE, N., KINWEL, T., HAM, S., THOMPSON, E. W., HUMBERT, P. O. & MÖLLER, A. 2018. Intermittent hypoxia induces a metastatic phenotype in breast cancer. *Oncogene,* 37**,** 4214-4225.

CHEN, W. L., WANG, C. C., LIN, Y. J., WU, C. P. & HSIEH, C. H. 2015. Cycling hypoxia induces chemoresistance through the activation of reactive oxygen species-mediated B-cell lymphoma extra-long pathway in glioblastoma multiforme. *J Transl Med,* 13**,** 389.

CHEN, X., ILIOPOULOS, D., ZHANG, Q., TANG, Q., GREENBLATT, M. B., HATZIAPOSTOLOU, M., LIM, E., TAM, W. L., NI, M., CHEN, Y., MAI, J., SHEN, H., HU, D. Z., ADORO, S., HU, B., SONG, M., TAN, C., LANDIS, M. D., FERRARI, M., SHIN, S. J., BROWN, M., CHANG, J. C., LIU, X. S. & GLIMCHER, L. H. 2014. XBP1 promotes triple-negative breast cancer by controlling the HIF1α pathway. *Nature,* 508**,** 103-107.

CLAVO, A. C., BROWN, R. S. & WAHL, R. L. 1995. Fluorodeoxyglucose uptake in human cancer cell lines is increased by hypoxia. *J Nucl Med,* 36**,** 1625-32.

COPPLE, B. L. 2010. Hypoxia stimulates hepatocyte epithelial to mesenchymal transition by hypoxia-inducible factor and transforming growth factor-beta-dependent mechanisms. *Liver Int,* 30**,** 669-82.

CYGLER, J., KLASSEN, N. V., ROSS, C. K., BICHAY, T. J. & RAAPHORST, G. P. 1994. The Survival of Aerobic and Anoxic Human Glioma and Melanoma Cells after Irradiation at Ultrahigh and Clinical Dose Rates. *Radiation Research,* 140**,** 79-84.

DA MOTTA, L. L., LEDAKI, I., PURSHOUSE, K., HAIDER, S., DE BASTIANI, M. A., BABAN, D., MOROTTI, M., STEERS, G., WIGFIELD, S., BRIDGES, E., LI, J. L., KNAPP, S., EBNER, D., KLAMT, F., HARRIS, A. L. & MCINTYRE, A. 2017. The BET inhibitor JQ1 selectively impairs tumour response to hypoxia and downregulates CA9 and angiogenesis in triple negative breast cancer. *Oncogene,* 36**,** 122-132.

DALY, L. A., BROWNRIDGE, P. J., BATIE, M., ROCHA, S., SÉE, V. & EYERS, C. E. 2021. Oxygen-dependent changes in binding partners and post-translational modifications regulate the abundance and activity of HIF-1α/2α. *Science Signaling,* 14**,** eabf6685.

DANEAU, G., BOIDOT, R., MARTINIVE, P. & FERON, O. 2010. Identification of Cyclooxygenase-2 as a Major Actor of the Transcriptomic Adaptation of Endothelial and Tumor Cells to Cyclic Hypoxia: Effect on Angiogenesis and Metastases. *Clinical Cancer Research,* 16**,** 410-419.

DAVID, A. R. & ZIMMERMAN, M. R. 2010. Cancer: an old disease, a new disease or something in between? *Nat Rev Cancer,* 10**,** 728-33.

DAVIES, M. A. & SAMUELS, Y. 2010. Analysis of the genome to personalize therapy for melanoma. *Oncogene,* 29**,** 5545-55.

DEWHIRST, M. W. 2009. Relationships between cycling hypoxia, HIF-1, angiogenesis and oxidative stress. *Radiat Res,* 172**,** 653-65.

DEWHIRST, M. W., KIMURA, H., REHMUS, S. W., BRAUN, R. D., PAPAHADJOPOULOS, D., HONG, K. & SECOMB, T. W. 1996. Microvascular studies on the origins of perfusion-limited hypoxia. *Br J Cancer Suppl,* 27**,** S247-51.

DEWHIRST, M. W., ONG, E. T., BRAUN, R. D., SMITH, B., KLITZMAN, B., EVANS, S. M. & WILSON, D. 1999. Quantification of longitudinal tissue pO2 gradients in window chamber tumours: impact on tumour hypoxia. *British Journal of Cancer,* 79**,** 1717-1722.

DUAN, C. 2016. Hypoxia-inducible factor 3 biology: complexities and emerging themes. *Am J Physiol Cell Physiol,* 310**,** C260-9.

EGEBLAD, M., NAKASONE, E. S. & WERB, Z. 2010. Tumors as organs: complex tissues that interface with the entire organism. *Dev Cell,* 18**,** 884-901.

ELLINGSEN, C., OVREBØ, K. M., GALAPPATHI, K., MATHIESEN, B. & ROFSTAD, E. K. 2012. pO_2 fluctuation pattern and cycling hypoxia in human cervical carcinoma and melanoma xenografts. *Int J Radiat Oncol Biol Phys,* 83**,** 1317-23.

ESTRELLA, V., CHEN, T., LLOYD, M., WOJTKOWIAK, J., CORNNELL, H. H., IBRAHIM-HASHIM, A., BAILEY, K., BALAGURUNATHAN, Y., ROTHBERG, J. M., SLOANE, B. F., JOHNSON, J., GATENBY, R. A. & GILLIES, R. J. 2013. Acidity generated by the tumor microenvironment drives local invasion. *Cancer Res,* 73**,** 1524-35.

EWING, D. 1998. The oxygen fixation hypothesis: a reevaluation. *Am J Clin Oncol,* 21**,** 355-61.

FOSKOLOU, I. P., JORGENSEN, C., LESZCZYNSKA, K. B., OLCINA, M. M., TARHONSKAYA, H., HAISMA, B., D'ANGIOLELLA, V., MYERS, W. K., DOMENE, C., FLASHMAN, E. & HAMMOND, E. M. 2017. Ribonucleotide Reductase Requires Subunit Switching in Hypoxia to Maintain DNA Replication. *Mol Cell,* 66**,** 206-220.e9.

FRANKEN, N. A. P., RODERMOND, H. M., STAP, J., HAVEMAN, J. & VAN BREE, C. 2006. Clonogenic assay of cells in vitro. *Nature Protocols,* 1**,** 2315-2319.

FRIDMAN, W. H., PAGÈS, F., SAUTÈS-FRIDMAN, C. & GALON, J. 2012. The immune contexture in human tumours: impact on clinical outcome. *Nature Reviews Cancer,* 12**,** 298-306.

FUHRMANN, D. C., WITTIG, I., HEIDE, H., DEHNE, N. & BRÜNE, B. 2013. Chronic hypoxia alters mitochondrial composition in human macrophages. *Biochimica et Biophysica Acta (BBA) - Proteins and Proteomics,* 1834**,** 2750-2760.

GNANT, M., THOMSSEN, C. & HARBECK, N. 2015. St. Gallen/Vienna 2015: A Brief Summary of the Consensus Discussion. *Breast Care,* 10**,** 124-130.

GONÇALVES, M. R., JOHNSON, S. P., RAMASAWMY, R., PEDLEY, R. B., LYTHGOE, M. F. & WALKER-SAMUEL, S. 2015. Decomposition of spontaneous fluctuations in tumour oxygenation using BOLD MRI and independent component analysis. *British Journal of Cancer,* 113**,** 1168-1177.

GÖTTGENS, E. L., BUSSINK, J., LESZCZYNSKA, K. B., PETERS, H., SPAN, P. N. & HAMMOND, E. M. 2019. Inhibition of CDK4/CDK6 Enhances Radiosensitivity of HPV Negative Head and Neck Squamous Cell Carcinomas. *Int J Radiat Oncol Biol Phys,* 105**,** 548-558.

GRAEBER, T. G., OSMANIAN, C., JACKS, T., HOUSMAN, D. E., KOCH, C. J., LOWE, S. W. & GIACCIA, A. J. 1996. Hypoxia-mediated selection of cells with diminished apoptotic potential in solid tumours. *Nature,* 379**,** 88-91.

GRAHAM, K. & UNGER, E. 2018. Overcoming tumor hypoxia as a barrier to radiotherapy, chemotherapy and immunotherapy in cancer treatment. *Int J Nanomedicine,* 13**,** 6049-6058.

GRAY, L. H., CONGER, A. D., EBERT, M., HORNSEY, S. & SCOTT, O. C. 1953. The concentration of oxygen dissolved in tissues at the time of irradiation as a factor in radiotherapy. *Br J Radiol,* 26**,** 638-48.

GRAY, M. J., ZHANG, J., ELLIS, L. M., SEMENZA, G. L., EVANS, D. B., WATOWICH, S. S. & GALLICK, G. E. 2005. HIF-1alpha, STAT3, CBP/p300 and Ref-1/APE are components of a transcriptional complex that regulates Src-dependent hypoxia-induced expression of VEGF in pancreatic and prostate carcinomas. *Oncogene,* 24**,** 3110-20.

GWAK, G. Y., YOON, J. H., KIM, K. M., LEE, H. S., CHUNG, J. W. & GORES, G. J. 2005. Hypoxia stimulates proliferation of human hepatoma cells through the induction of hexokinase II expression. *J Hepatol,* 42**,** 358-64.

HAIDER, S., MCINTYRE, A., VAN STIPHOUT, R. G. P. M., WINCHESTER, L. M., WIGFIELD, S., HARRIS, A. L. & BUFFA, F. M. 2016. Genomic alterations underlie a pan-cancer metabolic shift associated with tumour hypoxia. *Genome biology,* 17**,** 140-140.

HALL, E. J. & GIACCIA, A. J. 2011. *Radiobiology for the Radiologist,* Philadelphia, UNITED STATES, Wolters Kluwer Health.

HAMMOND, E. M., ASSELIN, M. C., FORSTER, D., O'CONNOR, J. P., SENRA, J. M. & WILLIAMS, K. J. 2014. The meaning, measurement and modification of hypoxia in the laboratory and the clinic. *Clin Oncol (R Coll Radiol),* 26**,** 277-88.

HAMMOND, E. M., DENKO, N. C., DORIE, M. J., ABRAHAM, R. T. & GIACCIA, A. J. 2002. Hypoxia links ATR and p53 through replication arrest. *Mol Cell Biol,* 22**,** 1834-43.

HAMMOND, E. M. & GIACCIA, A. J. 2005. The role of p53 in hypoxia-induced apoptosis. *Biochem Biophys Res Commun,* 331**,** 718-25.

HAN, J., MEI, Z., LU, C., QIAN, J., LIANG, Y., SUN, X., PAN, Z., KONG, D., XU, S., LIU, Z., GAO, Y., QI, G., SHOU, Y., CHEN, S., CAO, Z., ZHAO, Y., LIN, C., ZHAO, Y., GENG, Y., CHEN, J., YAN, X., MA, W. & YANG, G. 2021. Ultra-High Dose Rate FLASH Irradiation Induced Radio-Resistance of Normal Fibroblast Cells Can Be Enhanced by Hypoxia and Mitochondrial Dysfunction Resulting From Loss of Cytochrome C. *Front Cell Dev Biol,* 9**,** 672929.

HANAHAN, D. & WEINBERG, R. A. 2000. The hallmarks of cancer. *Cell,* 100**,** 57-70.

HANAHAN, D. & WEINBERG, R. A. 2011. Hallmarks of cancer: the next generation. *Cell,* 144**,** 646-74.

HANOT, M., BOIVIN, A., MALÉSYS, C., BEUVE, M., COLLIAUX, A., FORAY, N., DOUKI, T., ARDAIL, D. & RODRIGUEZ-LAFRASSE, C. 2012. Glutathione depletion and carbon ion radiation potentiate clustered DNA lesions, cell death and prevent chromosomal changes in cancer cells progeny. *PLoS One,* 7**,** e44367.

HE, M. Y., RANCOULE, C., REHAILIA-BLANCHARD, A., ESPENEL, S., TRONE, J. C., BERNICHON, E., GUILLAUME, E., VALLARD, A. & MAGNÉ, N. 2018. Radiotherapy in triple-negative breast cancer: Current situation and upcoming strategies. *Crit Rev Oncol Hematol,* 131**,** 96-101.

HICKEY, M. M. & SIMON, M. C. 2006. Regulation of angiogenesis by hypoxia and hypoxia-inducible factors. *Curr Top Dev Biol,* 76**,** 217-57.

HICKMAN, E. S., MORONI, M. C. & HELIN, K. 2002. The role of p53 and pRB in apoptosis and cancer. *Curr Opin Genet Dev,* 12**,** 60-6.

HILLESTAD, T., HOMPLAND, T., FJELDBO, C. S., SKINGEN, V. E., SALBERG, U. B., AARNES, E. K., NILSEN, A., LUND, K. V., EVENSEN, T. S., KRISTENSEN, G. B., STOKKE, T. & LYNG, H. 2020. MR Imaging Distinguishes Tumor Hypoxia Levels of Different Prognostic and Biological Significance in Cervical Cancer. *Cancer Res*.

HLOUSCHEK, J., HANSEL, C., JENDROSSEK, V. & MATSCHKE, J. 2018a. The Mitochondrial Citrate Carrier (SLC25A1) Sustains Redox Homeostasis and Mitochondrial Metabolism Supporting Radioresistance of Cancer Cells With Tolerance to Cycling Severe Hypoxia. *Front Oncol,* 8**,** 170.

HLOUSCHEK, J., RITTER, V., WIRSDÖRFER, F., KLEIN, D., JENDROSSEK, V. & MATSCHKE, J. 2018b. Targeting SLC25A10 alleviates improved antioxidant capacity and associated radioresistance of cancer cells induced by chronic-cycling hypoxia. *Cancer Lett,* 439**,** 24-38.

HOMPLAND, T., FJELDBO, C. S. & LYNG, H. 2021. Tumor Hypoxia as a Barrier in Cancer Therapy: Why Levels Matter. *Cancers (Basel),* 13.

HORSMAN, M. R., MORTENSEN, L. S., PETERSEN, J. B., BUSK, M. & OVERGAARD, J. 2012. Imaging hypoxia to improve radiotherapy outcome. *Nature Reviews Clinical Oncology,* 9**,** 674-687.

HOWLADER, N. N. A., KRAPCHO, M., NEYMAN, N., AMINOU, R., WALDRON, W., ALTEKRUSE, S. F., KOSARY, C. L., RUHL , J., TATALOVICH, Z., CHO, H., MARIOTTO, A., EISNER, M. P., LEWIS, D. R., CHEN, H. S., FEUER, E. J., CRONIN, K. A. & EDWARDS, B. K. 2011. *SEER cancer statistics review, 1975-2008* [Online]. National Cancer Institute, Bethesda. [Accessed].

HSIEH, C. H., LEE, C. H., LIANG, J. A., YU, C. Y. & SHYU, W. C. 2010. Cycling hypoxia increases U87 glioma cell radioresistance via ROS induced higher and long-term HIF-1 signal transduction activity. *Oncol Rep,* 24**,** 1629-36.

HSIEH, C. H., SHYU, W. C., CHIANG, C. Y., KUO, J. W., SHEN, W. C. & LIU, R. S. 2011. NADPH oxidase subunit 4-mediated reactive oxygen species contribute to cycling hypoxia-promoted tumor progression in glioblastoma multiforme. *PLoS One,* 6**,** e23945.

HSIEH, C. H., WU, C. P., LEE, H. T., LIANG, J. A., YU, C. Y. & LIN, Y. J. 2012. NADPH oxidase subunit 4 mediates cycling hypoxia-promoted radiation resistance in glioblastoma multiforme. *Free Radic Biol Med,* 53**,** 649-58.

HUBBI, M. E., LUO, W., BAEK, J. H. & SEMENZA, G. L. 2011. MCM proteins are negative regulators of hypoxia-inducible factor 1. *Mol Cell,* 42**,** 700-12.

HUSCHTSCHA, L. I. & REDDEL, R. R. 1999. p16INK4a and the control of cellular proliferative life span. *Carcinogenesis,* 20**,** 921-926.

JAFRI, M. A., ANSARI, S. A., ALQAHTANI, M. H. & SHAY, J. W. 2016. Roles of telomeres and telomerase in cancer, and advances in telomerase-targeted therapies. *Genome Med,* 8**,** 69.

JANES, P. W., ADIKARI, S. & LACKMANN, M. 2008. Eph/ephrin signalling and function in oncogenesis: lessons from embryonic development. *Curr Cancer Drug Targets,* 8**,** 473-9.

JING, X., YANG, F., SHAO, C., WEI, K., XIE, M., SHEN, H. & SHU, Y. 2019. Role of hypoxia in cancer therapy by regulating the tumor microenvironment. *Molecular Cancer,* 18**,** 157.

JOHNSON, A. B., DENKO, N. & BARTON, M. C. 2008. Hypoxia induces a novel signature of chromatin modifications and global repression of transcription. *Mutat Res,* 640**,** 174-9.

JOYCE, J. A. & POLLARD, J. W. 2009. Microenvironmental regulation of metastasis. *Nat Rev Cancer,* 9**,** 239-52.

KAELIN, W. G., JR. & RATCLIFFE, P. J. 2008. Oxygen sensing by metazoans: the central role of the HIF hydroxylase pathway. *Mol Cell,* 30**,** 393-402.

KAPLAN, R. N., RIBA, R. D., ZACHAROULIS, S., BRAMLEY, A. H., VINCENT, L., COSTA, C., MACDONALD, D. D., JIN, D. K., SHIDO, K., KERNS, S. A., ZHU, Z., HICKLIN, D., WU, Y., PORT, J. L., ALTORKI, N., PORT, E. R., RUGGERO, D., SHMELKOV, S. V., JENSEN, K. K., RAFII, S. & LYDEN, D. 2005. VEGFR1-positive haematopoietic bone marrow progenitors initiate the pre-metastatic niche. *Nature,* 438**,** 820-7.

KARNOUB, A. E., DASH, A. B., VO, A. P., SULLIVAN, A., BROOKS, M. W., BELL, G. W., RICHARDSON, A. L., POLYAK, K., TUBO, R. & WEINBERG, R. A. 2007. Mesenchymal stem cells within tumour stroma promote breast cancer metastasis. *Nature,* 449**,** 557-63.

KEATS, J. J., CHESI, M., EGAN, J. B., GARBITT, V. M., PALMER, S. E., BRAGGIO, E., VAN WIER, S., BLACKBURN, P. R., BAKER, A. S., DISPENZIERI, A., KUMAR, S., RAJKUMAR, S. V., CARPTEN, J. D., BARRETT, M., FONSECA, R., STEWART, A. K. & BERGSAGEL, P. L. 2012. Clonal competition with alternating dominance in multiple myeloma. *Blood,* 120**,** 1067-76.

KHARB, R., HAIDER, K., NEHA, K. & YAR, M. S. 2020. Aromatase inhibitors: Role in postmenopausal breast cancer. *Arch Pharm (Weinheim),* 353**,** e2000081.

KIM, J. W., TCHERNYSHYOV, I., SEMENZA, G. L. & DANG, C. V. 2006. HIF-1-mediated expression of pyruvate dehydrogenase kinase: a metabolic switch required for cellular adaptation to hypoxia. *Cell Metab,* 3**,** 177-85.

KIM, S. H., LEE, W. H., KIM, S. W., JE, H. U., LEE, J. C., CHANG, H. W., KIM, Y. M., KIM, K., KIM, S. Y. & HAN, M. W. 2018. EphA3 maintains radioresistance in head and neck cancers through epithelial mesenchymal transition. *Cell Signal,* 47**,** 122-130.

KIM, Y., NAM, H. J., LEE, J., PARK, D. Y., KIM, C., YU, Y. S., KIM, D., PARK, S. W., BHIN, J., HWANG, D., LEE, H., KOH, G. Y. & BAEK, S. H. 2016. Methylation-dependent regulation of HIF-1α stability restricts retinal and tumour angiogenesis. *Nature Communications,* 7**,** 10347.

KORITZINSKY, M., LEVITIN, F., VAN DEN BEUCKEN, T., RUMANTIR, R. A., HARDING, N. J., CHU, K. C., BOUTROS, P. C., BRAAKMAN, I. & WOUTERS, B. G. 2013. Two phases of disulfide bond formation have differing requirements for oxygen. *J Cell Biol,* 203**,** 615-27.

KOSHIJI, M., TO, K. K. W., HAMMER, S., KUMAMOTO, K., HARRIS, A. L., MODRICH, P. & HUANG, L. E. 2005. HIF-1α Induces Genetic Instability by Transcriptionally Downregulating MutSα Expression. *Molecular Cell,* 17**,** 793-803.

KUMARESWARAN, R., LUDKOVSKI, O., MENG, A., SYKES, J., PINTILIE, M. & BRISTOW, R. G. 2012. Chronic hypoxia compromises repair of DNA double-strand breaks to drive genetic instability. *J Cell Sci,* 125**,** 189-99.

KUO, Y. C., WU, H. T., HUNG, J. J., CHOU, T. Y., TENG, S. C. & WU, K. J. 2015. Nijmegen breakage syndrome protein 1 (NBS1) modulates hypoxia inducible factor-1α (HIF-1α) stability and promotes in vitro migration and invasion under ionizing radiation. *Int J Biochem Cell Biol,* 64**,** 229-38.

LANDO, D., PEET, D. J., GORMAN, J. J., WHELAN, D. A., WHITELAW, M. L. & BRUICK, R. K. 2002. FIH-1 is an asparaginyl hydroxylase enzyme that regulates the transcriptional activity of hypoxia-inducible factor. *Genes Dev,* 16**,** 1466-71.

LARDNER, A. 2001. The effects of extracellular pH on immune function. *J Leukoc Biol,* 69**,** 522-30.

LAU, K. W., TIAN, Y. M., RAVAL, R. R., RATCLIFFE, P. J. & PUGH, C. W. 2007. Target gene selectivity of hypoxia-inducible factor-alpha in renal cancer cells is conveyed by post-DNA-binding mechanisms. *Br J Cancer,* 96**,** 1284-92.

LEADON, S. A. 1996. Repair of DNA damage produced by ionizing radiation: A minireview. *Seminars in Radiation Oncology,* 6**,** 295-305.

LEE, E. Y. H. P. & MULLER, W. J. 2010. Oncogenes and tumor suppressor genes. *Cold Spring Harbor perspectives in biology,* 2**,** a003236-a003236.

LEE, J. Y., PARK, J. H., CHOI, H. J., WON, H. Y., JOO, H. S., SHIN, D. H., PARK, M. K., HAN, B., KIM, K. P., LEE, T. J., CROCE, C. M. & KONG, G. 2017. LSD1 demethylates HIF1α to inhibit hydroxylation and ubiquitin-mediated degradation in tumor angiogenesis. *Oncogene,* 36**,** 5512-5521.

LEONG, W. F., CHAU, J. F. L. & LI, B. 2009. p53 Deficiency Leads to Compensatory Up-Regulation of p16^{INK4a}. *Molecular Cancer Research,* 7**,** 354-360.

LEONTIEVA, O. V., NATARAJAN, V., DEMIDENKO, Z. N., BURDELYA, L. G., GUDKOV, A. V. & BLAGOSKLONNY, M. V. 2012. Hypoxia suppresses conversion from proliferative arrest to cellular senescence. *Proc Natl Acad Sci U S A,* 109**,** 13314-8.

LESZCZYNSKA, K. B., FOSKOLOU, I. P., ABRAHAM, A. G., ANBALAGAN, S., TELLIER, C., HAIDER, S., SPAN, P. N., O'NEILL, E. E., BUFFA, F. M. & HAMMOND, E. M. 2015. Hypoxia-induced p53 modulates both apoptosis and radiosensitivity via AKT. *The Journal of clinical investigation,* 125**,** 2385-2398.

LI, J., NI, M., LEE, B., BARRON, E., HINTON, D. R. & LEE, A. S. 2008. The unfolded protein response regulator GRP78/BiP is required for endoplasmic reticulum integrity and stress-induced autophagy in mammalian cells. *Cell Death & Differentiation,* 15**,** 1460-1471.

LI, L., REN, F., QI, C., XU, L., FANG, Y., LIANG, M., FENG, J., CHEN, B., NING, W. & CAO, J. 2018. Intermittent hypoxia promotes melanoma lung metastasis via oxidative stress and inflammation responses in a mouse model of obstructive sleep apnea. *Respiratory Research,* 19**,** 28.

LIM, J. H., LEE, Y. M., CHUN, Y. S., CHEN, J., KIM, J. E. & PARK, J. W. 2010. Sirtuin 1 modulates cellular responses to hypoxia by deacetylating hypoxia-inducible factor 1alpha. *Mol Cell,* 38**,** 864-78.

LIU, L., CASH, T. P., JONES, R. G., KEITH, B., THOMPSON, C. B. & SIMON, M. C. 2006. Hypoxia-induced energy stress regulates mRNA translation and cell growth. *Mol Cell,* 21**,** 521-31.

LIU, L., LIU, W., WANG, L., ZHU, T., ZHONG, J. & XIE, N. 2017. Hypoxia-inducible factor 1 mediates intermittent hypoxia-induced migration of human breast cancer MDA-MB-231 cells. *Oncol Lett,* 14**,** 7715-7722.

LIU, Y., SONG, X., WANG, X., WEI, L., LIU, X., YUAN, S. & LV, L. 2010. Effect of chronic intermittent hypoxia on biological behavior and hypoxia-associated gene expression in lung cancer cells. *J Cell Biochem,* 111**,** 554-63.

LOIBL, S. & GIANNI, L. 2017. HER2-positive breast cancer. *Lancet,* 389**,** 2415-2429.

LOIBL, S., POORTMANS, P., MORROW, M., DENKERT, C. & CURIGLIANO, G. 2021. Breast cancer. *The Lancet,* 397**,** 1750-1769.

LUO, D., WANG, J., LI, J. & POST, M. 2011. Mouse snail is a target gene for HIF. *Mol Cancer Res,* 9**,** 234-45.

LV, X., LI, J., ZHANG, C., HU, T., LI, S., HE, S., YAN, H., TAN, Y., LEI, M., WEN, M. & ZUO, J. 2017. The role of hypoxia-inducible factors in tumor angiogenesis and cell metabolism. *Genes Dis,* 4**,** 19-24.

MAKINO, Y., UENISHI, R., OKAMOTO, K., ISOE, T., HOSONO, O., TANAKA, H., KANOPKA, A., POELLINGER, L., HANEDA, M. & MORIMOTO, C. 2007. Transcriptional up-regulation of inhibitory PAS domain protein gene expression by hypoxia-inducible factor 1 (HIF-1): a negative feedback regulatory circuit in HIF-1-mediated signaling in hypoxic cells. *J Biol Chem,* 282**,** 14073-82.

MANTOVANI, F., COLLAVIN, L. & DEL SAL, G. 2019. Mutant p53 as a guardian of the cancer cell. *Cell Death & Differentiation,* 26**,** 199-212.

MARTIN-RENDON, E., HALE, S. J., RYAN, D., BABAN, D., FORDE, S. P., ROUBELAKIS, M., SWEENEY, D., MOUKAYED, M., HARRIS, A. L., DAVIES, K. & WATT, S. M. 2007.

Transcriptional profiling of human cord blood CD133+ and cultured bone marrow mesenchymal stem cells in response to hypoxia. *Stem Cells,* 25**,** 1003-12.

MARTINIVE, P., DEFRESNE, F., BOUZIN, C., SALIEZ, J., LAIR, F., GRÉGOIRE, V., MICHIELS, C., DESSY, C. & FERON, O. 2006. Preconditioning of the Tumor Vasculature and Tumor Cells by Intermittent Hypoxia: Implications for Anticancer Therapies. *Cancer Research,* 66**,** 11736-11744.

MATSUMOTO, S., YASUI, H., MITCHELL, J. B. & KRISHNA, M. C. 2010. Imaging cycling tumor hypoxia. *Cancer Res,* 70**,** 10019-23.

MAVADDAT, N., ANTONIOU, A. C., EASTON, D. F. & GARCIA-CLOSAS, M. 2010. Genetic susceptibility to breast cancer. *Mol Oncol,* 4**,** 174-91.

MIHAYLOVA, V. T., BINDRA, R. S., YUAN, J., CAMPISI, D., NARAYANAN, L., JENSEN, R., GIORDANO, F., JOHNSON, R. S., ROCKWELL, S. & GLAZER, P. M. 2003. Decreased expression of the DNA mismatch repair gene Mlh1 under hypoxic stress in mammalian cells. *Mol Cell Biol,* 23**,** 3265-73.

MIRZAYANS, R., ANDRAIS, B., SCOTT, A., PATERSON, M. C. & MURRAY, D. 2010. Single-cell analysis of p16INK4a and p21WAF1 expression suggests distinct mechanisms of senescence in normal human and Li-Fraumeni Syndrome fibroblasts. *Journal of Cellular Physiology,* 223**,** 57-67.

MISTRY, I. N., THOMAS, M., CALDER, E. D. D., CONWAY, S. J. & HAMMOND, E. M. 2017. Clinical Advances of Hypoxia-Activated Prodrugs in Combination With Radiation Therapy. *Int J Radiat Oncol Biol Phys,* 98**,** 1183-1196.

MOELLERING, R. E., BLACK, K. C., KRISHNAMURTY, C., BAGGETT, B. K., STAFFORD, P., RAIN, M., GATENBY, R. A. & GILLIES, R. J. 2008. Acid treatment of melanoma cells selects for invasive phenotypes. *Clin Exp Metastasis,* 25**,** 411-25.

MOLE, D. R., BLANCHER, C., COPLEY, R. R., POLLARD, P. J., GLEADLE, J. M., RAGOUSSIS, J. & RATCLIFFE, P. J. 2009. Genome-wide association of hypoxia-inducible factor (HIF)-1alpha and HIF-2alpha DNA binding with expression profiling of hypoxia-inducible transcripts. *J Biol Chem,* 284**,** 16767-16775.

MOO, T.-A., SANFORD, R., DANG, C. & MORROW, M. 2018. Overview of Breast Cancer Therapy. *PET clinics,* 13**,** 339-354.

MOYNAHAN, M. E., PIERCE, A. J. & JASIN, M. 2001. BRCA2 is required for homology-directed repair of chromosomal breaks. *Mol Cell,* 7**,** 263-72.

NAGELKERKE, A., BUSSINK, J., MUJCIC, H., WOUTERS, B. G., LEHMANN, S., SWEEP, F. C. & SPAN, P. N. 2013. Hypoxia stimulates migration of breast cancer cells via the PERK/ATF4/LAMP3-arm of the unfolded protein response. *Breast Cancer Res,* 15**,** R2.

NAGELKERKE, A., MUJCIC, H., BUSSINK, J., WOUTERS, B. G., VAN LAARHOVEN, H. W., SWEEP, F. C. & SPAN, P. N. 2011. Hypoxic regulation and prognostic value of LAMP3 expression in breast cancer. *Cancer,* 117**,** 3670-81.

NAGY, J. A., CHANG, S. H., SHIH, S. C., DVORAK, A. M. & DVORAK, H. F. 2010. Heterogeneity of the tumor vasculature. *Semin Thromb Hemost,* 36**,** 321-31.

O'CONNOR, J. P. B., ROBINSON, S. P. & WATERTON, J. C. 2019. Imaging tumour hypoxia with oxygen-enhanced MRI and BOLD MRI. *Br J Radiol,* 92**,** 20180642.

O'CONNOR, L., STRASSER, A., O'REILLY, L. A., HAUSMANN, G., ADAMS, J. M., CORY, S. & HUANG, D. C. 1998. Bim: a novel member of the Bcl-2 family that promotes apoptosis. *Embo j,* 17**,** 384-95.

O'RORKE, M. A., MURRAY, L. J., BRAND, J. S. & BHOO-PATHY, N. 2016. The value of adjuvant radiotherapy on survival and recurrence in triple-negative breast cancer: A systematic review and meta-analysis of 5507 patients. *Cancer Treat Rev,* 47**,** 12-21.

OLCINA, M. M., FOSKOLOU, I. P., ANBALAGAN, S., SENRA, J. M., PIRES, I. M., JIANG, Y., RYAN, A. J. & HAMMOND, E. M. 2013. Replication stress and chromatin context link ATM activation to a role in DNA replication. *Mol Cell,* 52**,** 758-66.

OLCINA, M. M., LESZCZYNSKA, K. B., SENRA, J. M., ISA, N. F., HARADA, H. & HAMMOND, E. M. 2016. H3K9me3 facilitates hypoxia-induced p53-dependent apoptosis through repression of APAK. *Oncogene,* 35**,** 793-799.

OLTVAI, Z. N., MILLIMAN, C. L. & KORSMEYER, S. J. 1993. Bcl-2 heterodimerizes in vivo with a conserved homolog, Bax, that accelerates programmed cell death. *Cell,* 74**,** 609-19.

PANTHER, E., CORINTI, S., IDZKO, M., HEROUY, Y., NAPP, M., LA SALA, A., GIROLOMONI, G. & NORGAUER, J. 2003. Adenosine affects expression of membrane molecules, cytokine and chemokine release, and the T-cell stimulatory capacity of human dendritic cells. *Blood,* 101**,** 3985-90.

PAPANDREOU, I., CAIRNS, R. A., FONTANA, L., LIM, A. L. & DENKO, N. C. 2006. HIF-1 mediates adaptation to hypoxia by actively downregulating mitochondrial oxygen consumption. *Cell Metab,* 3**,** 187-97.

PASQUALE, E. B. 2008. Eph-Ephrin Bidirectional Signaling in Physiology and Disease. *Cell,* 133**,** 38-52.

PAWLIK, T. M. & KEYOMARSI, K. 2004. Role of cell cycle in mediating sensitivity to radiotherapy. *Int J Radiat Oncol Biol Phys,* 59**,** 928-42.

PAWLUS, M. R., WANG, L. & HU, C. J. 2014. STAT3 and HIF1α cooperatively activate HIF1 target genes in MDA-MB-231 and RCC4 cells. *Oncogene,* 33**,** 1670-9.

PETITPREZ, F., SUN, C.-M., LACROIX, L., SAUTÈS-FRIDMAN, C., DE REYNIÈS, A. & FRIDMAN, W. H. 2018. Quantitative Analyses of the Tumor Microenvironment Composition and Orientation in the Era of Precision Medicine. *Frontiers in oncology,* 8**,** 390-390.

PING, Q., YAN, R., CHENG, X., WANG, W., ZHONG, Y., HOU, Z., SHI, Y., WANG, C. & LI, R. 2021. Cancer-associated fibroblasts: overview, progress, challenges, and directions. *Cancer Gene Therapy,* 28**,** 984-999.

PIRES, I. M., BENCOKOVA, Z., MCGURK, C. & HAMMOND, E. M. 2010a. Exposure to acute hypoxia induces a transient DNA damage response which includes Chk1 and TLK1. *Cell Cycle,* 9**,** 2502-2507.

PIRES, I. M., BENCOKOVA, Z., MILANI, M., FOLKES, L. K., LI, J.-L., STRATFORD, M. R., HARRIS, A. L. & HAMMOND, E. M. 2010b. Effects of acute versus chronic hypoxia on DNA damage responses and genomic instability. *Cancer research,* 70**,** 925-935.

PIRES, I. M., OLCINA, M. M., ANBALAGAN, S., POLLARD, J. R., REAPER, P. M., CHARLTON, P. A., MCKENNA, W. G. & HAMMOND, E. M. 2012. Targeting radiation-resistant hypoxic tumour cells through ATR inhibition. *Br J Cancer,* 107**,** 291-9.

POLYAK, K. & WEINBERG, R. A. 2009. Transitions between epithelial and mesenchymal states: acquisition of malignant and stem cell traits. *Nat Rev Cancer,* 9**,** 265-73.

RAK, J., MITSUHASHI, Y., BAYKO, L., FILMUS, J., SHIRASAWA, S., SASAZUKI, T. & KERBEL, R. S. 1995. Mutant ras oncogenes upregulate VEGF/VPF expression: implications for induction and inhibition of tumor angiogenesis. *Cancer Res,* 55**,** 4575-80.

RAMACHANDRAN, S., MA, T. S., GRIFFIN, J., NG, N., FOSKOLOU, I. P., HWANG, M.-S., VICTORI, P., CHENG, W.-C., BUFFA, F. M., LESZCZYNSKA, K. B., EL-KHAMISY, S. F., GROMAK, N.

& HAMMOND, E. M. 2021. Hypoxia-induced SETX links replication stress with the unfolded protein response. *Nature Communications,* 12**,** 3686.

RANKIN, E. B., FUH, K. C., CASTELLINI, L., VISWANATHAN, K., FINGER, E. C., DIEP, A. N., LAGORY, E. L., KARIOLIS, M. S., CHAN, A., LINDGREN, D., AXELSON, H., MIAO, Y. R., KRIEG, A. J. & GIACCIA, A. J. 2014. Direct regulation of GAS6/AXL signaling by HIF promotes renal metastasis through SRC and MET. *Proc Natl Acad Sci U S A,* 111**,** 13373-8.

RANKIN, E. B. & GIACCIA, A. J. 2016. Hypoxic control of metastasis. *Science,* 352**,** 175-80.

ROBERTS, S. A., LAWRENCE, M. S., KLIMCZAK, L. J., GRIMM, S. A., FARGO, D., STOJANOV, P., KIEZUN, A., KRYUKOV, G. V., CARTER, S. L., SAKSENA, G., HARRIS, S., SHAH, R. R., RESNICK, M. A., GETZ, G. & GORDENIN, D. A. 2013. An APOBEC cytidine deaminase mutagenesis pattern is widespread in human cancers. *Nat Genet,* 45**,** 970-6.

ROFSTAD, E. K., GALAPPATHI, K., MATHIESEN, B. & RUUD, E. B. 2007. Fluctuating and diffusion-limited hypoxia in hypoxia-induced metastasis. *Clin Cancer Res,* 13**,** 1971-8.

ROFSTAD, E. K., GAUSTAD, J.-V., EGELAND, T. A. M., MATHIESEN, B. & GALAPPATHI, K. 2010. Tumors exposed to acute cyclic hypoxic stress show enhanced angiogenesis, perfusion and metastatic dissemination. *International Journal of Cancer,* 127**,** 1535-1546.

RON, A., DEÁN-BEN, X. L., GOTTSCHALK, S. & RAZANSKY, D. 2019. Volumetric Optoacoustic Imaging Unveils High-Resolution Patterns of Acute and Cyclic Hypoxia in a Murine Model of Breast Cancer. *Cancer Res,* 79**,** 4767-4775.

SAHLGREN, C., GUSTAFSSON, M. V., JIN, S., POELLINGER, L. & LENDAHL, U. 2008. Notch signaling mediates hypoxia-induced tumor cell migration and invasion. *Proc Natl Acad Sci U S A,* 105**,** 6392-7.

SALMINEN, A., KAARNIRANTA, K. & KAUPPINEN, A. 2016. Hypoxia-Inducible Histone Lysine Demethylases: Impact on the Aging Process and Age-Related Diseases. *Aging and disease,* 7**,** 180-200.

SÁNCHEZ-ELSNER, T., BOTELLA, L. M., VELASCO, B., CORBÍ, A., ATTISANO, L. & BERNABÉU, C. 2001. Synergistic cooperation between hypoxia and transforming growth factor-beta pathways on human vascular endothelial growth factor gene expression. *J Biol Chem,* 276**,** 38527-35.

SCHÖDEL, J., OIKONOMOPOULOS, S., RAGOUSSIS, J., PUGH, C. W., RATCLIFFE, P. J. & MOLE, D. R. 2011. High-resolution genome-wide mapping of HIF-binding sites by ChIP-seq. *Blood,* 117**,** e207-17.

SCHWAB, L. P., PEACOCK, D. L., MAJUMDAR, D., INGELS, J. F., JENSEN, L. C., SMITH, K. D., CUSHING, R. C. & SEAGROVES, T. N. 2012. Hypoxia-inducible factor 1α promotes primary tumor growth and tumor-initiating cell activity in breast cancer. *Breast Cancer Res,* 14**,** R6.

SEMENZA, G. L. 2010a. Defining the role of hypoxia-inducible factor 1 in cancer biology and therapeutics. *Oncogene,* 29**,** 625-34.

SEMENZA, G. L. 2010b. HIF-1: upstream and downstream of cancer metabolism. *Curr Opin Genet Dev,* 20**,** 51-6.

SEMENZA, G. L. 2017. A compendium of proteins that interact with HIF-1α. *Experimental cell research,* 356**,** 128-135.

SHAH, S. P., MORIN, R. D., KHATTRA, J., PRENTICE, L., PUGH, T., BURLEIGH, A., DELANEY, A., GELMON, K., GULIANY, R., SENZ, J., STEIDL, C., HOLT, R. A., JONES, S., SUN, M., LEUNG, G., MOORE, R., SEVERSON, T., TAYLOR, G. A., TESCHENDORFF, A. E., TSE, K., TURASHVILI, G., VARHOL, R., WARREN, R. L., WATSON, P., ZHAO, Y., CALDAS, C.,

HUNTSMAN, D., HIRST, M., MARRA, M. A. & APARICIO, S. 2009. Mutational evolution in a lobular breast tumour profiled at single nucleotide resolution. *Nature,* 461**,** 809-13.

SHCHORS, K., SHCHORS, E., ROSTKER, F., LAWLOR, E. R., BROWN-SWIGART, L. & EVAN, G. I. 2006. The Myc-dependent angiogenic switch in tumors is mediated by interleukin 1beta. *Genes Dev,* 20**,** 2527-38.

SHILOH, Y. & ZIV, Y. 2013. The ATM protein kinase: regulating the cellular response to genotoxic stress, and more. *Nature Reviews Molecular Cell Biology,* 14**,** 197-210.

SHIMIZU, T., IWANAGA, M., YASUNAGA, A., URATA, Y., GOTO, S., SHIBATA, S. & KONDO, T. 1998. Protective role of glutathione synthesis on radiation-induced DNA damage in rabbit brain. *Cell Mol Neurobiol,* 18**,** 299-310.

SILVA, S. N., TOMAR, M., PAULO, C., GOMES, B. C., AZEVEDO, A. P., TEIXEIRA, V., PINA, J. E., RUEFF, J. & GASPAR, J. F. 2010. Breast cancer risk and common single nucleotide polymorphisms in homologous recombination DNA repair pathway genes XRCC2, XRCC3, NBS1 and RAD51. *Cancer Epidemiol,* 34**,** 85-92.

SINCLAIR, W. K. & MORTON, R. A. 1963. VARIATIONS IN X-RAY RESPONSE DURING THE DIVISION CYCLE OF PARTIALLY SYNCHRONIZED CHINESE HAMSTER CELLS IN CULTURE. *Nature,* 199**,** 1158-60.

SINCLAIR, W. K. & MORTON, R. A. 1965. X-RAY AND ULTRAVIOLET SENSITIVITY OF SYNCHRONIZED CHINESE HAMSTER CELLS AT VARIOUS STAGES OF THE CELL CYCLE. *Biophys J,* 5**,** 1-25.

SINCLAIR, W. K. & MORTON, R. A. 1966. X-ray sensitivity during the cell generation cycle of cultured Chinese hamster cells. *Radiat Res,* 29**,** 450-74.

SLAMON, D. J., LEYLAND-JONES, B., SHAK, S., FUCHS, H., PATON, V., BAJAMONDE, A., FLEMING, T., EIERMANN, W., WOLTER, J., PEGRAM, M., BASELGA, J. & NORTON, L. 2001. Use of chemotherapy plus a monoclonal antibody against HER2 for metastatic breast cancer that overexpresses HER2. *N Engl J Med,* 344**,** 783-92.

SNELL, C. E., TURLEY, H., MCINTYRE, A., LI, D., MASIERO, M., SCHOFIELD, C. J., GATTER, K. C., HARRIS, A. L. & PEZZELLA, F. 2014. Proline-hydroxylated hypoxia-inducible factor 1α (HIF-1α) upregulation in human tumours. *PLoS One,* 9**,** e88955.

SPIVAK-KROIZMAN, T. R., HOSTETTER, G., POSNER, R., AZIZ, M., HU, C., DEMEURE, M. J., VON HOFF, D., HINGORANI, S. R., PALCULICT, T. B., IZZO, J., KIRIAKOVA, G. M., ABDELMELEK, M., BARTHOLOMEUSZ, G., JAMES, B. P. & POWIS, G. 2013. Hypoxia triggers hedgehog-mediated tumor-stromal interactions in pancreatic cancer. *Cancer Res,* 73**,** 3235-47.

STEIN, G. H., DRULLINGER, L. F., SOULARD, A. & DULIĆ, V. 1999. Differential roles for cyclin-dependent kinase inhibitors p21 and p16 in the mechanisms of senescence and differentiation in human fibroblasts. *Mol Cell Biol,* 19**,** 2109-17.

SUNG, H., FERLAY, J., SIEGEL, R. L., LAVERSANNE, M., SOERJOMATARAM, I., JEMAL, A. & BRAY, F. 2021. Global Cancer Statistics 2020: GLOBOCAN Estimates of Incidence and Mortality Worldwide for 36 Cancers in 185 Countries. *CA Cancer J Clin,* 71**,** 209-249.

TAN, E. Y., YAN, M., CAMPO, L., HAN, C., TAKANO, E., TURLEY, H., CANDILORO, I., PEZZELLA, F., GATTER, K. C., MILLAR, E. K., O'TOOLE, S. A., MCNEIL, C. M., CREA, P., SEGARA, D., SUTHERLAND, R. L., HARRIS, A. L. & FOX, S. B. 2009. The key hypoxia regulated gene CAIX is upregulated in basal-like breast tumours and is associated with resistance to chemotherapy. *Br J Cancer,* 100**,** 405-11.

TANNOCK, I. F., LEE, C. M., TUNGGAL, J. K., COWAN, D. S. & EGORIN, M. J. 2002. Limited penetration of anticancer drugs through tumor tissue: a potential cause of resistance of solid tumors to chemotherapy. *Clin Cancer Res,* 8**,** 878-84.

THIERY, J. P., ACLOQUE, H., HUANG, R. Y. & NIETO, M. A. 2009. Epithelial-mesenchymal transitions in development and disease. *Cell,* 139**,** 871-90.

TO, C., FARNSWORTH, R. H., VAIL, M. E., CHHEANG, C., GARGETT, C. E., MURONE, C., LLERENA, C., MAJOR, A. T., SCOTT, A. M., JANES, P. W. & LACKMANN, M. 2014. Hypoxia-controlled EphA3 marks a human endometrium-derived multipotent mesenchymal stromal cell that supports vascular growth. *PLoS One,* 9**,** e112106.

TOLEDO, LUIS I., ALTMEYER, M., RASK, M.-B., LUKAS, C., LARSEN, DORTHE H., POVLSEN, LOU K., BEKKER-JENSEN, S., MAILAND, N., BARTEK, J. & LUKAS, J. 2013. ATR Prohibits Replication Catastrophe by Preventing Global Exhaustion of RPA. *Cell,* 155**,** 1088-1103.

TURNBULL, C. & RAHMAN, N. 2008. Genetic predisposition to breast cancer: past, present, and future. *Annu Rev Genomics Hum Genet,* 9**,** 321-45.

VAN TONDER, A., JOUBERT, A. M. & CROMARTY, A. D. 2015. Limitations of the 3-(4,5-dimethylthiazol-2-yl)-2,5-diphenyl-2H-tetrazolium bromide (MTT) assay when compared to three commonly used cell enumeration assays. *BMC research notes,* 8**,** 47-47.

VARLEY, K. E., MUTCH, D. G., EDMONSTON, T. B., GOODFELLOW, P. J. & MITRA, R. D. 2009. Intra-tumor heterogeneity of MLH1 promoter methylation revealed by deep single molecule bisulfite sequencing. *Nucleic Acids Res,* 37**,** 4603-12.

VASSIN, V. M., ANANTHA, R. W., SOKOLOVA, E., KANNER, S. & BOROWIEC, J. A. 2009. Human RPA phosphorylation by ATR stimulates DNA synthesis and prevents ssDNA accumulation during DNA-replication stress. *Journal of cell science,* 122**,** 4070-4080.

VAUPEL, P., BRIEST, S. & HÖCKEL, M. 2002. Hypoxia in breast cancer: pathogenesis, characterization and biological/therapeutic implications. *Wien Med Wochenschr,* 152**,** 334-42.

VAUPEL, P., KALLINOWSKI, F. & OKUNIEFF, P. 1989. Blood flow, oxygen and nutrient supply, and metabolic microenvironment of human tumors: a review. *Cancer Res,* 49**,** 6449-65.

VESELY, M. D., KERSHAW, M. H., SCHREIBER, R. D. & SMYTH, M. J. 2011. Natural Innate and Adaptive Immunity to Cancer. *Annual Review of Immunology,* 29**,** 235-271.

WANG, G. L., JIANG, B. H., RUE, E. A. & SEMENZA, G. L. 1995. Hypoxia-inducible factor 1 is a basic-helix-loop-helix-PAS heterodimer regulated by cellular O2 tension. *Proc Natl Acad Sci U S A,* 92**,** 5510-4.

WANG, P., ZHANG, X., SUN, N., ZHAO, Z. & HE, J. 2020. Comprehensive Analysis of the Tumor Microenvironment in Cutaneous Melanoma associated with Immune Infiltration. *Journal of Cancer,* 11**,** 3858-3870.

WARBURG, O. 1956. On the origin of cancer cells. *Science,* 123**,** 309-14.

WIJFFELS, K. I., KAANDERS, J. H., RIJKEN, P. F., BUSSINK, J., VAN DEN HOOGEN, F. J., MARRES, H. A., DE WILDE, P. C., RALEIGH, J. A. & VAN DER KOGEL, A. J. 2000. Vascular architecture and hypoxic profiles in human head and neck squamous cell carcinomas. *Br J Cancer,* 83**,** 674-83.

WILSON, D. F., RUMSEY, W. L., GREEN, T. J. & VANDERKOOI, J. M. 1988. The oxygen dependence of mitochondrial oxidative phosphorylation measured by a new optical method for measuring oxygen concentration. *Journal of Biological Chemistry,* 263**,** 2712-2718.

WILSON, J. D., HAMMOND, E. M., HIGGINS, G. S. & PETERSSON, K. 2019. Ultra-High Dose Rate (FLASH) Radiotherapy: Silver Bullet or Fool's Gold? *Front Oncol,* 9**,** 1563.

WINTERS, S., MARTIN, C., MURPHY, D. & SHOKAR, N. K. 2017. Chapter One - Breast Cancer Epidemiology, Prevention, and Screening. *In:* LAKSHMANASWAMY, R. (ed.) *Progress in Molecular Biology and Translational Science.* Academic Press.

WONG, C. C., GILKES, D. M., ZHANG, H., CHEN, J., WEI, H., CHATURVEDI, P., FRALEY, S. I., WONG, C. M., KHOO, U. S., NG, I. O., WIRTZ, D. & SEMENZA, G. L. 2011. Hypoxia-inducible factor 1 is a master regulator of breast cancer metastatic niche formation. *Proc Natl Acad Sci U S A,* 108**,** 16369-74.

WYCKOFF, J. B., WANG, Y., LIN, E. Y., LI, J. F., GOSWAMI, S., STANLEY, E. R., SEGALL, J. E., POLLARD, J. W. & CONDEELIS, J. 2007. Direct visualization of macrophage-assisted tumor cell intravasation in mammary tumors. *Cancer Res,* 67**,** 2649-56.

WYKOFF, C. C., BEASLEY, N. J., WATSON, P. H., TURNER, K. J., PASTOREK, J., SIBTAIN, A., WILSON, G. D., TURLEY, H., TALKS, K. L., MAXWELL, P. H., PUGH, C. W., RATCLIFFE, P. J. & HARRIS, A. L. 2000. Hypoxia-inducible expression of tumor-associated carbonic anhydrases. *Cancer Res,* 60**,** 7075-83.

XIANG, L., GILKES, D. M., HU, H., LUO, W., BULLEN, J. W., LIANG, H. & SEMENZA, G. L. 2015. HIF-1α and TAZ serve as reciprocal co-activators in human breast cancer cells. *Oncotarget,* 6**,** 11768-78.

XU, L., FUKUMURA, D. & JAIN, R. K. 2002. Acidic extracellular pH induces vascular endothelial growth factor (VEGF) in human glioblastoma cells via ERK1/2 MAPK signaling pathway: mechanism of low pH-induced VEGF. *J Biol Chem,* 277**,** 11368-74.

YAMAURA, H. & MATSUZAWA, T. 1979. Tumor regrowth after irradiation; an experimental approach. *Int J Radiat Biol Relat Stud Phys Chem Med,* 35**,** 201-19.

YANG, M. H., WU, M. Z., CHIOU, S. H., CHEN, P. M., CHANG, S. Y., LIU, C. J., TENG, S. C. & WU, K. J. 2008. Direct regulation of TWIST by HIF-1alpha promotes metastasis. *Nat Cell Biol,* 10**,** 295-305.

YANG, S.-J., PARK, Y. S., CHO, J. H., MOON, B., AN, H.-J., LEE, J. Y., XIE, Z., WANG, Y., POCALYKO, D., LEE, D. C., SOHN, H. A., KANG, M., KIM, J. Y., KIM, E., PARK, K. C., KIM, J.-A. & YEOM, Y. I. 2017. Regulation of hypoxia responses by flavin adenine dinucleotide-dependent modulation of HIF-1α protein stability. *The EMBO journal,* 36**,** 1011-1028.

YASUI, H., MATSUMOTO, S., DEVASAHAYAM, N., MUNASINGHE, J. P., CHOUDHURI, R., SAITO, K., SUBRAMANIAN, S., MITCHELL, J. B. & KRISHNA, M. C. 2010. Low-Field Magnetic Resonance Imaging to Visualize Chronic and Cycling Hypoxia in Tumor-Bearing Mice. *Cancer Research,* 70**,** 6427-6436.

YIN, C., KNUDSON, C. M., KORSMEYER, S. J. & VAN DYKE, T. 1997. Bax suppresses tumorigenesis and stimulates apoptosis in vivo. *Nature,* 385**,** 637-40.

YU, J., WANG, Z., KINZLER, K. W., VOGELSTEIN, B. & ZHANG, L. 2003. PUMA mediates the apoptotic response to p53 in colorectal cancer cells. *Proc Natl Acad Sci U S A,* 100**,** 1931-6.

ZACKRISSON, B. U., NYSTRÖM, U. H. & OSTBERGH, P. 1991. Biological Response In Vitro to Pulsed High Dose Rate Electrons from a Clinical Accelerator. *Acta Oncologica,* 30**,** 747-751.

ZHANG, B., BEEGHLY-FADIEL, A., LONG, J. & ZHENG, W. 2011. Genetic variants associated with breast-cancer risk: comprehensive research synopsis, meta-analysis, and epidemiological evidence. *Lancet Oncol,* 12**,** 477-88.

ZHANG, W., SHI, X., PENG, Y., WU, M., ZHANG, P., XIE, R., WU, Y., YAN, Q., LIU, S. & WANG, J. 2015. HIF-1α Promotes Epithelial-Mesenchymal Transition and Metastasis through Direct Regulation of ZEB1 in Colorectal Cancer. *PLoS One,* 10**,** e0129603.

ZHOU, C.-H., ZHANG, X.-P., LIU, F. & WANG, W. 2015. Modeling the interplay between the HIF-1 and p53 pathways in hypoxia. *Scientific Reports,* 5**,** 13834.

APPENDIX: Published papers from this MSc by Research

Bader, S. B., Ma, T. S., **Simpson, C. J**., Liang, J., Maezono, S. E. B., Olcina, M. M., Buffa, F. M. & Hammond, E. M. 2021. Replication catastrophe induced by cyclic hypoxia leads to increased APOBEC3B activity. Nucleic Acids Res. 2021 Jul 21;49(13):7492-7506